

Critical Phenomena in the

Random Ising Model

Thesis

submitted by

Alasdair Stewart Brown

for the degree of

Doctor of Philosophy

Department of Physics,

University of Edinburgh

February, 1986



To Susie and my family

The truth is rarely pure, and never simple

(Oscar Wilde)

Declaration

I hereby declare that this thesis is my own work except where explicitly stated otherwise

Alvin S. M.

14th February, 1986

Acknowledgments

The work presented in this thesis would not have been possible without the friendship and support of many people who have made my time in Edinburgh most enjoyable. Principally, I would like to thank my supervisors, Professor D.J. Wallace and Dr. A.D. Bruce for many helpful and illuminating discussions in relation to academic problems encountered during the course of my research. I would also like to thank all the students and staff in the Theory group, amongst whom I have made many lasting friendships. Especially important to me has been the support and encouragement of my friends outside of the Theory group, and of the help extended to me by my family. I would like to acknowledge the financial support of the Science and Engineering Research Council during the period of my research.

Abstract

The modern techniques of field theory applied to critical phenomena are briefly discussed, with particular emphasis on the use of the ϵ -expansion to extract the asymptotic behaviour in the critical region. The dimensional regularisation and minimal subtraction method of renormalisation, introduced by 't Hooft and Veltman, is outlined. These methods, along with a Monte Carlo simulation on a highly parallel computer, are utilised in extracting information pertaining to the behaviour near criticality of the random, site-diluted Ising model.

The universal ratio of the susceptibility amplitude above and below the critical temperature is determined to one higher order than previously in an ϵ -expansion, within the framework of the replica formalism. The calculation is performed using a Taylor expansion, in the number of replicas, of the transverse propagator appearing in the Hamiltonian, about the longitudinal. This higher order correction goes in the right direction for agreement with experiment.

An extension of the formalism to embrace the presence of two sets of replica spins is used to derive the $o(\epsilon^{1/2})$ term in an expansion of the additional static correlation function, $C^{(s)}(q)$, arising from the non-interchangeability of the thermal and configurational averages in the random model. The appearance of $C^{(s)}(q)$ in the structure factor implies that results of neutron scattering experiments to measure the susceptibility amplitude ratio must be re-interpreted.

Finally, analysis of the properties of block spin variables in a Monte Carlo simulation is used to determine the phase diagram and critical exponents in two-dimensions. Possible interpretations of the observed evolution of the exponent ratio, β/ν , under increasing dilution are discussed.

TABLE OF CONTENTS

1 Introduction to Field Theory and Critical Phenomena	1
1.1 Introduction to Critical Phenomena	1
1.2 Field Theory and Critical Phenomena	3
1.3 Perturbative Expansions in Field Theory	9
1.4 Renormalisation	16
1.5 Random Systems	20
1.6 Research Projects	24
2 Susceptibility Amplitude Ratios in the Random Ising Model	26
2.1 Introduction	26
2.2 The Random Ising Model	27
2.3 The Replica Trick	29
2.4 Universal Form of the equation of State	31
2.5 One-Loop expansion of Susceptibility Amplitude Ratio	33
2.6 Two-Loop expansion of Susceptibility Amplitude Ratio	53
2.7 Conclusions	62
3 Structure Factor in the Random Ising Model	64
3.1 Introduction	64
3.2 Double Replica Trick	66
3.3 Calculation of $C^{(s)}(q=0)$	70
3.4 Conclusions	77
4 Monte Carlo Simulation of the Random Ising Model	79
4.1 Introduction	79
4.2 Critical Behaviour in the Pure Ising Model	89
4.3 Critical Behaviour in the Diluted Ising Model	100
4.4 Discussion of results	108
References	122

1.1. Introduction to Critical Phenomena

Many physical systems exhibit phase transitions. A phase transition occurs when there is a discontinuous or singular behaviour resulting from the continuous change of a control variable and is often associated with a change in the symmetry of the system. Phase transitions are evidence of the macroscopic cooperative behaviour of the microscopic constituents of the system. The classic example of a phase transition is the gas-liquid transition in water, where the density changes discontinuously as the temperature reaches a critical value. The discontinuity in the density across the coexistence curve plays the role of an order parameter, taking a non-zero value below the critical temperature, and zero above.

Ehrenfest classified phase transitions as

" n^{th} order if the n^{th} derivative of the free energy is the first discontinuous or singular derivative."

The modern classification is that a transition is first order if the first derivative is discontinuous or singular, otherwise the transition is of second order or continuous.

Throughout this thesis we will be concerned with ferromagnetic systems and will therefore adopt the terminology of magnetism.

If a ferromagnetic system acquires a non-zero magnetisation via a second-order phase transition as we lower the temperature through T_c , then

T_c is a critical point. As we approach a critical point various physical quantities either vanish, or behave asymptotically as a power of the reduced temperature, i.e., $T - T_c$. For example, in a ferromagnet the order parameter is the bulk magnetisation, M , and as we approach T_c from below (in zero external field, H)

$$M(T, H=0) \sim (T_c - T)^\beta \quad (1.1)$$

β is called a critical exponent.

Another important concept is that of scaling near a critical point (Widom, 1965). To illustrate, the equation of state relates the external, applied magnetic field to the internal magnetisation and temperature, viz.,

$$H = f(M, T) \quad (1.2)$$

Near the critical point f is a generalised homogeneous function of M and $T - T_c$, i.e.,

$$f(\lambda^a x, \lambda^b y) = \lambda^c f(x, y) \quad (1.3)$$

$$\Rightarrow H = M^\delta f\left(\frac{T - T_c}{M^{1/\beta}}\right) \quad (1.4)$$

This can be used to derive expressions for the critical exponents and scaling laws relating these exponents to one another.

The concept of universality embodies the idea that the critical exponents and the functional form of f are independent of the details of the microscopic interaction. However, they do depend on the number of space dimensions, the

internal symmetry of the system and the range of the interaction (e.g., if it is long-range as opposed to nearest neighbour, dipolar as opposed to spherically symmetric, &c.)

Theoretical understanding of the above phenomena has greatly advanced in the last 15 years due to the introduction of the renormalisation group (Wilson, 1972) and the use of field theory in which the lattice model of statistical mechanics is transformed into a representation by continuous classical fields (Brézin *et al*, 1973).

In the remainder of this chapter we review the techniques of field theory with reference to statistical mechanics. In section (1.2) we highlight the main features of the approach and show how to obtain the Greens functions which contain the essential physics. In section (1.3) we describe the main calculational method in field theory, a perturbative expansion about an exactly soluble model. Section (1.4) shows how the divergences arising in perturbation series can be systematically handled by renormalisation of the theory. Random systems and their importance are discussed in section (1.5) and in section (1.6) research projects detailed in this thesis are summarised.

1.2. Field Theory and Critical Phenomena

This section reviews the main aspects of the continuous field description of critical phenomena and discusses how to abstract the Greens functions which contain the essential physics from this approach. For a modern, detailed description of Field Theory applied to this topic the reader is referred to the excellent book by Amit (1984).

The first stage in describing a system using a continuous field

representation is to construct the Hamiltonian in terms of the continuous field variables. This enables one to write down the partition function,

$$Z = \sum_{\{spins\}} e^{-\beta H} \quad (1.5)$$

which generates all the correlation functions of the order parameter. If we start from a lattice formulation with spin variable s_i on site i and a Hamiltonian of the general form

$$-\beta H = \sum_{ij} s_i K_{ij} s_j \quad (1.6)$$

provided the coupling constant matrix, K , is symmetric and positive definite, we can transform Z to a continuous field description by means of the identity (Berlin and Kac, 1952; Hubbard, 1958; Stratonovich, 1957; Baker, 1962)

$$e^{\sum_{ij} s_i K_{ij} s_j} = N \int \prod_{i=1}^N d\phi_i e^{-\frac{1}{4} \sum_{ij} \phi_i K_{ij}^{-1} \phi_j + \sum_i \phi_i s_i} \quad (1.7)$$

Here, N is a constant.

This transformation decouples the spin variables, $\{s_i\}$ on the right-hand side of (1.7) and the sum over the spin configurations in the partition function can now be evaluated. This gives rise to a term in the resulting Hamiltonian which on Taylor expansion produces local interactions of the field ϕ , e.g., ϕ^2 , ϕ^4 , &c., whereas the $\phi_i K_{ij}^{-1} \phi_j$ term produces non-local derivative interactions, e.g., $\nabla \phi^2$, &c. An alternative route to constructing an Hamiltonian for the system is to appeal to symmetry considerations and include in the Hamiltonian all terms which are consistent with the symmetries present in the lattice model (Mukamel and Krinsky, 1976). In both of these approaches the resulting series of interaction terms must be truncated at some point to enable us to

carry out calculations using the field theoretic Hamiltonian, $\mathcal{H}\{\Phi\}$. All terms which correspond to relevant perturbations of the system are retained, and the other, so-called irrelevant interactions are discarded. The meaning of the terms relevant and irrelevant in this context will be more precisely defined when we consider the renormalisation group later in this chapter. The general form of the Hamiltonian is thus

$$\mathcal{H} = \int d^d x \left\{ \frac{1}{2} (\nabla\Phi)^2 + \frac{1}{2} r_0 \Phi^2 + \frac{1}{4!} u_0 \Phi^4 + \dots - H_0 \Phi \right\} \quad (1.8)$$

where we have adjusted the scale of the field Φ to produce a coefficient of $\frac{1}{2}$ for the gradient term and we have included an external field, H_0 . The ellipsis indicates other possible relevant terms contributing to the Hamiltonian.

If we consider the simplest case in which the only terms in \mathcal{H} are those shown above, we see immediately that $u > 0$ if the potential,

$$V = \frac{1}{2} r_0 \phi^2 + \frac{1}{4!} u_0 \phi^4 \quad (1.9)$$

is to be bounded below. For r_0 there are two possibilities, $r_0 < 0$ or $r_0 > 0$. In the first case, the potential has the familiar, "double-well" shape and the likely value of ϕ is ~~zero~~^{non-zero} in the second, there is only one minimum and the likely value of ϕ is zero. Thus r_0 plays the role of temperature, with $r_0 > 0$ corresponding to $T > T_c$, and $r_0 < 0$ to $T < T_c$ - within the approximations of mean field theory criticality corresponds to the condition $r_0 = 0$.

Expectation values of operators are defined through

$$\langle O \rangle = \frac{1}{Z} \int D\phi O e^{-\mathcal{H}} \quad (1.10)$$

where the notation $\int D\phi$ implies an integral over all functional forms of the

field $\Phi(x)$.

If we introduce a source term, J , into the Hamiltonian which couples linearly to the field Φ , all the correlation functions of the order parameter, or Greens functions, are generated by taking functional derivatives of the partition function with respect to the source, i.e.,

$$G_T^{(N)}(x_1, \dots, x_N) = \langle \phi(x_1) \dots \phi(x_N) \rangle = \left. \frac{\delta^N Z\{J\}}{\delta J(x_1) \dots \delta J(x_N)} \right|_{J=0} \quad (1.11)$$

$Z\{J\}$ is therefore also known as the generating functional for these quantities.

We can also define a free energy functional $F\{J\}$ for our continuous field description, analogous to the lattice model free energy, through the definition

$$F\{J\} = \ln Z\{J\} \quad (1.12)$$

Taking appropriate derivatives with respect to J , we find that $F\{J\}$ is the generating functional for the **connected** Greens functions, or cumulants,

$$G_c^{(N)}(x_1, \dots, x_N) = \left. \frac{\delta^N F\{J\}}{\delta J(x_1) \dots \delta J(x_N)} \right|_{J=0} \quad (1.13)$$

These correspond to an expansion of the correlation function of N fields from which all possible factorisations have been subtracted, e.g.,

$$G_c^{(2)}(x_1, x_2) = \langle \phi(x_1) \phi(x_2) \rangle - \langle \phi(x_1) \rangle \langle \phi(x_2) \rangle \quad (1.14)$$

$$= G^{(2)}(x_1, x_2) - G^{(1)}(x_1) G^{(1)}(x_2) \quad (1.15)$$

The terminology *connected* will become clear once we discuss the graphical

interpretation of a perturbative expansion of the Greens functions.

If we now study the Legendre transformation to conjugate variables (in the Hamiltonian mechanics sense (Goldstein,1980)) defined by

$$\Gamma\{\bar{\phi}\} + F\{J\} = \int d^d x [\mathcal{J}(x) + H(x)] \bar{\phi}(x) \quad (1.16)$$

where

$$\bar{\phi}(x) = \langle \phi(x) \rangle = \frac{\delta F\{J\}}{\delta \mathcal{J}(x)} = M \quad (1.17)$$

we find that $\Gamma\{\bar{\phi}\}$ is the generating functional for the vertex functions, $\Gamma^{(N)}(x_1, \dots, x_N)$, the matrix inverse of the connected Greens function (again, the description *vertex* function will be clarified by our discussion of the Feynman graph expansion). The functional derivatives in this case are taken with respect to the variable $\bar{\phi}$, not J , viz.,

$$\Gamma^{(N)}(x_1, \dots, x_N) = \left. \frac{\delta \Gamma\{\bar{\phi}\}}{\delta \bar{\phi}(x_1) \dots \delta \bar{\phi}(x_N)} \right|_{\bar{\phi}=M} \quad (1.18)$$

To complete the list of functions we shall need to consider when we come to study renormalisation of a field theory, we must include Greens functions involving composite operators, e.g., higher powers of the fields at a given point. We shall not need these in their full generality; for our purpose it will be sufficient to consider the Greens functions containing the ϕ^2 operator,

$$G^{(N,P)}(x_1 \dots x_N; y_1 \dots y_P) = \left(\frac{1}{i}\right)^P \langle \phi(x_1) \dots \phi(x_N) \phi^2(y_1) \dots \phi^2(y_P) \rangle \quad (1.19)$$

In an analogous fashion to the preceding definitions we can define a generating functional $Z'\{J,t\}$ for the $G^{(N,P)}$ by

$$Z'\{J,t\} = \frac{1}{Z} \int \mathcal{D}\phi \exp\{-H + \int d^d x [J\phi + \frac{1}{2}t\phi^2]\} \quad (1.20)$$

Then

$$F'\{J,t\} = \ln Z'\{J,t\} \quad (1.21)$$

is the generating functional for the connected pieces of $G^{(N,P)}$, $G_c^{(N,P)}$, and, similarly, the vertex functions $\Gamma^{(N,P)}$ defined as

$$\Gamma^{(N,P)}(x_1, \dots, x_N; y_1, \dots, y_P) = \frac{\delta^{N+P} \Gamma'\{\bar{\phi}, t\}}{\delta \bar{\phi}(x_1) \dots \delta \bar{\phi}(x_N) \delta t(y_1) \dots \delta t(y_P)} \Big|_{\bar{\phi}=\eta} \quad (1.22)$$

are generated by the functional $\Gamma'\{\bar{\phi}, t\}$ defined through the Legendre transformation

$$\Gamma'\{\bar{\phi}, t\} + F'\{J,t\} = \int d^d x (J + H) \bar{\phi} \quad (1.23)$$

Up to this point our discussion of correlation functions has been confined to real space. As the Hamiltonian is invariant under a spatial translation the Greens functions simplify if we transform to momentum space and study their Fourier transforms. The translational invariance in the real space representation then manifests itself as an overall momentum conservation factor, $\delta(\Sigma_i k_i)$, multiplying the Fourier transformed Greens function. The Fourier transform of $G^{(N)}(x_1, \dots, x_N)$ is defined as

$$G^{(N)}(k_1, \dots, k_N) \delta(k_1 + \dots + k_N) = \int \frac{d^d x_1}{(2\pi)^{d/2}} \dots \int \frac{d^d x_N}{(2\pi)^{d/2}} e^{i \sum_{j=1}^N k_j \cdot x_j} G^{(N)}(x_1, \dots, x_N) \quad (1.24)$$

and for the function $G^{(N,P)}(x_1, \dots, x_N; y_1, \dots, y_P)$ we have

$$G^{(N,P)}(k_1, \dots, k_N; q_1, \dots, q_P) \delta(k_1 + \dots + k_N + q_1 + \dots + q_P) \\ = \int \frac{d^d x_1}{(2\pi)^{d/2}} \dots \int \frac{d^d x_N}{(2\pi)^{d/2}} e^{i \sum_{j=1}^N k_j \cdot x_j} \int \frac{d^d y_1}{(2\pi)^{d/2}} \dots \int \frac{d^d y_P}{(2\pi)^{d/2}} e^{i \sum_{l=1}^P q_l \cdot y_l} G^{(N,P)}(x_1, \dots, x_N; y_1, \dots, y_P) \quad (1.25)$$

Similar expressions hold for the other functions described above.

The foregoing are the exact integral expressions for the Greens functions, &c. Unfortunately, in all but the most trivial models, these integrals cannot be carried out explicitly. Therefore we must employ some approximation technique to provide ourselves with a systematic framework for the evaluation of any desired quantity. This is provided by a perturbative expansion of the correlation functions about an exactly soluble quadratic form of the Hamiltonian, \mathcal{H} . This approach is the subject of the next section.

1.3. Perturbative Expansions in Field Theory

As we remarked at the end of the previous section, the problem of evaluating Greens functions exactly in any non-trivial case is intractable. We must therefore turn to approximations, such as **perturbation theory**. The use of this technique in classical mechanics dates back to the time of Newton, and the principles apply equally to the present discussion.

Perturbation theory relies on the existence of an Hamiltonian, \mathcal{H}_0 , which differs from the Hamiltonian of the system being studied, \mathcal{H} , only "slightly", but

for which we can perform the integrals enumerated in section 1.2 exactly. The physical system functions are then obtained as power series in the difference $(\mathcal{H} - \mathcal{H}_0)$. In this section we will discuss the resulting series and use the ϕ^4 Hamiltonian,

$$\mathcal{H} = \int d^d x \left\{ \frac{1}{2} (\nabla \phi)^2 + \frac{1}{2} m_0^2 \phi^2 + \frac{g_0}{4!} \phi^4 \right\} \quad (1.26)$$

with g_0 "small", as an illustrative example. In this case the exactly soluble \mathcal{H}_0 is

$$\mathcal{H}_0 = \int d^d x \left\{ \frac{1}{2} (\nabla \phi)^2 + \frac{1}{2} m_0^2 \phi^2 \right\} \quad (1.27)$$

the so-called Gaussian, or free, theory.

Consider the general case

$$\mathcal{H} = \int d^d x \left\{ \frac{1}{2} (\nabla \phi)^2 + \frac{1}{2} m_0^2 \phi^2 + V(\phi) \right\} \quad (1.28)$$

where we shall perturb in the potential $V(\phi)$. It may be shown (Amit, 1984; Ramond, 1981) that the partition function of section (1.1) can be written in the form

$$Z\{J\} = [Z\{0\}]^{-1} e^{\left\{ -\int d^d x V\left(\frac{\delta}{\delta J}\right) \right\}} e^{\left\{ \frac{1}{2} \int d^d x d^d y J(x) G_0(x-y) J(y) \right\}} \quad (1.29)$$

where

$$G_0(x-y) = \int_{|p| < \Lambda} \frac{d^d p}{(2\pi)^d} \frac{e^{i p \cdot (x-y)}}{p^2 + m_0^2} \quad (1.30)$$

In this expression the momentum integral has a cut-off, Λ , at high p values corresponding to the maximum allowed p -vector in the Fourier decomposition of G_0 . This cut-off arises naturally when we consider the continuous field description of critical phenomena in a lattice system, where Λ is proportional to the inverse lattice spacing.

The perturbation expansion is generated by expanding the first exponential in (1.30) as a Taylor series in the potential and acting on the second exponential term with the resulting functional derivatives. Since the Greens functions $G^{(N)}$ are generated by taking N functional derivatives of $Z\{J\}$ with respect to the source, J , and then setting J equal to zero, for the result to be non-zero the derivatives must group in pairs (in all possible combinations). Corresponding to each pair of derivatives,

$$\frac{\delta}{\delta J(x)} \frac{\delta}{\delta J(y)} \quad (1.31)$$

a factor of $G_0(x-y)$ will be present in the expansion. This correspondence led Feynman to introduce a graphical representation of the series in powers of g , which has proved invaluable in the application of perturbation expansions in Field Theory. The denominator, $Z\{0\}$, in (1.29) acts to cancel all graphs not topologically connected to an exterior coordinate, i.e., one appearing in $G^{(N)}(x_1, \dots, x_N)$. The rules for constructing the graphs are:

- draw a point for every external coordinate and every interaction term; label each point by its coordinate
- for all $G_0(x-y)$ present draw a line connecting the point labelled by x to the point labelled by y .

To construct the term in the algebraic series from a Feynman graph the following rules are used (using (1.26) as an illustration)

1. for each internal point include a factor of $-g/4!$
2. for each line joining x to y include a factor of $G_0(x-y)$
3. integrate over all internal coordinates
4. multiply by $1/n!$ where n is the order of g in the expansion
5. multiply by the number of ways of constructing the graph of given topology.

The above is for an expansion in real space - the expansion of the momentum space Greens functions can be similarly represented as a graphical series. In this case each line corresponds to a factor of

$$G_0(p) = \frac{1}{p^2 + m_0^2} \quad (1.32)$$

and the overall momentum is conserved. The rules for constructing and computing the contribution of a graph to the expansion of $G^{(N)}(p_1, \dots, p_N)$ are as follows - we consider here

$$V(\phi) = \sum_r \lambda_r \phi^r \quad (1.33)$$

1. draw N external lines
2. distribute the N external momenta, p_i , about the N external lines ($N!$ possible ways of carrying this step out)
3. for each of the n_r vertices of the interaction ϕ^r draw a point at which r lines meet
4. join all lines in the graphs in pairs; label each internal line with a momentum q_j in such a way as to conserve momentum at each vertex
5. for each vertex of type r include a factor $\lambda_r/r!$
6. for each line with momentum k include a factor of $G_0(k)$
7. integrate over all internal momenta q_j , $\int d^d q_j / (2\pi^d)$
8. multiply by $1/(n_1!n_2!\dots n_r!)$
9. multiply by the number of ways of constructing the graph of given topology.

The above Feynman rules summarise the procedure for calculating $G^{(N)}(p_1, \dots, p_N)$ to all orders in perturbation theory.

If we study the graphical expansions of the other quantities defined in the previous section we discover that they fall into topologically distinct sets - hence the names associated with them, e.g, connected functions. The

expansion of $G_c^{(N)}(p_1, \dots, p_N)$ contains only graphs which are topologically connected. One particle irreducible (1PI) graphs are defined as those which cannot be separated into two disparate pieces by cutting one internal line. The vertex functions, $\Gamma^{(N)}(p_1, \dots, p_N)$, are defined as minus the sum of all 1PI graphs with N external legs. Note that by definition the external propagators $G_0(p_i)$ are not included in the vertex function. When we consider Greens functions involving the composite operator, ϕ^2 , the above rules are unchanged if we consider the term containing ϕ^2 as an interaction vertex with momentum conserved on the two incoming lines. An overall factor of $(\frac{1}{2})^P$ is included in the rules for the computation of a graph having P ϕ^2 insertions in its structure. Note here that there is no overall factor of $1/P!$ as one might expect from having P vertices.

The graphical expansion as a power series in the coupling constants can be reformulated as a systematic expansion in the number of closed loops the graphs contain. This is the technique we shall adopt throughout this thesis, and gives rise to the classification of approximations as " n^{th} -loop order"; this corresponds to an expansion about the classical theory. The lowest level, the tree approximation, corresponds to the mean field theory, first introduced by Weiss (1932), which neglects the effect of fluctuations and at this level we can recover the mean-field values of the critical exponents and amplitudes.

As an example of a calculation using the loop expansion we shall calculate the magnetic susceptibility to one-loop using the Hamiltonian of (1.26). Now

$$\chi = \frac{\partial M}{\partial H} \Big|_{H=0} \quad (1.34)$$

$$= \int d^d y \langle (\phi(y) - \langle \phi(y) \rangle) (\phi(0) - \langle \phi(0) \rangle) \rangle \quad (1.35)$$

$$= G_{\tau_c}^{(2)}(q=0) \quad (1.36)$$

$$= \left\{ \Gamma^{(2)}(q=0) \right\}^{-1} \quad (1.37)$$

so we must calculate $\Gamma^{(2)}(q=0)$ to one loop order. Applying the rules given above we obtain

$$\chi^{-1} = \Gamma^{(2)}(q=0) \quad (1.38)$$

$$= m_0^2 + \frac{1}{2} g_0 \int_{|k| < \Lambda} \frac{d^d k}{k^2 + m_0^2} \quad (1.39)$$

A second-order phase transition is signalled by the divergence of the susceptibility as the temperature, T , approaches the critical temperature, T_c . As we remarked earlier, in section (1.2), the temperature dependence enters the continuous field description through the parameter m_0 - we therefore solve $\chi^{-1} = 0$ for m_0 to obtain the critical value, m_c , at which the transition occurs. To lowest order this gives

$$m_c^2 = -\frac{1}{2} g_0 \int_{|k| < \Lambda} \frac{d^d k}{k^2} \quad (1.40)$$

Introducing the reduced temperature, τ_0 , defined through

$$\tau_0 = m_0^2 - m_c^2 \quad (1.41)$$

we have, again to lowest order,

$$\chi^{-1} = \tau_0 - \frac{1}{2} g_0 \tau_0 \int_{|k| < \Lambda} \frac{d^d k}{k^2 (k^2 + \tau_0)} \quad (1.42)$$

The integral in (1.42) converges for any dimension $d > 4$, but for $d < 4$ it has an infra-red ($k \rightarrow 0$) divergence. The dimension at which these infra-red singularities appear in thermodynamic quantities calculated in field theory is known as the **upper-critical dimension**, denoted d_c . The singularities persist to all orders in the loop expansion and must be removed by the process of **renormalisation**, the topic of the next section. Above d_c the integrals are convergent and the mean-field results are recovered; for example, (1.42) implies that for $d > 4$, $\chi \sim \tau^{-1}$, or $\gamma = 1$.

(The above manipulations are only defined if the integral has a high-momentum cut-off. This is provided in statistical physics by the inherent upper limit, Λ , reflecting the existence of an underlying physical length scale, usually the lattice spacing. In quantum field theory the integrals are also ultra-violet divergent)

We shall now turn our attentions to the handling of the divergences for dimensions less than the upper critical dimension.

1.4. Renormalisation

At the end of section (1.3) we encountered one of the main problems associated with perturbation expansions in the continuous field description of critical phenomena.

Thankfully these divergences may be handled in a systematic manner by redefining the parameters in the theory to absorb the divergences and obtain finite results. In studying phase transition physics the interesting limit is $m_0 \rightarrow 0$ with Λ fixed - in quantum field theory the limit considered is the "continuum limit", i.e., $\Lambda \rightarrow \infty$. In the latter case the integrals considered at the end of section (1.3) suffer from ultra-violet divergences for

any dimension $d > 2$ (the lower critical dimension). However, if we define

$$m^2 = m_0^2 + \frac{1}{2} g_0 \int \frac{d^d k}{k^2 + m_0^2} \quad (1.43)$$

we obtain

$$\Gamma^{(2)}(q) = q^2 + m^2 + o(g_0^2) \quad (1.44)$$

which is finite as $\Lambda \rightarrow \infty$; this is an example of mass renormalisation. The infinity has been absorbed in a redefinition of our original parameter, m_0 , which is related to our new, arbitrary parameter m by

$$m_0^2 = m^2 - \frac{1}{2} g_0 \int \frac{d^d k}{k^2 + m^2} \quad (1.45)$$

In the case of critical phenomena the integrals converge in the ultra-violet and the consequent redefinition of m_0 is unnecessary. However, renormalising the theory in such a way that the limit $\Lambda \rightarrow \infty$ is finite for all $d < d_c$ provides us with a natural description of the approach to a phase transition (and a computationally effective method of calculation (Brézin *et al*, 1974)). The presence of a short-distance cut-off is unimportant near the transition, where the physics is dominated by large length scale fluctuations, and taking $\Lambda \rightarrow \infty$ introduces corrections which are negligible in the critical region. The cut-off, Λ , on the momentum integral is one method of regularising the theory, that is, a method by which we can define a finite expression corresponding to an infinite Feynman integral in such a way that there exists a well-defined limiting procedure which recovers the original value of the Feynman integral in its domain of definition. The regularisation procedure we shall adopt is the dimensional regularisation scheme of 't Hooft and Veltman (1972). This

consists of analytically continuing the integrals in the number of space dimensions by partial integration of the integrand (Ramond,1981). Similarly, many (an infinite number in theory!) methods of renormalising a field theory are possible. The approach we use is again to follow 't Hooft and Veltman and adopt the minimal subtraction scheme, tied to dimensional regularisation. This leads naturally to the ϵ -expansion, which we discuss below. For details of this method we refer the reader to 't Hooft and Veltman (1972) and 't Hooft (1973); in the context of critical phenomena the technique is described in Lawrie (1975) and Amit (1984). We shall only sketch the main ideas here.

In the study of critical phenomena we are interested in the infra-red behaviour of our theory, i.e., the low momentum region. In the ϵ -expansion the infra-red divergences in the Feynman diagrams are forced to appear as logarithms, through an expansion such as

$$\chi^\epsilon = 1 + \epsilon \ln x + \frac{\epsilon^2}{2!} (\ln x)^2 + \dots \quad (1.46)$$

where $\epsilon = d_c - d$. This necessitates a double expansion, in the number of loops and in ϵ , to study the critical behaviour of the model.

To handle the ultra-violet divergences in the theory the 't Hooft and Veltman scheme sets the momentum cut-off to infinity, and calculates the resulting integrals in dimensional regularisation, analytically continuing in ϵ . The ultra-violet divergences then appear as poles in ϵ and the renormalisation is achieved by defining new, renormalised parameters of the theory in such a way that the Greens functions at criticality are finite as $\epsilon \rightarrow 0$, i.e., we "remove the poles in ϵ ". The details of this are to be found in Amit (1984) and Ramond (1981); in Chapters 2 and 3 of this thesis the process is illuminated by explicit calculation.

To render the vertex functions $\Gamma^{(N)}$ finite in the limit $\epsilon \rightarrow 0$ we must renormalise the coupling constant and the wavefunction by defining new quantities

$$g_R = \mu^{-\epsilon} A_1(g_0, \epsilon) \quad (1.47)$$

and

$$\phi_R = Z_\phi^{-1/2} \phi_0 \quad (1.48)$$

such that

$$\Gamma_R^{(N)}(p_i, g_R, \mu) = Z_\phi^{N/2} \Gamma^{(N)}(p_i, g_0) \quad (1.49)$$

has a finite $\epsilon \rightarrow 0$ limit. Here μ is an arbitrary momentum scale chosen to make g_R dimensionless. The functions A_1 and Z_ϕ are fixed by demanding that they minimally subtract off the poles in ϵ . A further renormalisation is necessary to render finite the vertex functions $\Gamma^{(N,P)}$. This is achieved by renormalising the temperature via the definition

$$\tau_R = \mu^{-2} Z_\phi^{-1} \tau_0 \quad (1.50)$$

and demanding that

$$\Gamma_R^{(N,P)}(p_i, q_i, g_R, \mu) = Z_\phi^P Z_\phi^N \Gamma^{(N,P)}(p_i, q_i, g_0) \quad (1.51)$$

has a finite $\epsilon \rightarrow 0$ limit. Again, this is carried out by choosing Z_ϕ^2 to minimally subtract off the poles in ϵ . The vertex function $\Gamma^{(0,2)}$ requires an additional, additive renormalisation.

These definitions are sufficient to render all the quantities calculated in our theory finite outside the critical region if we define a renormalised field, H_R , a renormalised source, J_R , and a renormalised magnetisation, M_R , by

$$H_R = Z_\phi^{-1/2} H_0 \quad (1.52)$$

$$M_R = \mu^{\frac{\epsilon}{2}-1} Z_\phi^{-1/2} M_0 \quad (1.53)$$

and

$$J_R = Z_\phi^{-1/2} J_0 \quad (1.54)$$

The method of approach that was adopted for the calculations detailed later in this thesis was to calculate the desired function in the original, bare theory and to substitute in the renormalised values at the end of the calculation, knowing that we are guaranteed finite results, thanks to the work of 't Hooft and Veltman.

In the next section we turn our attention to the specific area of random systems in critical phenomena and give a brief outline of this wide ranging topic of current research.

1.5. Random Systems

In the study of random systems we are primarily interested in the effect on the critical behaviour of a system of introducing disorder. This disorder is described by a wide variety of terms (disorder, amorphous, defects, noise) depending on the context of the discussion and in recent years the subject

area has generated a vast amount of literature. The motivation behind studying disordered systems is the belief that they are a closer approximation to the real, physical systems than homogeneous, perfect crystals. A review of earlier work in the field may be found in Balian *et al.* (1979), whilst Stinchcombe (in Domb and Lebowitz, 1983) gives an overview of the theory pertaining to dilute magnetism, mainly from the real-space viewpoint. This latter article contains a comprehensive set of references in the general field of dilute magnetism. The brief resumé comprising this section will concentrate on the static properties of substitutionally diluted magnets since this is most relevant to the current work.

The term **diluted magnet** is used here to refer to a magnetic system diluted with non-magnetic ions. We consider the case of substitutional disorder in which a certain fraction, $(1 - p)$, of the magnetic ions are replaced by non-magnetic atoms. This disorder may be classified as **quenched** or **annealed**; in the former, the configurational averages over the random variables are independent of the thermal averages, and in the latter, the disorder variables are in thermal equilibrium with the other degrees of freedom in the system. Substitutional disorder can also be of either **site** or **bond** type - in site-disorder the randomness is associated with the atoms (**site-dilution**) whereas in the case of bond-disorder the randomness is associated with the exchange constants between the ions (**bond-dilution**). The expectation is that the two types of randomness lie in the same universality class. Here we are interested in the first case, that of site-dilution.

In quenched, dilute magnets, in addition to the thermodynamic phase transitions which can occur, there also exists the purely geometric transition associated with **percolation** (see the article by Stinchcombe and references

therein). For concentrations of magnetic ions, p , less than a threshold value, p_c , a phase transition cannot occur because there is no infinite cluster of connected ions to support long-range order. However, for concentrations $p > p_c$ this infinite cluster exists and long-range ordering can occur. The dependence on p of the critical temperature at which this ordering occurs is shown schematically in Figure 1-1. Since the transition is of second order in simple magnets the thermal behaviour at criticality is characterised by a set of critical exponents. These are expected to be the same as for the pure system if the pure system specific heat exponent, α , is negative, and may be modified otherwise (Harris,1974). This is known as the **Harris criterion** and can be stated for the Ising model in the language of the renormalisation group as

"The Ising fixed point is stable if the specific heat exponent of the corresponding Ising model is negative"

(Amit,1984)

This has been proved to all orders in the ϵ -expansion by Jug and Carneiro (1982).

The three-dimensional (pure) Ising model has $\alpha > 0$ so the dilution may modify the transition and lead to new exponent values. Khmel'nitski (1975) summed the parquet diagrams for the random Ising model and obtained a new random fixed point of $o(\epsilon^{1/2})$. So far, this is the only example of an $o(\epsilon^{1/2})$ fixed point to be found; it arises due to the β functions being proportional at lowest order (given a suitable definition of the coupling constants). Jayaprakash and Katz (1982) calculated higher order corrections to the β functions and proved the stability of this fixed point, which is therefore expected to characterise the critical behaviour of the random Ising model.

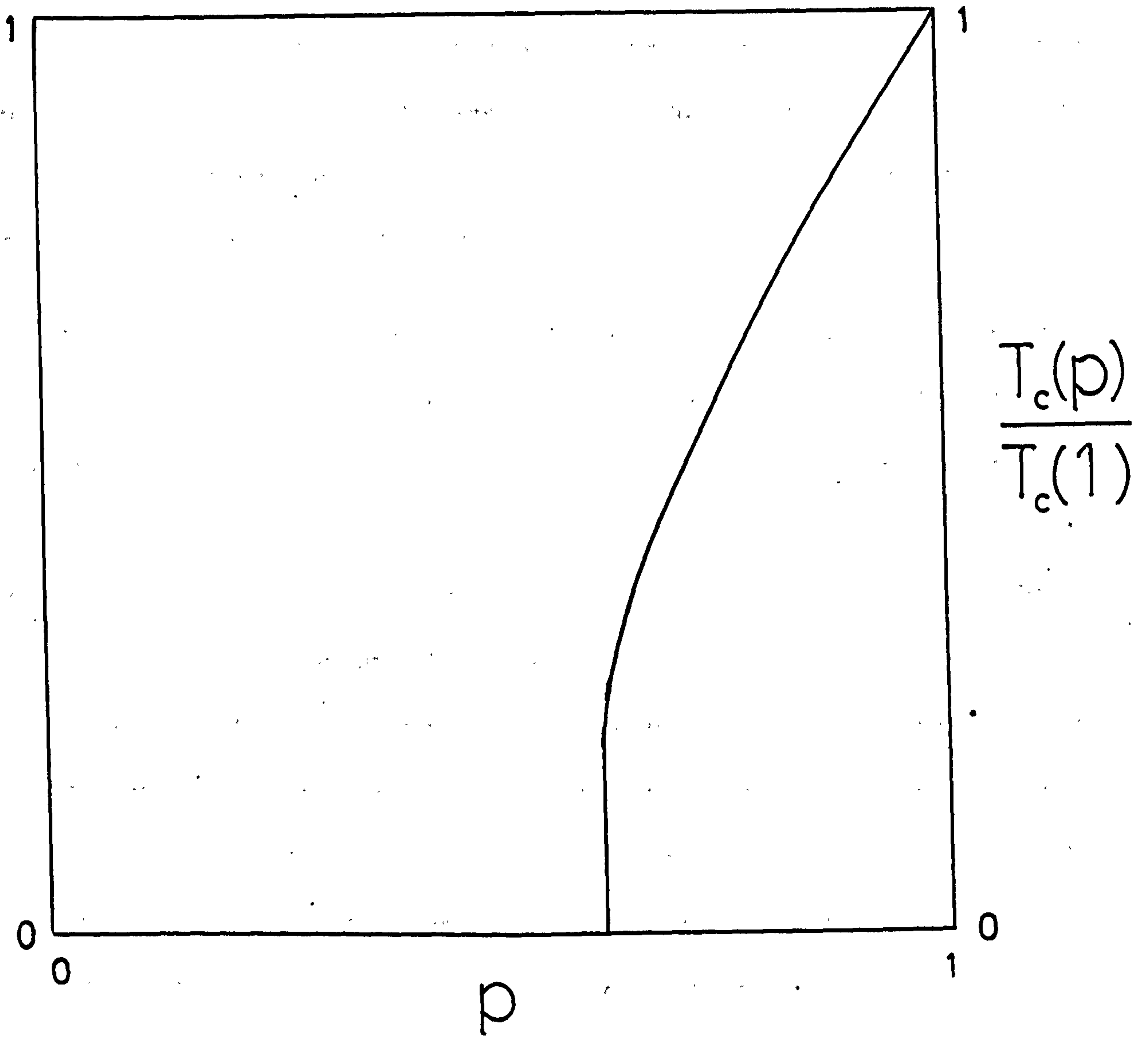


Figure 1-1: Schematic phase diagram of a dilute magnet

These authors calculated the exponents η and ν to second order in an $\epsilon^{1/2}$ -expansion, and Newlove (1983) has derived the first order results for the universal amplitude ratios at criticality. This latter calculation is extended to two-loops for the susceptibility amplitude ratio in the present work.

1.6. Research Projects

The remainder of this thesis contains a study of the critical behaviour of a particular random system, the random site-diluted Ising model, using the techniques of field theory detailed in this introduction and a Monte Carlo simulation on a highly parallel computer.

Neutron scattering experiments to study the critical behaviour of a site-diluted Ising magnet were carried out by Birgeneau *et al* (1983). Results for the critical amplitude ratios were markedly different from experiments on the pure system; this motivated Newlove (1983) to perform a one-loop ϵ -expansion for these quantities. Again, these analytic results differed significantly from the results of a one-loop treatment for the pure case (Brézin *et al*, 1974). In Chapter 2 of this thesis we derive a two loop expression for the susceptibility amplitude ratio at criticality by a field theoretic calculation of the equation of state from the replicated Hamiltonian. This is achieved by expanding the transverse propagator as a power series in n , the number of replicas, about the longitudinal propagator. This enables us to identify and discard early on in the calculation terms which vanish in the limit $n \rightarrow 0$.

As was initially pointed out by Grinstein, Ma and Mazenko (1977), the introduction of dilution into the Ising model gives rise to a new, static correlation function, $C^{(s)}(q)$, because of the fluctuations in the local, quenched magnetisation. Aharony and Pelcovits (1985) showed that this function has

important consequences for the interpretation of neutron scattering measurements of the susceptibility amplitude ratio, and calculated the correction to lowest order. In Chapter 3 we detail a field theory calculation of $C^{(s)}(q=0)$ to obtain the next order term in the ϵ -expansion, by employing an extension of the replica trick to embrace two sets of replica spins.

Chapter 4 reports the details of a Monte Carlo simulation of the site-diluted Ising model, designed to study the effects of dilution on the critical behaviour of the system. A study of the scaling properties of sub-block magnetisations, as suggested by Binder (1981), is used to extract the critical temperature and to obtain estimates for the critical exponents. The method is applied initially to the pure Ising model for verification and then the diluted case is treated. The observed limiting behaviour of the cumulant studied is discussed with reference to the influence of the competing fixed points in the model.

2.1. Introduction

In this chapter we shall be concerned with the effect of the introduction of quenched impurities on the critical amplitudes of a system. Our attention will be confined to the case of site-dilution, where the sites of a regular lattice are occupied by a magnetic ion with probability p , and a non-magnetic ion with probability $1 - p$. In such a case, a phase transition is only possible if there exists an infinite, connected cluster of spins. Below a critical value of the concentration, say p_c , there is no such cluster and the critical temperature, $T_c(p)$, is zero, whilst for $p > p_c$, $T_c(p)$ is greater than zero and a phase transition may occur. This is the purely geometric phenomenon of percolation. The reader is referred to the article by Shante and Kirkpatrick (1971) for a review.

The remainder of this chapter is laid out in the following way. In section 2.2 we describe the random Ising model and some experimental results on a realisation of it in nature, $\text{Fe}_{1-x}\text{Zn}_x\text{F}_2$ (Birgeneau *et al*, 1976). In section 2.3 we introduce the Replica Trick for calculating averages over the random variables in the model. The universal form of the equation of state is discussed in section 2.4. Section 2.5 describes a one-loop calculation of the equation of state from which we extract a value for the universal ratio of susceptibility amplitudes. This section is included as motivation for a two-loop calculation of the amplitude ratio and to introduce the techniques which are essential in the higher order calculation which is presented in section 2.6. Conclusions are contained in section 2.7.

2.2. The Random Ising Model

In this section we describe a simple model exhibiting a phase transition and discuss the effects of the addition of quenched impurities on the critical behaviour of the system. The model we shall consider is the random, site-diluted Ising model.

In the Ising model magnetic ions occupy the sites of a square lattice and interact through nearest-neighbour interactions. The Hamiltonian describing the system is

$$\beta H = -\frac{1}{2} \sum_{\langle ij \rangle} J_{ij} s_i s_j, \quad s_i = \pm 1, \quad \beta = \frac{1}{kT} \quad (2.1)$$

where s_i is the spin at site i , $J_{ij} = J$ is the interaction strength between sites i and j , and the summation is over nearest neighbouring sites. The model has been extensively studied and an exact solution is known in two dimensions (Onsager, 1944).

Site-dilution is introduced by associating an occupation number, p_i , with the site i , where $p_i=1$ if the site contains a magnetic ion ("occupied") and $p_i=0$ if the site contains a non-magnetic impurity ("vacant"). The probability of any given site being occupied is p , $0 < p < 1$, independent of the state of all other sites and the occupation numbers have a distribution described by the function

$$P(p_i) = p \delta(p_i - 1) + (1-p) \delta(p_i) \quad (2.2)$$

This is the random, site-diluted Ising model. The Hamiltonian for this system is

$$\beta \mathcal{H}(\{p_i, s_i\}) = -\frac{1}{2} \sum_{\langle ij \rangle} J_{ij} p_i p_j s_i s_j \quad (2.3)$$

and the partition function is given by

$$Z(\{p_i\}) = \int \prod_i ds_i e^{-\mathcal{H}(\{p_i, s_i\})} \quad (2.4)$$

The quenched impurity average is taken over the free energy of the system

$$\bar{F} = -\frac{1}{\beta} \int \prod_i dp_i P(p_i) \ln Z(\{p_i\}) \quad (2.5)$$

where the bar indicates an average with respect to the impurity distribution. In the following we have absorbed the factor of β into a redefinition of the coupling in the Hamiltonian, (2.3).

The partition function may be rewritten in terms of a continuous field description by use of the Hubbard-Stratonovich identity (see section 1.2). The resulting partition function is

$$Z(\psi) = \int \mathcal{D}\phi e^{-\mathcal{H}(\{\phi, \psi, J_0\})} \quad (2.6)$$

with Hamiltonian

$$\begin{aligned} \mathcal{H}(\{\phi, \psi, J_0\}) = \int d^d x \left\{ \frac{1}{2} (\nabla \phi(x))^2 + \frac{1}{2} r_0 \phi(x)^2 + \frac{v_0}{4!} \phi(x)^4 \right. \\ \left. + \frac{1}{2} \psi(x) \phi(x)^2 - J_0(x) \phi(x) \right\} \end{aligned} \quad (2.7)$$

where the spins in the lattice description are replaced by the continuous field ϕ . $\psi(x)$ is a random field with probability distribution function satisfying

$$\int \psi(x) \psi(x') P(\psi) \mathcal{D}\psi = \Delta \delta(x-x') \quad (2.8)$$

and we have we introduced the source term $J(x)$ which couples linearly to ϕ . This was first written down by Grinstein and Luther (1976). The temperature dependence enters through the variable $r_0=r_0(T)$. The field theoretic description was shown to have an order $\sqrt{\epsilon}$ fixed point by Khmel'nitski (1975), the stability of which was proved by Jayaprakash and Katz (1982).

To calculate quantities in this theory we have to perform the impurity average over the free energy. The replica formalism allows us to carry out this step.

2.3. The Replica Trick

In systems containing quenched impurities, the mathematically non-trivial impurity average is taken over the free energy, $F = -kT \ln Z$. In the case of a Gaussian distribution of impurities this average can be performed explicitly by employing the replica, or $n=0$, trick (Grinstein and Luther, 1976; Edwards and Anderson, 1975; Emery, 1975).

The replica trick is based on the identity

$$\ln Z = \lim_{n \rightarrow 0} \frac{Z^n - 1}{n} \quad (2.9)$$

and the quenched impurity average over the free energy becomes

$$\overline{F\{\gamma\}} = \int D\psi P(\psi) \ln Z(\{\psi\}) \quad (2.10)$$

$$= \lim_{n \rightarrow 0} \frac{1}{n} \int D\psi P(\psi) \{Z^n(\{\psi\}) - 1\} \quad (2.11)$$

assuming we can swap the orders of the limit and integration. The validity of

this has never been placed on a sound mathematical footing and it has been shown to fail to reproduce the correct results in some instances (Verbaarschot and Zirnbauer, 1985). Our model does not seem to have any of the features which have been postulated for the breakdown of the replica trick.

If we assume a Gaussian probability distribution for ψ

$$P(\psi) = \frac{1}{(2\pi\Delta)^{N/2}} e^{-\int \frac{\psi^2(x)}{2\Delta} dx} \quad (2.12)$$

where we will let $N \rightarrow \infty$ at the end, then $P(\psi)$ satisfies

$$\int P(\psi) D\psi = 1 \quad (2.13)$$

$$\int \psi P(\psi) D\psi = 0 \quad (2.14)$$

$$\int \psi(x) \psi(x') P(\psi) D\psi = \Delta \delta(x-x') \quad (2.15)$$

and

$$\begin{aligned} \overline{F(\phi, J_0)} = \lim_{n \rightarrow 0} \int \prod_{\alpha=1}^n D\phi^\alpha \exp \left\{ - \int d^d x \left[\frac{1}{2} \sum_{\alpha=1}^n (\nabla \phi^\alpha)^2 + \frac{1}{2} t_0 \sum_{\alpha=1}^n \phi^\alpha(x)^2 \right. \right. \\ \left. \left. + \frac{v_0}{4!} \sum_{\alpha=1}^n \phi^\alpha(x)^4 + \frac{u_0}{4!} \left(\sum_{\alpha=1}^n \phi^\alpha(x)^2 \right)^2 - \sum_{\alpha=1}^n J_0^\alpha(x) \phi^\alpha(x) \right] \right\} \quad (2.16) \end{aligned}$$

where $u_0 = -3\Delta$.

The Hamiltonian may be written more compactly in vector notation as

$$\begin{aligned} \mathcal{H} = \int d^d x \left\{ \frac{1}{2} (\nabla \underline{\phi}(x))^2 + \frac{1}{2} t_0 \underline{\phi}(x)^2 + \frac{v_0}{4!} \sum_{\alpha=1}^n \phi^\alpha(x)^4 \right. \\ \left. + \frac{u_0}{4!} (\underline{\phi}(x)^2)^2 - \underline{J}_0(x) \cdot \underline{\phi}(x) \right\} \quad (2.17) \end{aligned}$$

with the definitions

$$\underline{\phi}(x) = (\phi^1(x), \phi^2(x), \dots, \phi^n(x)) \quad (2.18)$$

$$(\underline{\phi}(x))^2 = \sum_{\alpha=1}^n \phi^\alpha(x)^2 \quad (2.19)$$

$$(\nabla \underline{\phi}(x))^2 = \sum_{\alpha=1}^n (\nabla \phi^\alpha(x))^2 \quad (2.20)$$

In this form it is recognisable as being the Hamiltonian of an n-component spin with a cubic anisotropy term (see Amit (1984) for a general discussion). The calculations detailed in the remainder of this thesis use this Hamiltonian as their starting point.

2.4. Universal Form of the equation of State

The renormalisation of a theory can be carried out in many different schemes as was indicated in section 1.4. However, since the different renormalised theories all describe the same underlying physical model they must be related by a group of transformations. The expression of this group of transformations in differential equation form is embedded in the renormalisation group equations. These describe how vertex functions behave under a change in the scale of the momenta. At a fixed point in coupling constant space, where the β functions are zero, scaling behaviour of the Greens functions is found, leading to identification of the universal critical exponents, η and ν , and hence, by the scaling laws, all the other exponents of the theory.

As the renormalised equation of state is a sum of renormalised vertex functions of the same type, it immediately follows that the equation of state satisfies a renormalisation group equation, viz.,

$$\left\{ \mu \frac{\partial}{\partial \mu} + \beta(g) \frac{\partial}{\partial g} - \frac{1}{2} \gamma_{\phi}(g) \left(1 + M \frac{\partial}{\partial M} \right) - \gamma_{\phi^2} t \frac{\partial}{\partial t} \right\} H(t, M, \mu, g) = 0 \quad (2.21)$$

where H is the external field, t is the reduced temperature, M , the magnetisation, μ , the momentum scale and g , the coupling constant. This can be solved by the method of characteristics and at the fixed point has the solution

$$H(t, M, \mu, g^*) = \mu^{1/2} h\left(\mu M^{2/2}, \mu t^{\frac{1}{\nu^{-1}-2}}\right) \quad (2.22)$$

where we have written $\gamma_{\phi}(g^*) = \eta$, and $\gamma_{\phi^2}(g^*) = \nu^{-1} - 2$. Dimensional analysis allows us to write this in a form in which the function h depends only on dimensionless ratios and all the dimensional behaviour is explicitly extracted as a prefactor. Introducing p as a momentum scale we obtain

$$H(t, M, \mu) = \rho^{\frac{d+2-\eta}{2}} \mu^{\eta/2} h\left(\frac{\mu}{\rho} \left(\frac{M}{\rho^{d/2}}\right)^{2/\eta}, \frac{\mu}{\rho} \left(\frac{t}{\rho^2}\right)^{\frac{1}{\nu^{-1}-2}}\right) \quad (2.23)$$

and choosing p such that the first factor in h is 1 we are lead to the equation

$$H(t, M, \mu) = \mu^{\frac{d+2}{2}} \left[\frac{M}{\mu^{d/2}} \right]^{\frac{d+2-\eta}{d-2+\eta}} h\left[\frac{t}{\mu^2} \left(\frac{M}{\mu^{d/2}} \right)^{-\frac{2}{\nu(d-2+\eta)}} \right] \quad (2.24)$$

Comparing with the scaling form of the equation of state conjectured by Widom (1965)

$$h = M^{\delta} f\left(\frac{t}{M^{1/\nu}}\right) \quad (2.25)$$

we can make the identifications

$$\delta = \frac{d+2-\eta}{d-2+\eta} \quad (2.26)$$

$$\beta = \frac{\nu}{2} (d-2+\eta) \quad (2.27)$$

As the general form of the renormalisation group equation in the critical region admits only two independent, universal critical exponents, it follows that there are only two independent amplitudes in the theory. However, these are non-universal, although it is possible to construct universal combinations of them. The universal combinations of main interest are given in Amit (1984).

In the remainder of this chapter we shall employ the techniques described in outline in Chapter 1 to calculate the susceptibility amplitude ratio in the epsilon expansion to order two-loops.

In the next section we calculate the equation of state, and hence the susceptibility amplitude ratio, C_+/C_- , to one-loop.

2.5. One-Loop expansion of Susceptibility Amplitude Ratio

In this section we calculate the equation of state to one-loop order in the ϵ -expansion using a technique due to Brézin, Wallace and Wilson (1972). From the renormalised equation of state the universal ratio of susceptibility amplitudes above and below T_c can be derived in a very efficient manner.

The approach is to shift the value of the field ϕ by its expectation value in the ordered state and perform the perturbation expansion in terms of the new, shifted field

$$\bar{\Phi} = \phi - \langle \phi \rangle \quad (2.28)$$

(Wallace, in Domb and Green, 1976). This removes the so-called "tadpole" diagrams from the expansion. The equation of state is then defined by the condition

$$\langle \bar{\Phi} \rangle = 0 \quad (2.29)$$

The first stage is therefore to find the expectation value of the field ϕ below T_c by solving the Euler-Lagrange equations simultaneously for all n replicas. Using this procedure the ordered phase is found to be

$$\langle \phi^\alpha \rangle = M_0 \quad \alpha = 1, \dots, n \quad (2.30)$$

i.e., all the replica fields have the same expectation value. This should not be surprising as we have a *permutation* symmetry amongst the replicas in the Lagrangian. If we had assumed that one replica had expectation value M_0 , and all others zero, we would have found that the arguments of some of the logarithms in the calculation were negative; this thermodynamic instability is traceable to the coupling constant, $u_0 = -3\Delta$, being negative.

In the random Ising Hamiltonian we therefore rotate the coordinate system until the 1 direction lies along the body diagonal of the n -dimensional hypercube and then shift the field in the 1 direction by M_0 to obtain new fields $\bar{\Phi}$, such that

$$\underline{\phi} = (\bar{\Phi}_1 + n^{1/2} M_0) \underline{e}_1 + \sum_{j=2}^n \bar{\Phi}_j \underline{e}_j \quad (2.31)$$

$$\equiv (\bar{\Phi}_{||} + n^{1/2} M_0) \underline{e}_1 + \bar{\Phi}_{\perp} \quad (2.32)$$

where the $\{e_i\}$ form a complete, orthonormal set. The $\{e_i\}$ satisfy

$$\underline{e}_i = n^{-1/2} (1, 1, \dots, 1) \quad (2.33)$$

$$\underline{e}_i \cdot \underline{e}_j = \sum_{\alpha=1}^n e_i^\alpha e_j^\alpha = \delta_{ij} \quad (2.34)$$

$$\sum_{\alpha=1}^n e_i^\alpha = 0 \quad i \neq 1 \quad (2.35)$$

$$\sum_{i=2}^n e_i^\alpha e_i^\beta = \delta^{\alpha\beta} - \frac{1}{n} \quad (2.36)$$

and are in fact the set of vectors which define the n vertices of an hypertetrahedron in $n-1$ dimensional space (Wallace and Zia, 1975). Defining

$$\underline{M}_0 = M_0 (1, 1, \dots, 1) = n^{1/2} M_0 \underline{e}_1 \quad (2.37)$$

$$\underline{H}_0 = H_0 (1, 1, \dots, 1) = n^{1/2} H_0 \underline{e}_1 \quad (2.38)$$

the Hamiltonian in the presence of a field H_0

$$\mathcal{H} = \int d^d x \left\{ \frac{1}{2} (\nabla \Phi)^2 + \frac{1}{2} t_0 \Phi^2 + \frac{u_0}{4!} (\Phi^2)^2 + \frac{v_0}{4!} \sum_{\alpha=1}^n (\Phi_\alpha)^4 - \underline{H}_0 \cdot \underline{\Phi} \right\} \quad (2.39)$$

becomes in terms of the shifted fields Φ

$$\begin{aligned}
\mathbb{H} = \int d^d x \{ & \frac{1}{2} (\nabla \Phi_{||})^2 + \frac{1}{2} (\nabla \Phi_{\perp})^2 + \frac{1}{2} (t_0 + \frac{1}{2} u_0 n M_0^2 + \frac{1}{2} v_0 M_0^2) \Phi_{||}^2 \\
& + \frac{1}{2} (t_0 + \frac{1}{6} u_0 n M_0^2 + \frac{1}{2} v_0 M_0^2) \Phi_{\perp}^2 + [(t_0 + \frac{1}{6} u_0 n M_0^2 + \frac{1}{2} v_0 M_0^2) n^{\mu} M_0 - n^{\mu} H_0] \Phi_{||} \\
& + \frac{1}{6} u_0 n^{\mu} M_0 \Phi_{||} (\Phi_{||}^2 + \Phi_{\perp}^2) \\
& + \frac{1}{6} v_0 n^{\mu} M_0 (n^{\nu} \Phi_{||}^3 + 3 n^{\nu} \Phi_{||} \Phi_{\perp}^2 + n^{-1/2} \sum_{i,j,k=2}^n a_{ijk} \Phi_{\perp}^i \Phi_{\perp}^j \Phi_{\perp}^k \\
& + \frac{u_0}{4!} (\Phi_{||}^4 + \Phi_{||}^2 \Phi_{\perp}^2 + (\Phi_{\perp}^2)^2) \\
& + \frac{v_0}{4!} (n^{\nu} \Phi_{||}^4 + 6 n^{\nu} \Phi_{||}^2 \Phi_{\perp}^2 + 4 n^{-1/2} \Phi_{||} \sum_{i,j,k=2}^n a_{ijk} \Phi_{\perp}^i \Phi_{\perp}^j \Phi_{\perp}^k + \sum_{i,j,k,l=2}^n b_{ijkl} \Phi_{\perp}^i \Phi_{\perp}^j \Phi_{\perp}^k \Phi_{\perp}^l) \} \quad (2.40)
\end{aligned}$$

where

$$a_{ijk} = \sum_{\alpha=1}^n e_i^{\alpha} e_j^{\alpha} e_k^{\alpha} \quad (2.41)$$

$$b_{ijkl} = \sum_{\alpha=1}^n e_i^{\alpha} e_j^{\alpha} e_k^{\alpha} e_l^{\alpha}, \quad i, j, k, l = 2, \dots, n \quad (2.42)$$

and we have dropped irrelevant constant terms. This equation is identical to Aharony (1974) apart from a rescaling of M_0 , H_0 , u_0 and v_0 . The equation of state now follows from the requirement that $\langle \Phi_{||} \rangle = 0$ (the relations $\langle \Phi_i \rangle = 0$, $i = 2, \dots, n$ are trivially satisfied due to the orthonormality of the basis vectors and the definitions of the tensors a_{ijk} and b_{ijkl}).

Perusal of the above Hamiltonian reveals the presence of two bare masses

$$\Gamma_{||} = t_0 + \frac{1}{2} v_0 M_0^2 + \frac{1}{2} u_0 n M_0^2 \quad (2.43)$$

$$\Gamma_{\perp} = t_0 + \frac{1}{2} v_0 M_0^2 + \frac{1}{6} u_0 n M_0^2, \quad (n-1 \text{-fold degenerate}) \quad (2.44)$$

and therefore two propagators

$$G_{||}^{-1}(q) = q^2 + \Gamma_{||} \quad (2.45)$$

$$G_{\perp}^{-1}(q) = q^2 + \Gamma_{\perp} \quad (2.46)$$

in the model. For later convenience we define the variable b by the equation

$$b = t_0 + \frac{1}{2} v_0 M_0^2 \quad (2.47)$$

We proceed with the renormalisation using the techniques of dimensional regularisation and minimal subtraction developed by 't Hooft and Veltman (1972). It is sufficient to renormalise the theory above T_c to obtain finite Greens functions in the ordered phase (Amit, 1984). The renormalisation is further simplified by noting that any graph containing a first order self-energy insertion vanishes at criticality, since integration of the loop momentum yields a factor of the reduced temperature multiplying the graph.

The graphs contributing to $\langle \Phi_{||} \rangle = 0$ to one loop are given in Figure 2-1. To zeroth order we have

$$0 = - \left\{ \left(t_0 + \frac{1}{6} u_0 n M_0^2 + \frac{1}{6} v_0 M_0^2 \right) n^2 M_0 - n^{1/2} H_0 \right\} \quad (2.48)$$

$$\Rightarrow \frac{H_0}{M_0} = t_0 + \frac{1}{6} u_0 n M_0^2 + \frac{1}{6} v_0 M_0^2 \quad (T < T_c) \quad (2.49)$$

To lowest order we can just replace the bare quantities (2.49) by their renormalised counterparts to obtain a renormalised equation of state, viz.,

$$\frac{H_R}{M_R} = \mu^2 \left\{ t_R + \frac{1}{6} (u_R n + v_R) M_R^2 \right\} \quad (2.50)$$

where the subscript R denotes a dimensionless, renormalised quantity. All the dimensional dependence has been extracted using dimensional analysis and is

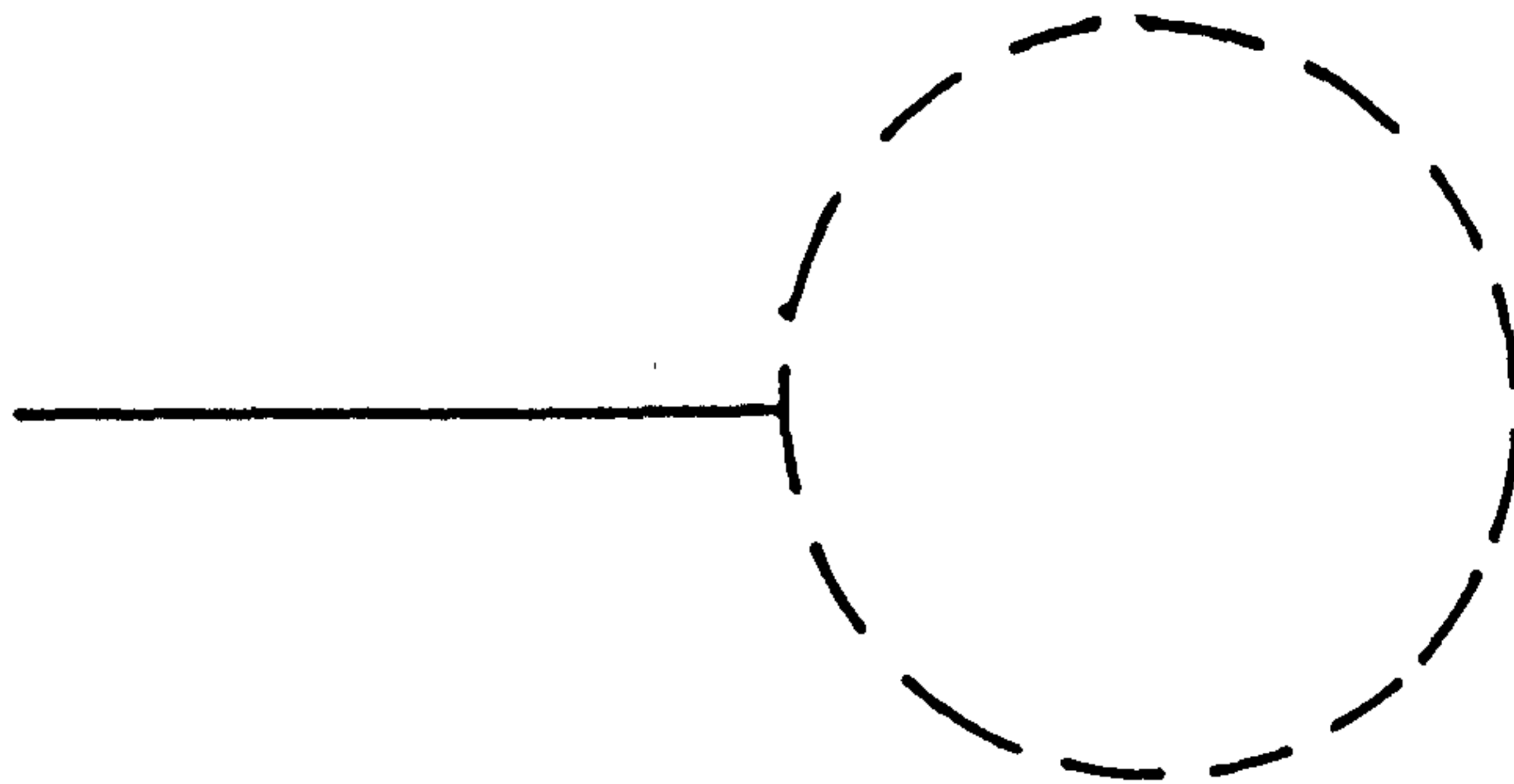
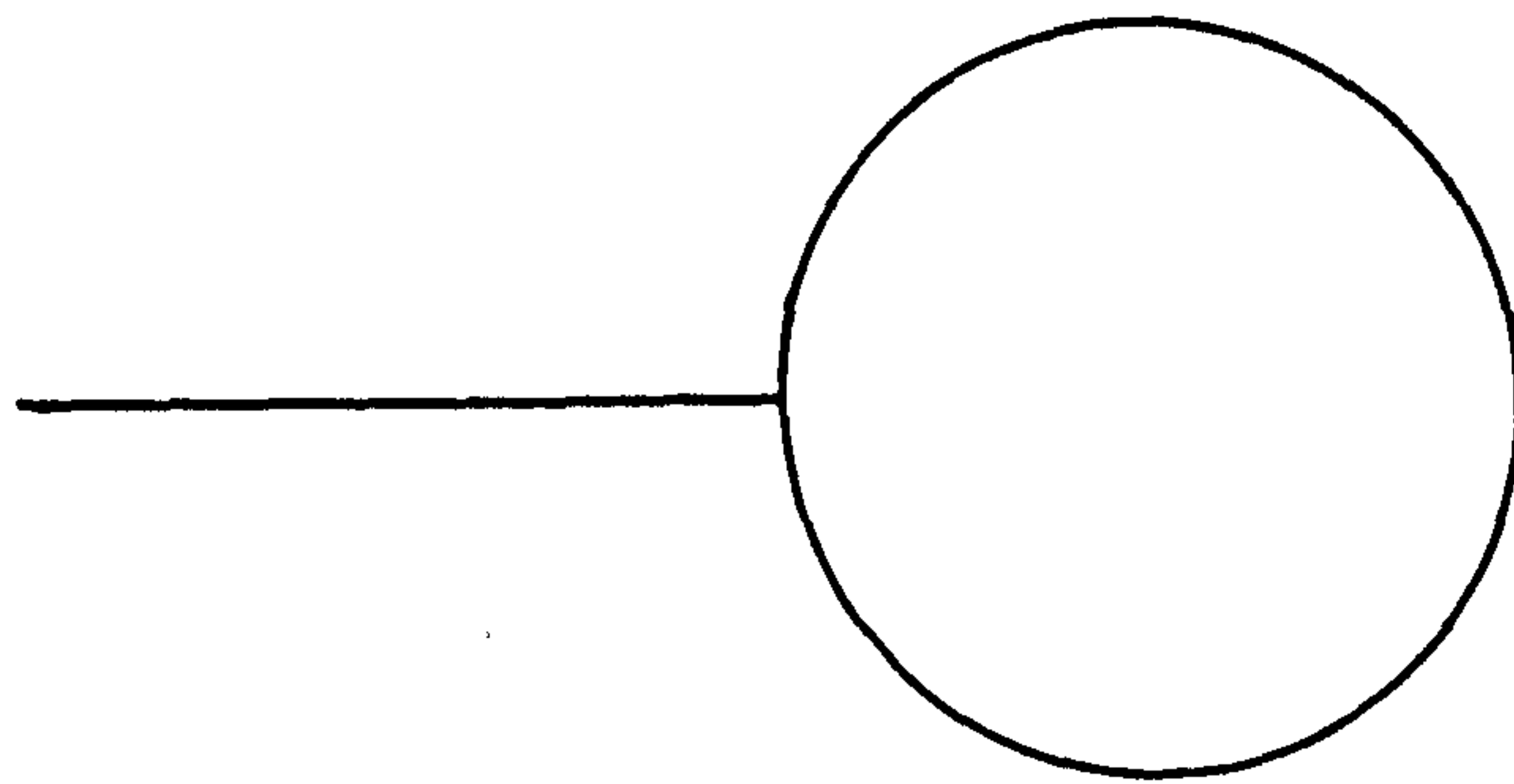


Figure 2-1: Graphs in expansion of $\langle \phi_{11} \rangle$ to one loop

explicitly shown in the momentum scale prefactor.

We now carry out the prescription outlined in section 1.4 to calculate a renormalised equation of state to one loop level. Above T_c the Hamiltonian may be written

$$\mathcal{H} = \int d^d x \left\{ \frac{1}{2} (\nabla \phi)^2 + \frac{1}{2} t_0 \phi^2 + \frac{1}{4!} \sum_{i,j,k,l=1}^n (u_0 S_{ijkl} + v_0 F_{ijkl}) \phi_i \phi_j \phi_k \phi_l \right\} \quad (2.51)$$

where the tensors S_{ijkl} and F_{ijkl} are defined as

$$S_{ijkl} = \frac{1}{3} (\delta_{ij} \delta_{kl} + \delta_{ik} \delta_{jl} + \delta_{il} \delta_{jk}) \quad (2.52)$$

$$F_{ijkl} = \delta_{ij} \delta_{kl} \delta_{ik} \quad (2.53)$$

The Feynman diagrams thus have two types of vertex present and a tensorial factor associated with each graph - by this we mean that the internal replica indices in the graphs are summed over. We denote an S vertex as a circle and an F vertex as a square.

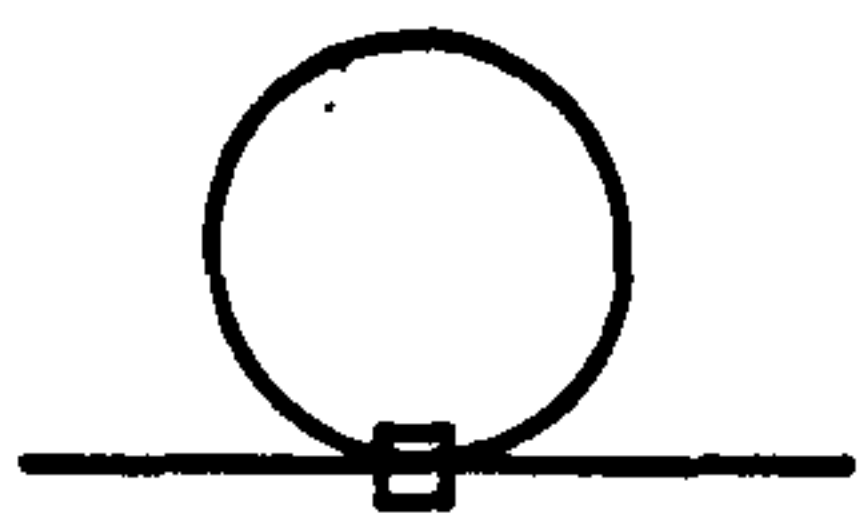
Mass Renormalisation

Above T_c the two point vertex function is given by the graphs in Figure 2-2. These give, for the bare quantity

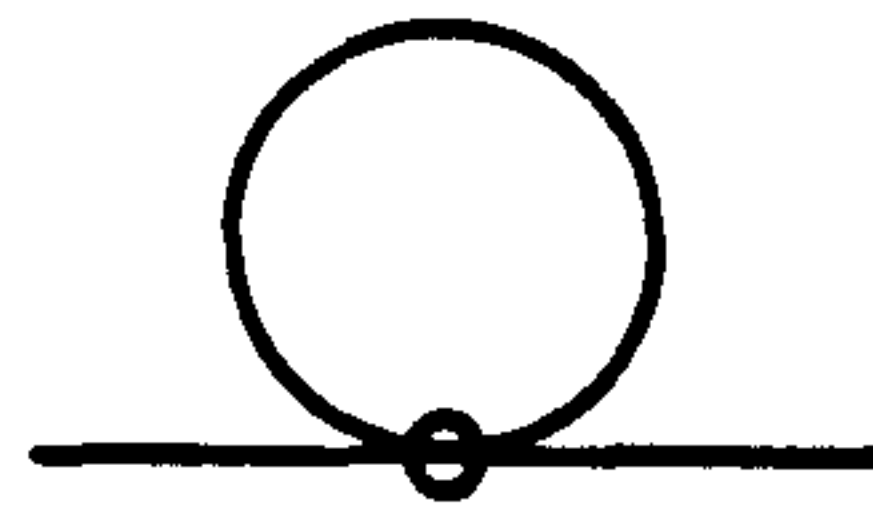
$$\Gamma^{(2)} = q^2 + t_0 + 12 \cdot \frac{1}{4!} \cdot \left\{ \frac{1}{3} u_0 (n+2) + v_0 \right\} \int \frac{d^d k}{k^2 + t_0} \quad (2.54)$$

$$= q^2 + t_0 \left\{ 1 - \frac{1}{2\epsilon} \frac{S_d}{(2\pi)^d} \left(\frac{1}{3} (n+2) u_0 + v_0 \right) \right\} + \mathcal{O}(\epsilon) \quad (2.55)$$

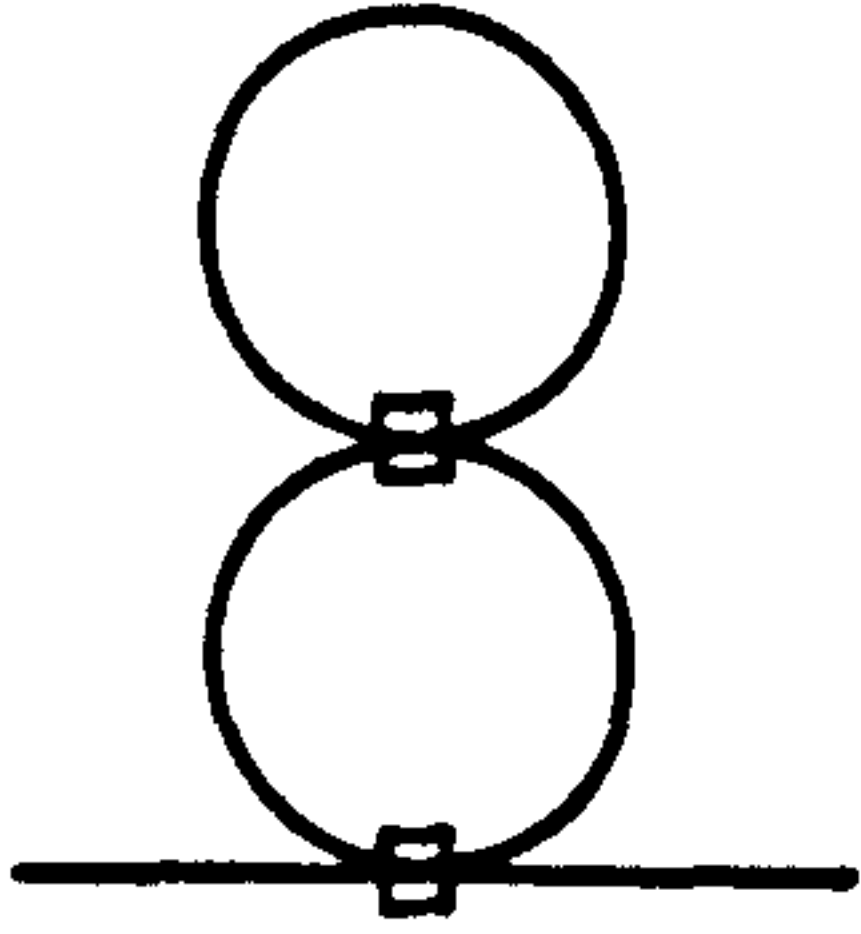
where S_d is the area of the unit sphere in d -dimensions. In the rest of this chapter the factors of $S_d / (2\pi)^d$ will be omitted for ease of writing - they are



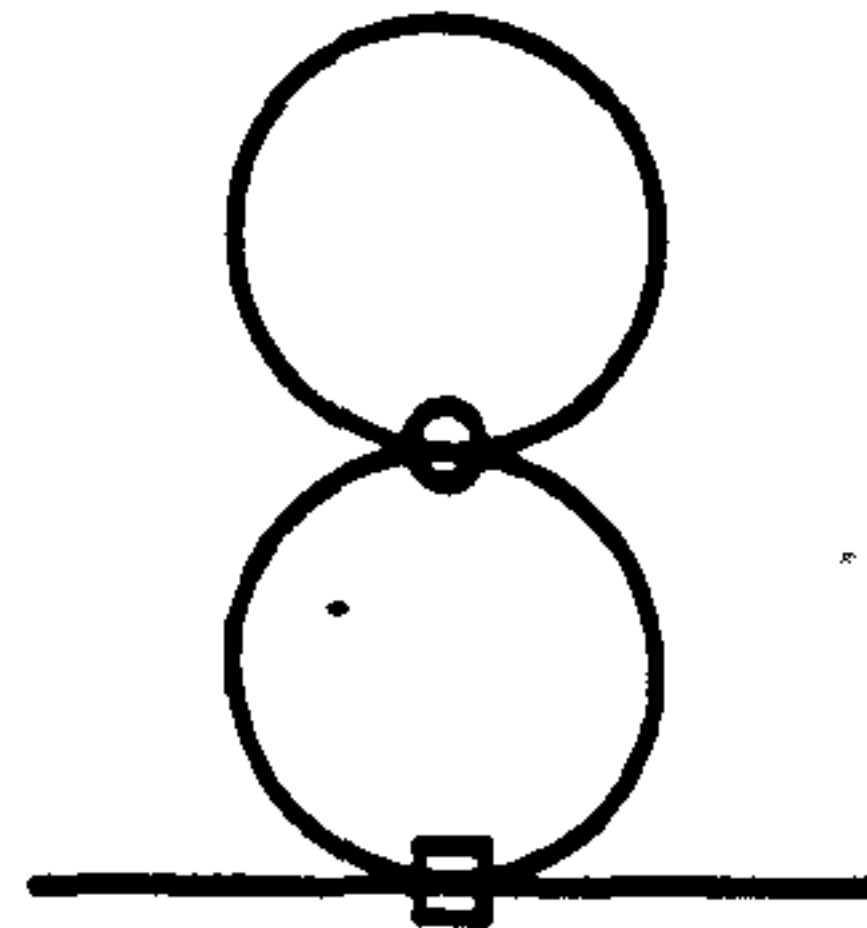
$v/2$



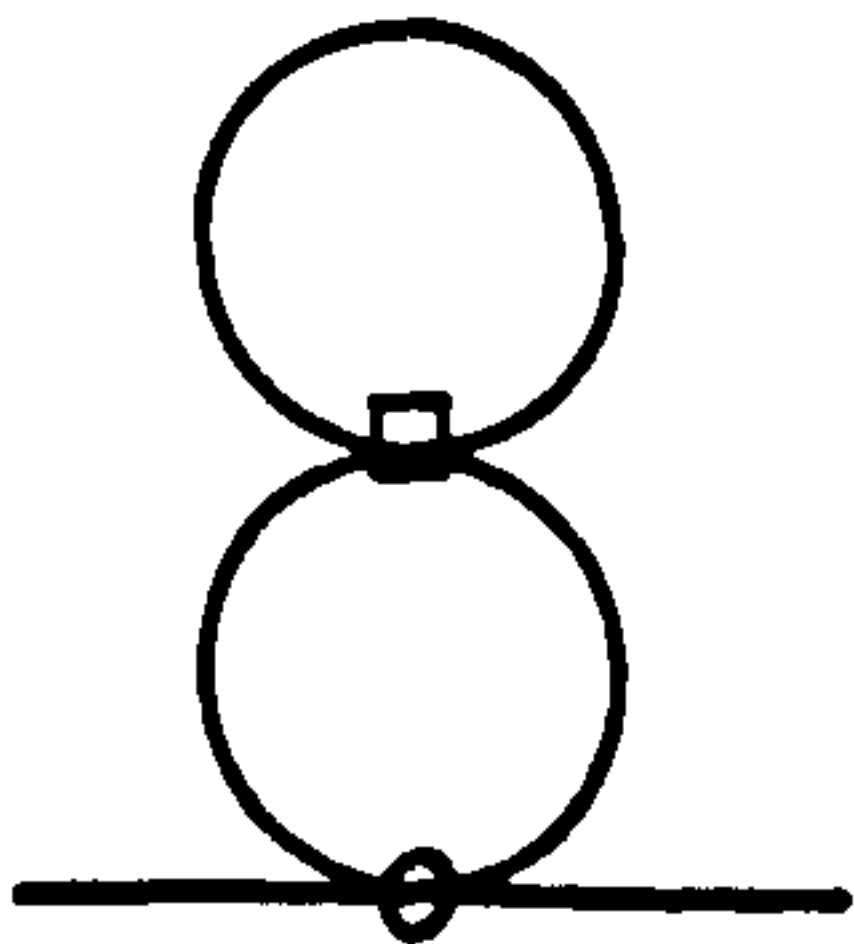
$u(n+2)/6$



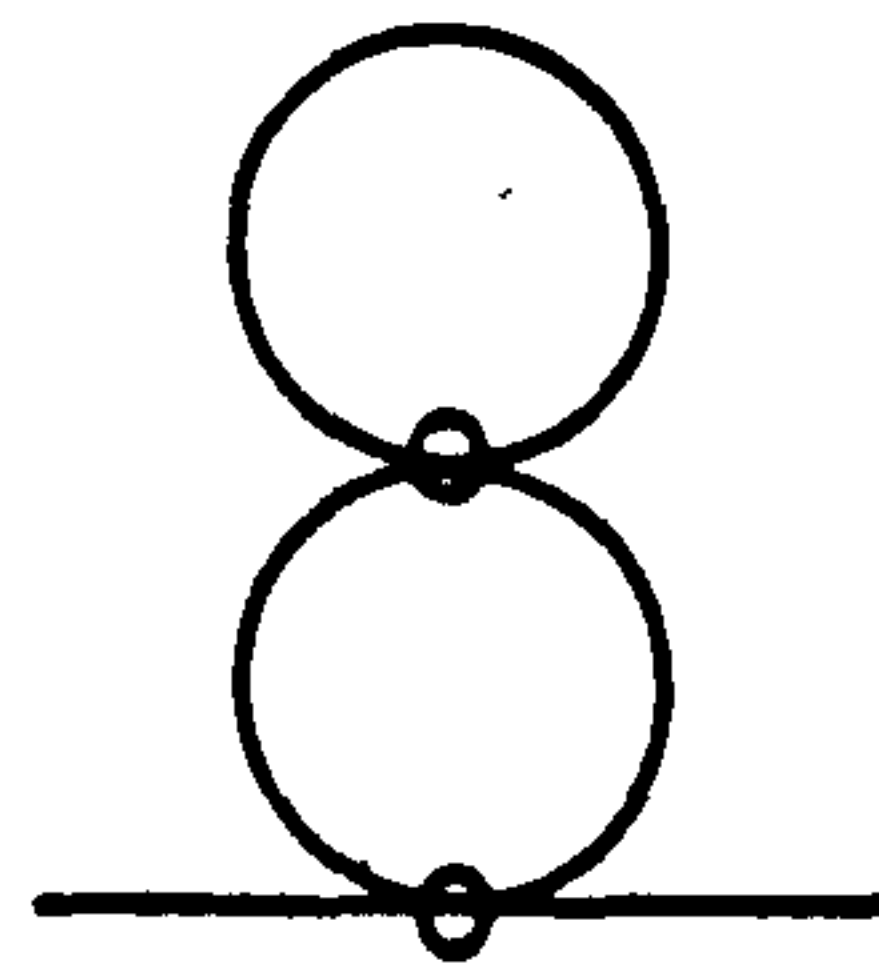
$-v^2/4$



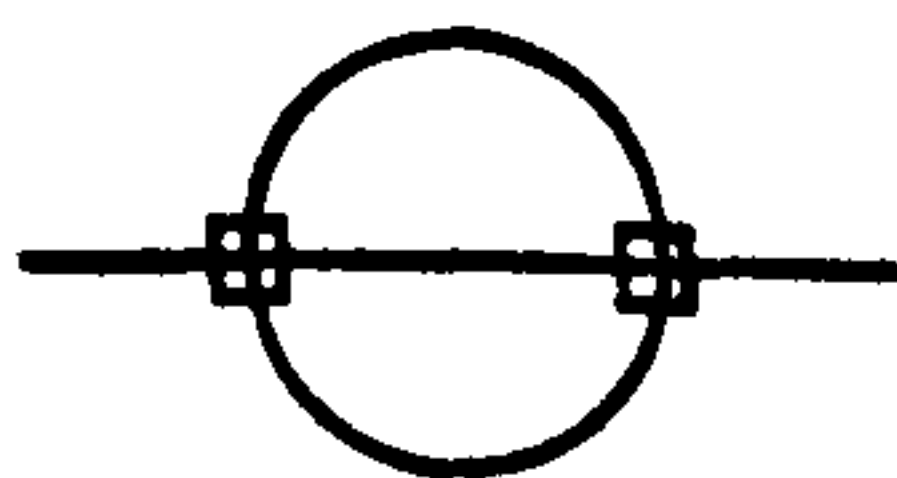
$-uv(n+2)/12$



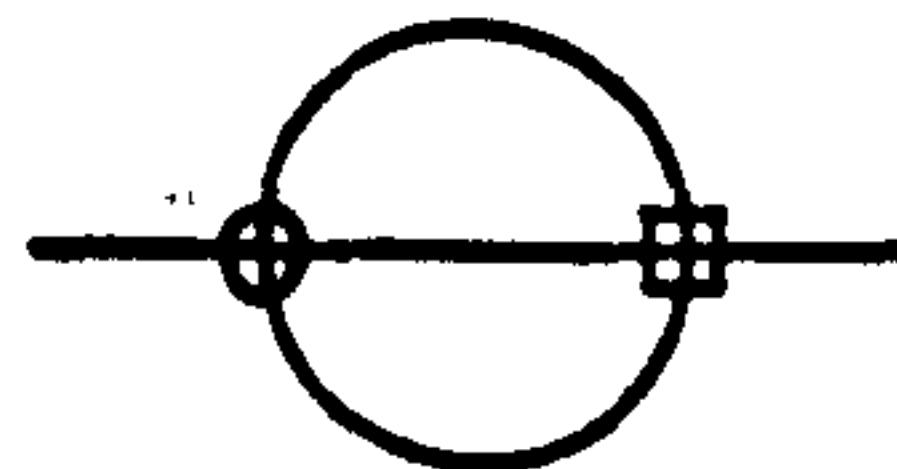
$-uv(n+2)/12$



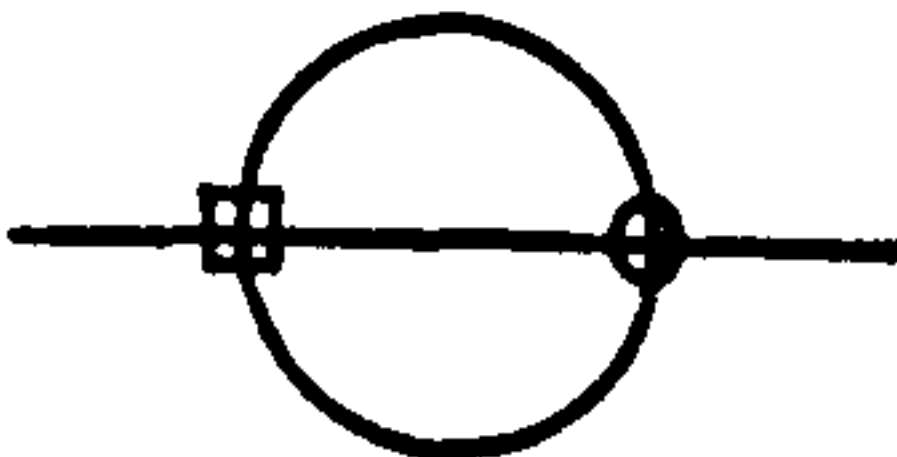
$-u^2(n+2)^2/36$



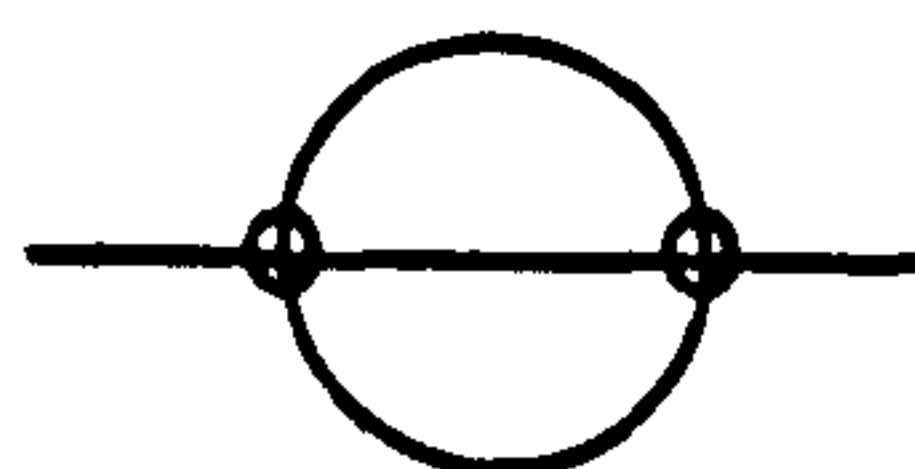
$-v^2/6$



$-uv/6$



$-uv/6$



$-u^2(n+2)/18$

Figure 2-2: One loop graphs, with weights, for the two point function

easily recovered as a factor for every loop. We therefore define (minimally) a renormalised temperature by

$$t = \mu^2 t_R = t_0 \left\{ 1 - \frac{1}{2\epsilon} \left(\frac{1}{3}(n+2)u_0 + v_0 \right) \right\} \quad (2.56)$$

i.e.,

$$t_0 = \mu^2 t_R \left\{ 1 + \frac{1}{2\epsilon} \left(\frac{1}{3}(n+2)u_R + v_R \right) \right\} \quad (2.57)$$

since to this order $u = u_0 \mu^{-\epsilon} = u_R$ and $v = v_0 \mu^{-\epsilon} = v_R$. Then

$$\mu^2 \Gamma_R^{(u)} = q^2 + t + \text{higher orders} \quad (2.58)$$

Wave function Renormalisation

To render $\Gamma_R^{(2)}$ finite at four dimensions the two point vertex function $\Gamma^{(2)}$ is multiplied by the wave function renormalisation constant Z_ϕ . As we shall see in the next section, to order one loop, $Z_\phi = 1$. This is a consequence of the only one loop diagram contributing to $\Gamma_b^{(2)}$ being proportional to the reduced temperature and hence vanishing at criticality.

Coupling Constant Renormalisation

To obtain finite Greens functions we must also renormalise the coupling constants in the theory. This is achieved by imposing the condition that

$$\mu^\epsilon \Gamma_R^{(4)} = Z_\phi^2 \Gamma_b^{(4)} \quad (2.59)$$

must have a finite limit as $d \rightarrow 4$. As we have remarked above, wave function renormalisation is a two-loop effect and therefore at this one-loop level it is sufficient to demand that a renormalisation of the coupling constants (and temperature) removes the poles in ϵ in $\Gamma_b^{(4)}$. At one loop the graphs which contribute to $\Gamma_b^{(4)}$ are shown in Figure 2-3. It is easily checked that on setting $n = 1$, $u_0 = 0$ and $F_{ijkl} = 1$ one recovers the graphs of an ordinary ϕ^4 theory. A second check on the factors listed is to set $v_0 = 0$, $S_{ijkl} = 1$ and we obtain the results appropriate to an $O(n)$ symmetric, bosonic field theory. Finally, setting $u_0 = v_0 = g$, $S_{ijkl} = F_{ijkl} = 1$ and dividing by the number of graphs of a given topology, the ϕ^4 results are once more recovered. These checks provide important confirmation of the correctness of the intermediate stages in the calculation, over and above the inbuilt checks of the method of minimal subtraction allied to dimensional regularisation.

Collecting the factors together, the bare four-point function is given by

$$\begin{aligned} \Gamma_{ijkl}^{(4) \text{ bare}} &= \mu^\epsilon \left\{ v F_{ijkl} + u S_{ijkl} \right. \\ &\quad - \frac{1}{\epsilon} [v F_{ijkl} (3v + 4u) + u S_{ijkl} (2v + \frac{1}{2} u(n+8))] \\ &\quad \left. + [\mathcal{I}(k_1+k_2) + \mathcal{I}(k_1+k_3) + \mathcal{I}(k_1+k_4)] \right\} \end{aligned} \quad (2.60)$$

where the integral $\mathcal{I}(k)$ is

$$\mathcal{I}(k) = \int \frac{d^4 q}{q^2 (q^2 + k^2)} = \frac{1}{\epsilon} \left[1 - \frac{1}{2} \epsilon - \frac{1}{2} \epsilon L(k) \right] + \text{finite} \quad (2.61)$$

in which q and k are dimensionless, and

$$L(k) = \int_0^1 dx \ln [x(1-x)k^2] \quad (2.62)$$

We now expand u and v as double power series in the renormalised couplings

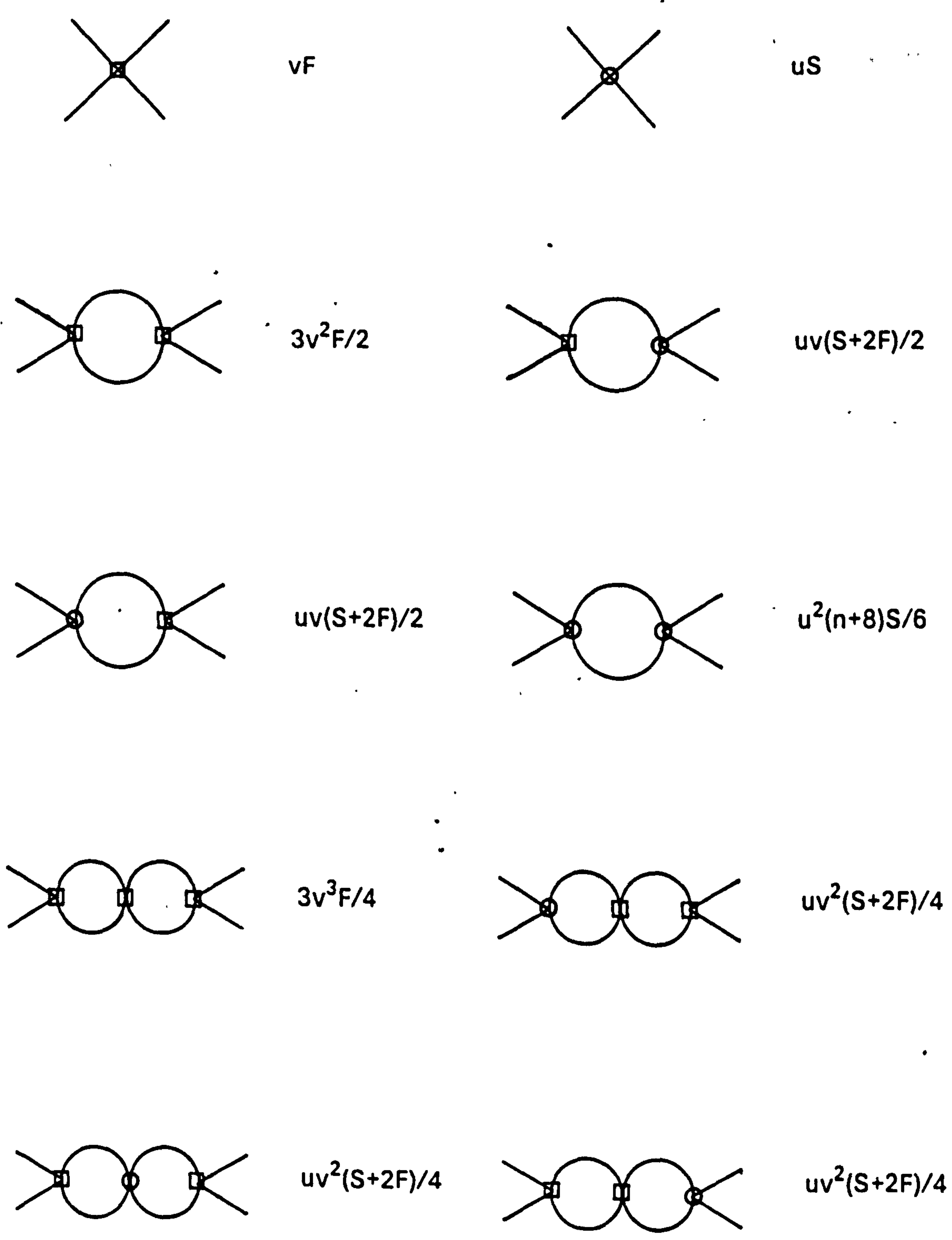
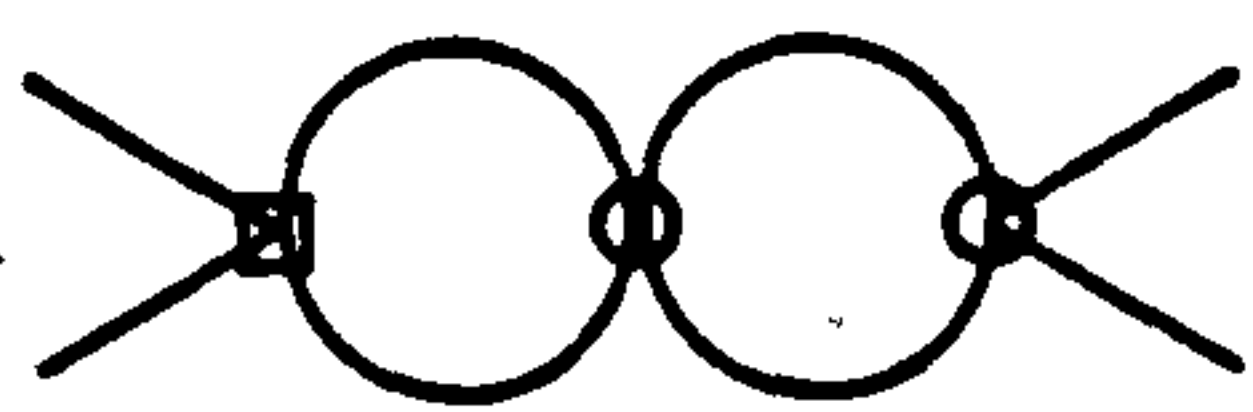
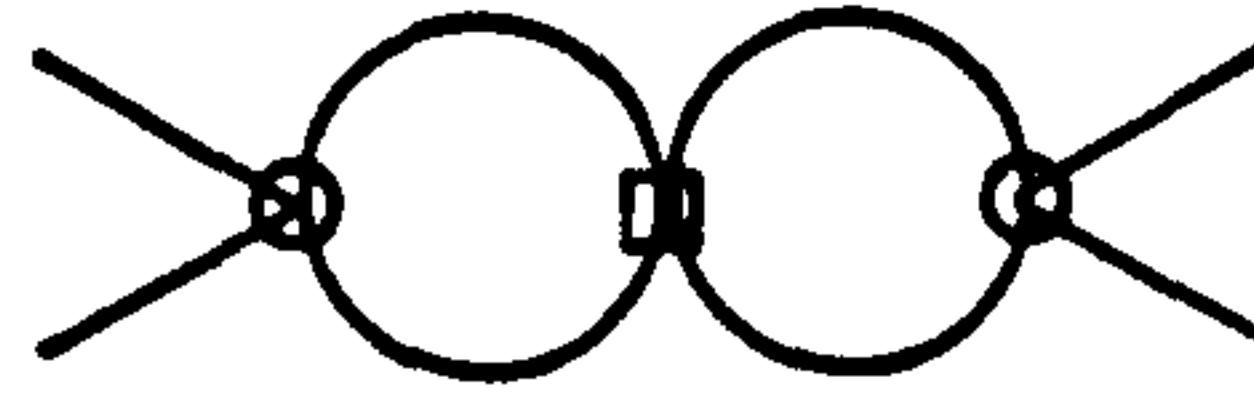


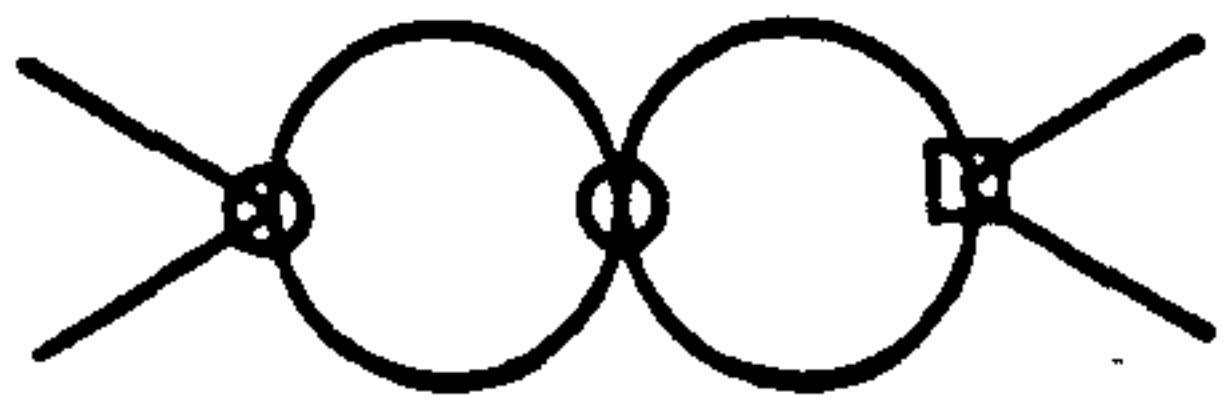
Figure 2-3: One loop graphs, with weights, for the four point function



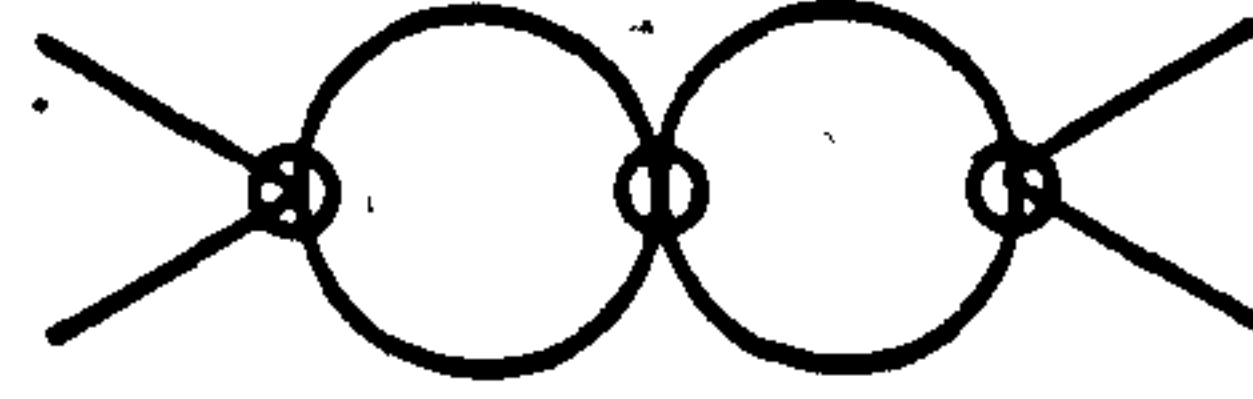
$$u^2v[(n+4)S+4F]/12$$



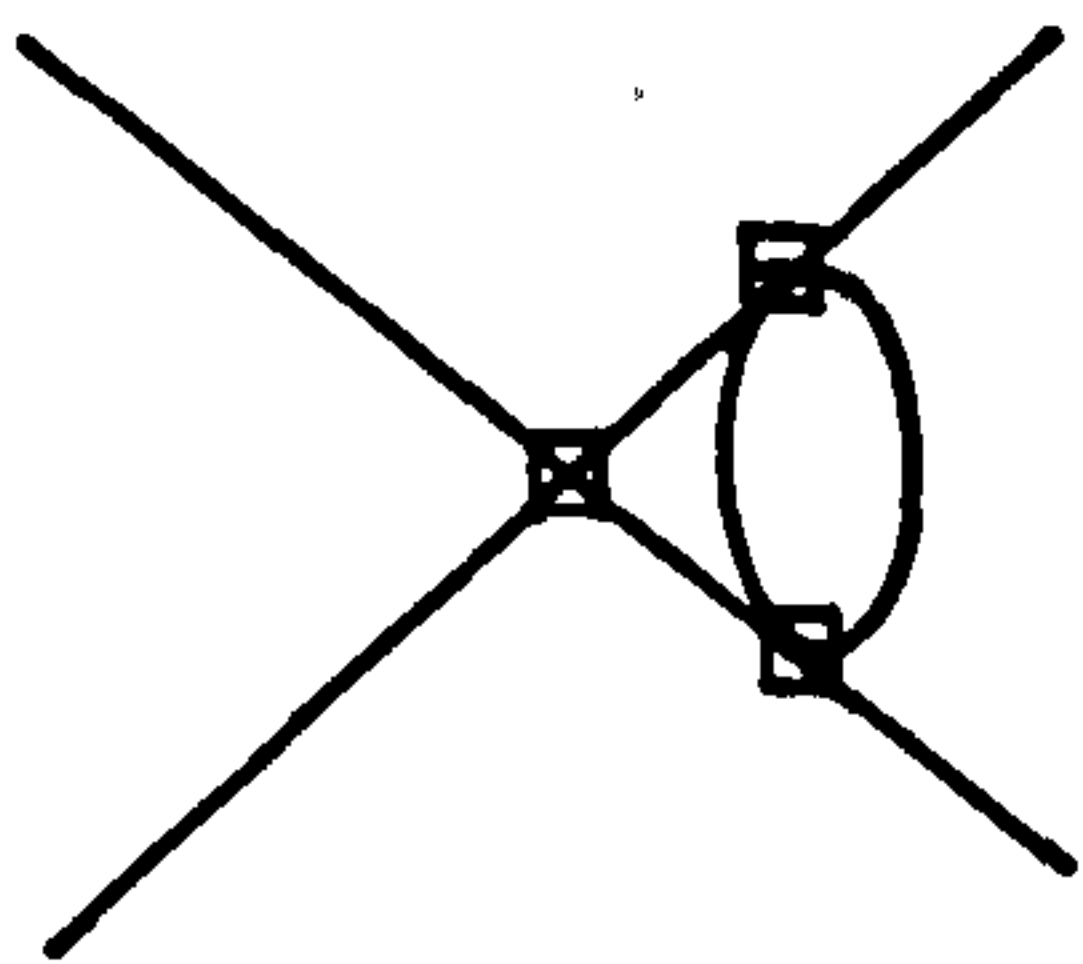
$$u^2v[(n+4)S+4F]/12$$



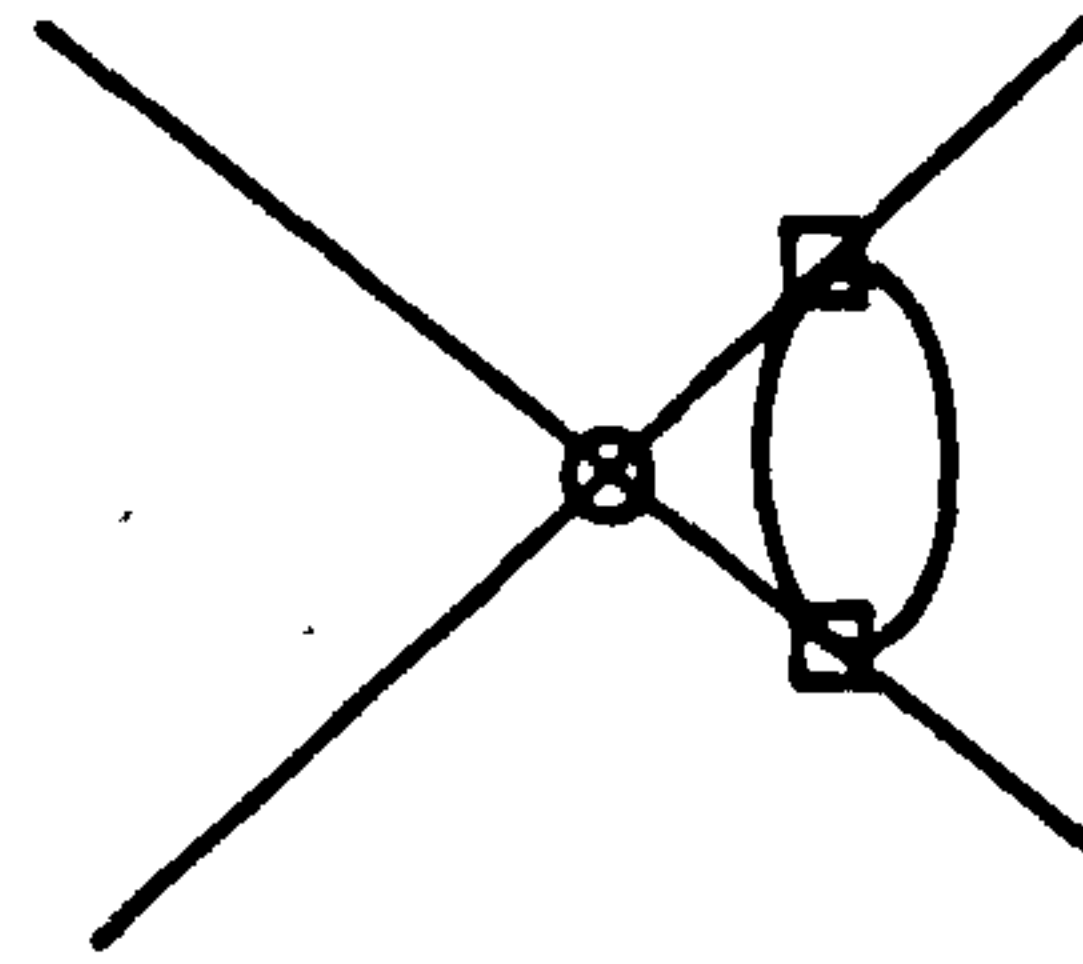
$$u^2v[(n+4)S+4F]/12$$



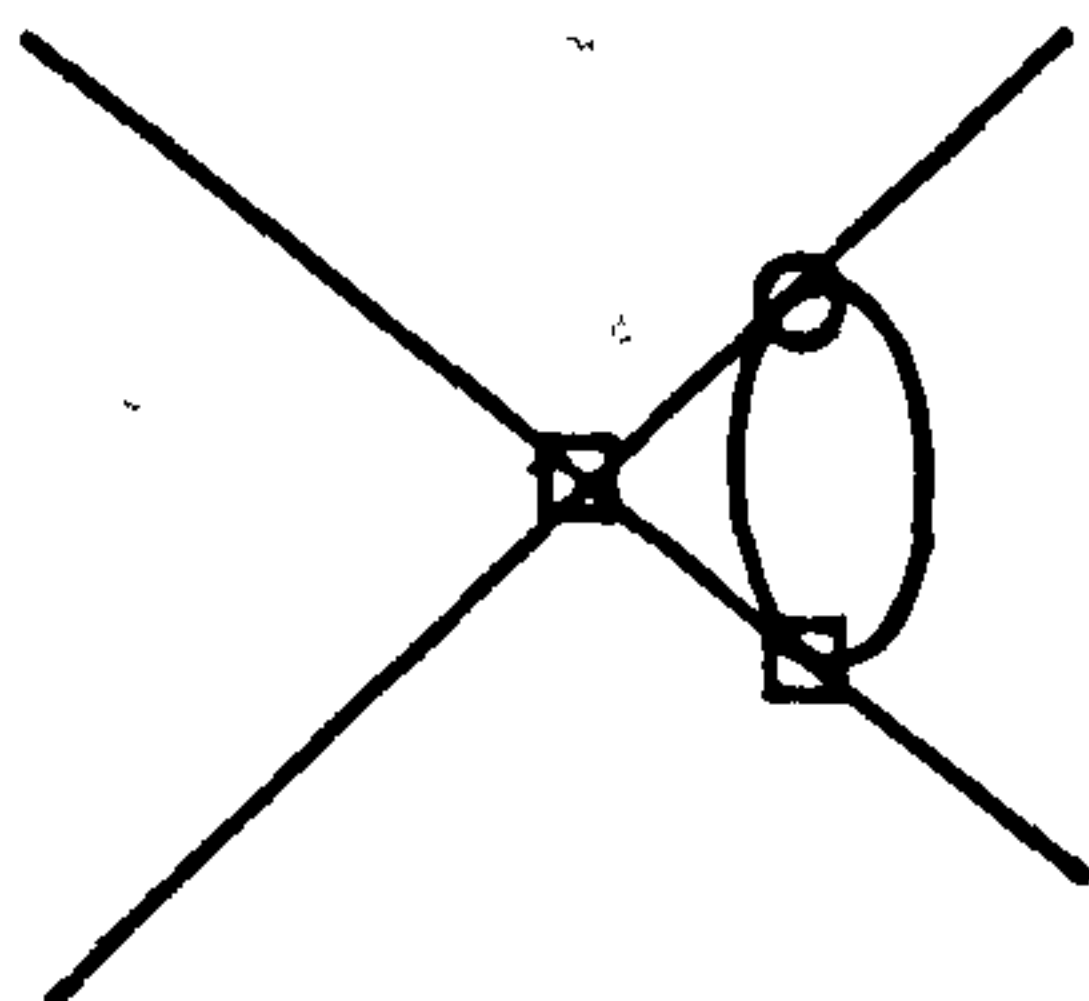
$$u^3(n^2+6n+20)S/36$$



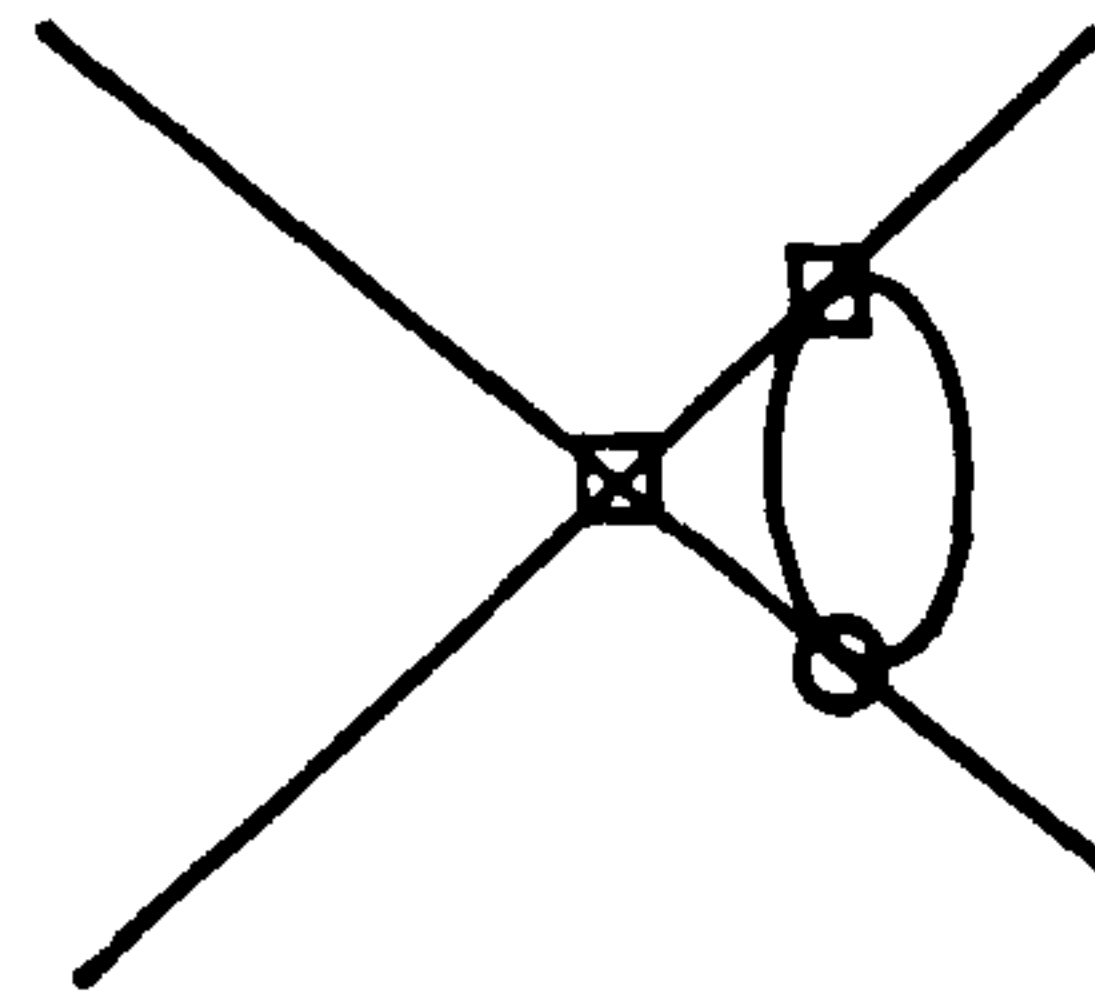
$$3v^3F$$



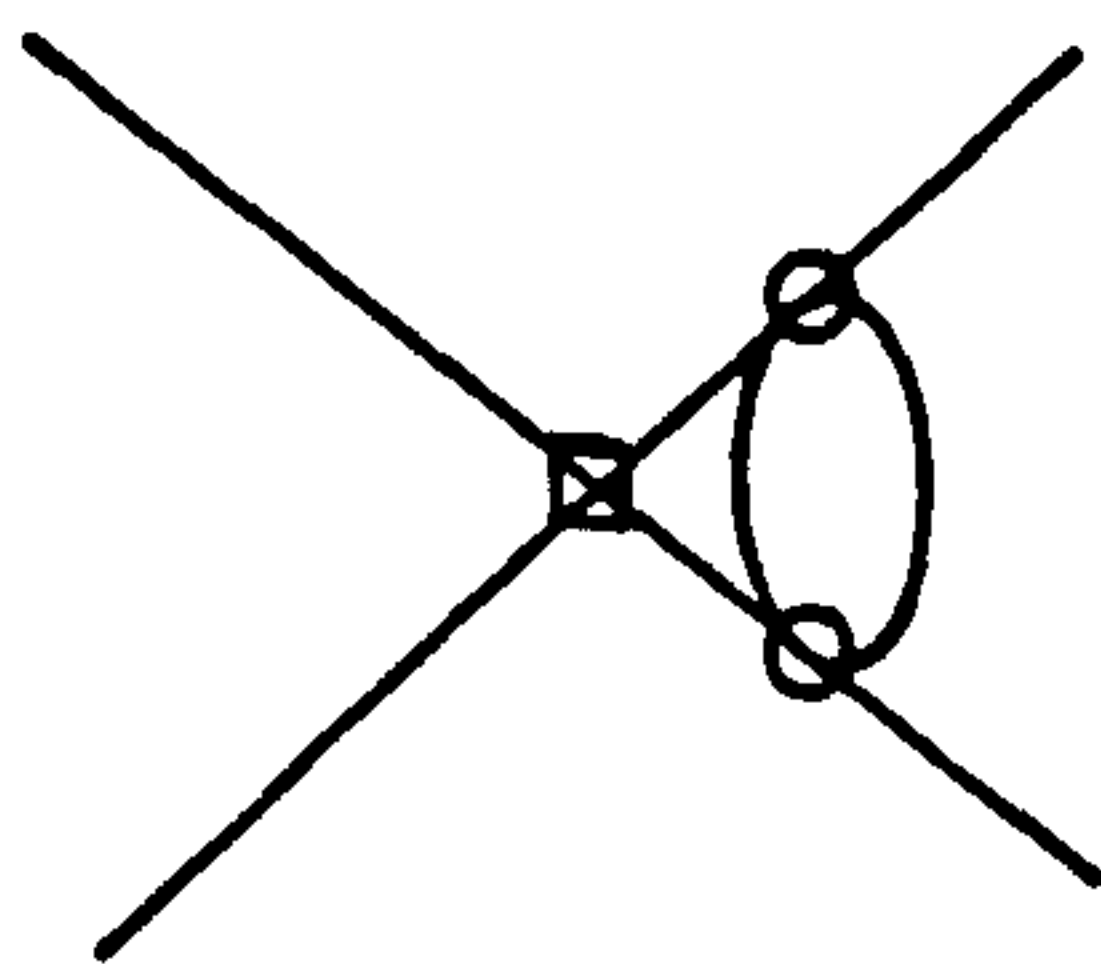
$$uv^2(S+2F)$$



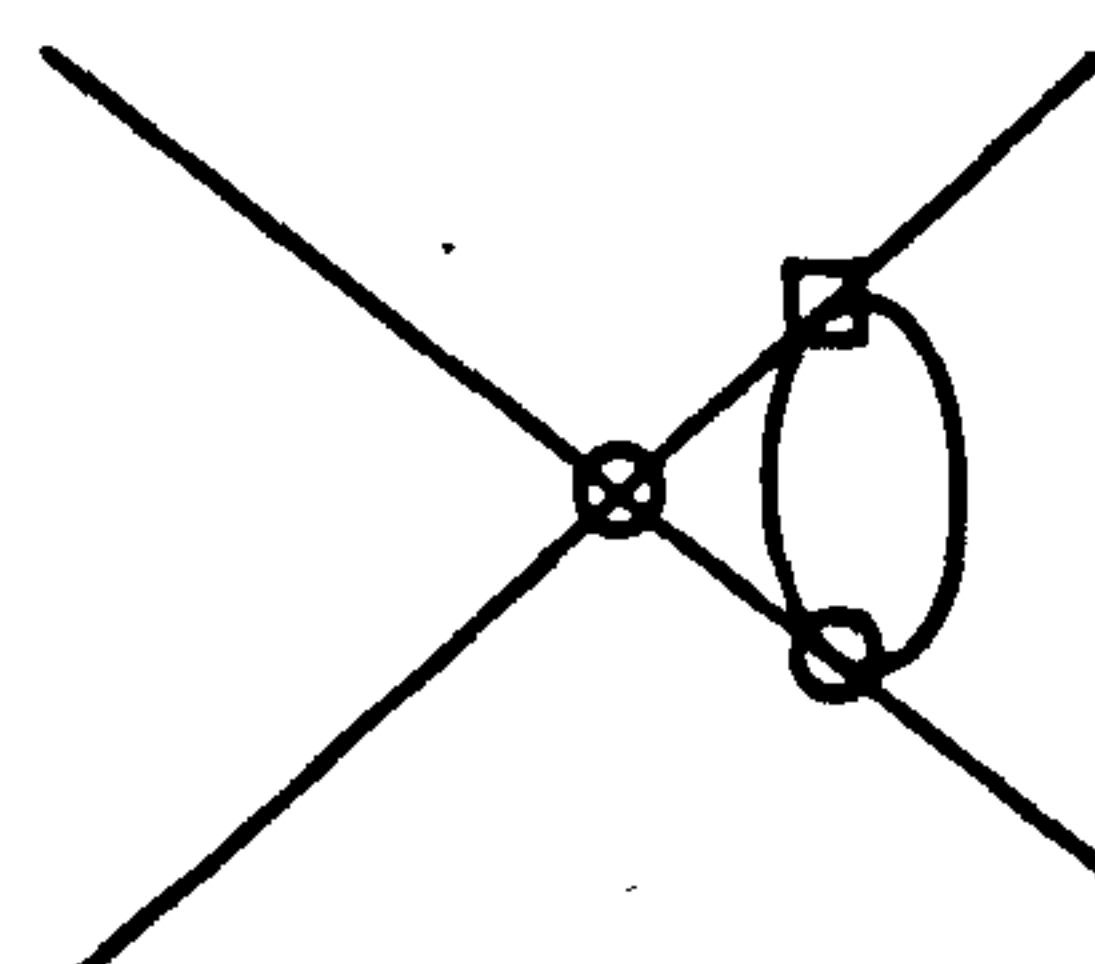
$$3uv^2$$



$$3uv^2$$

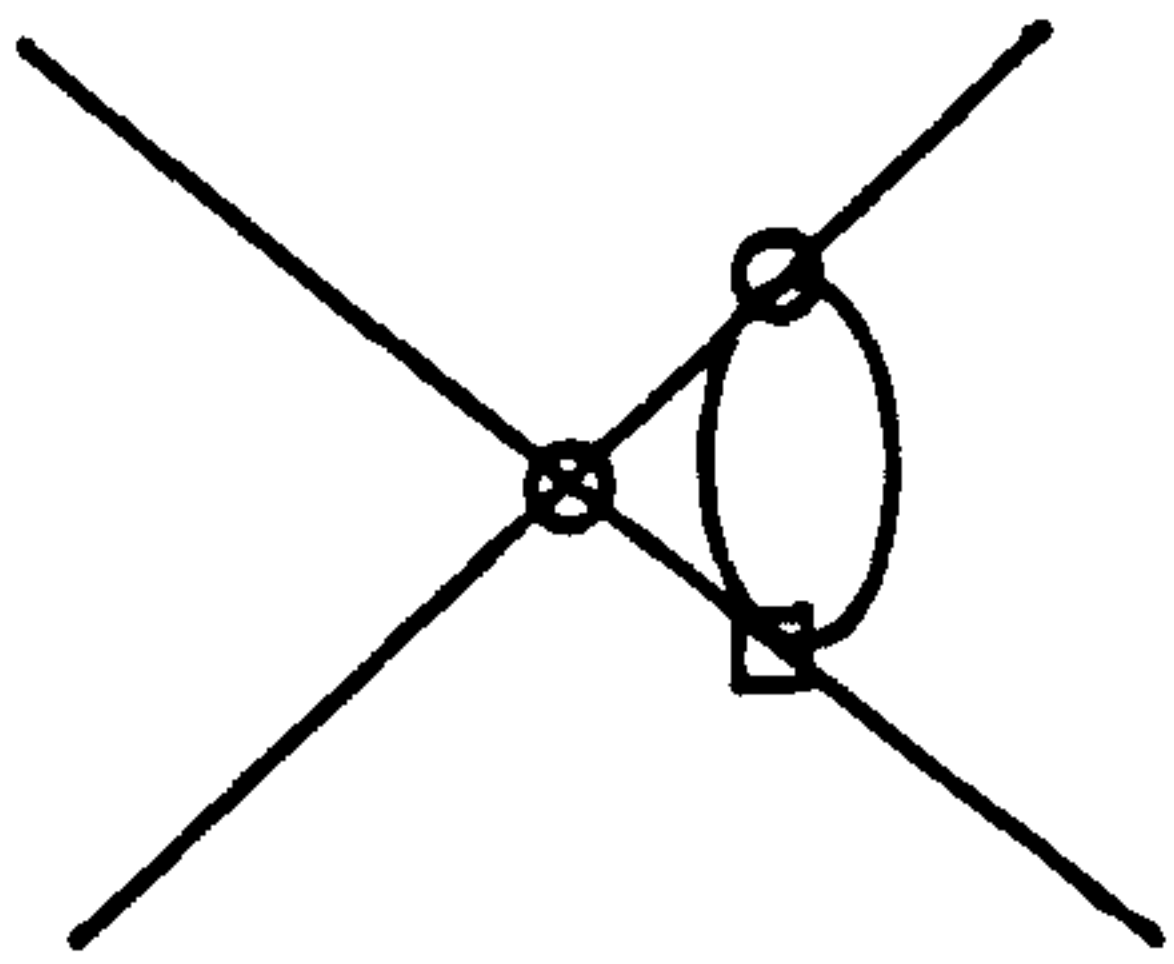


$$u^2v[2S+(n+6)F]/3$$

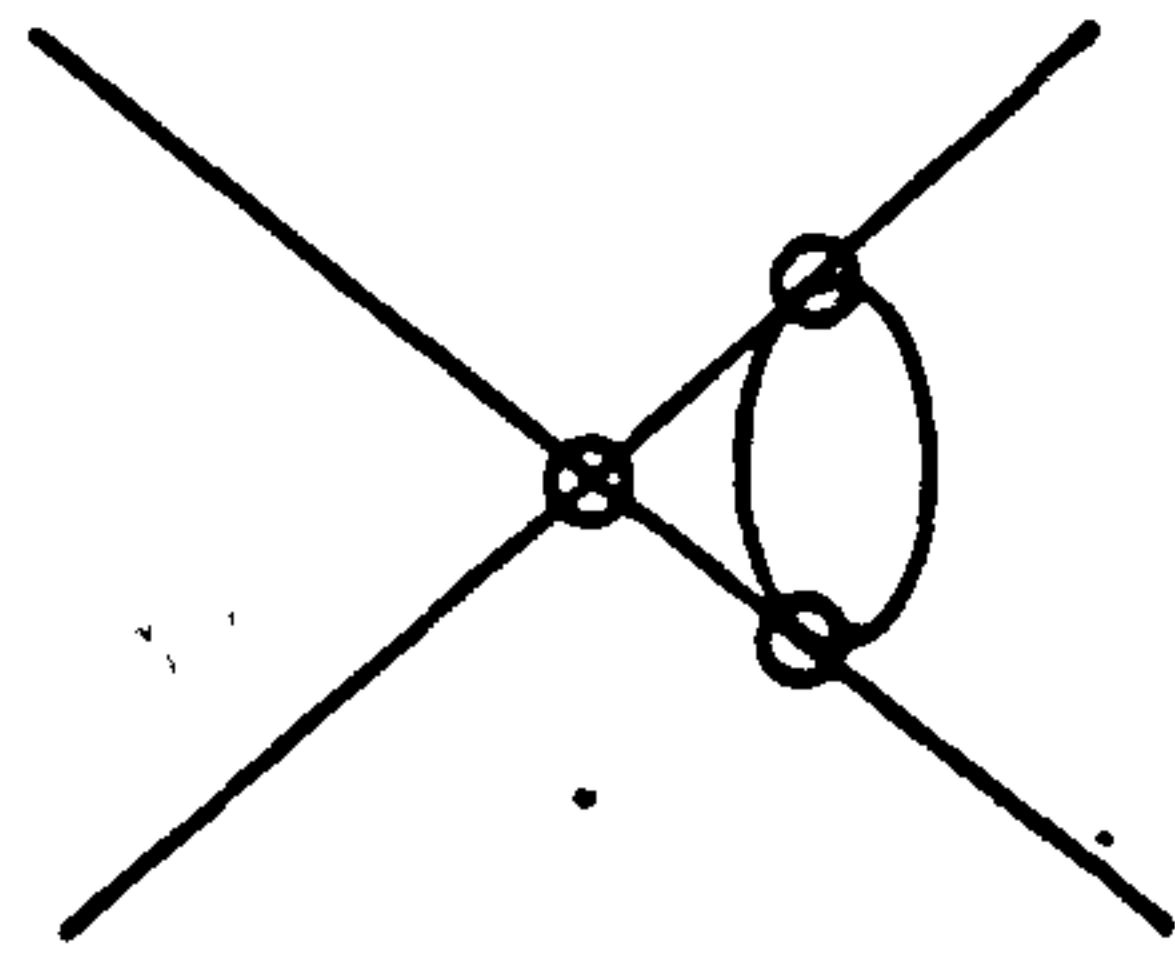


$$u^2v[5S+4F]/3$$

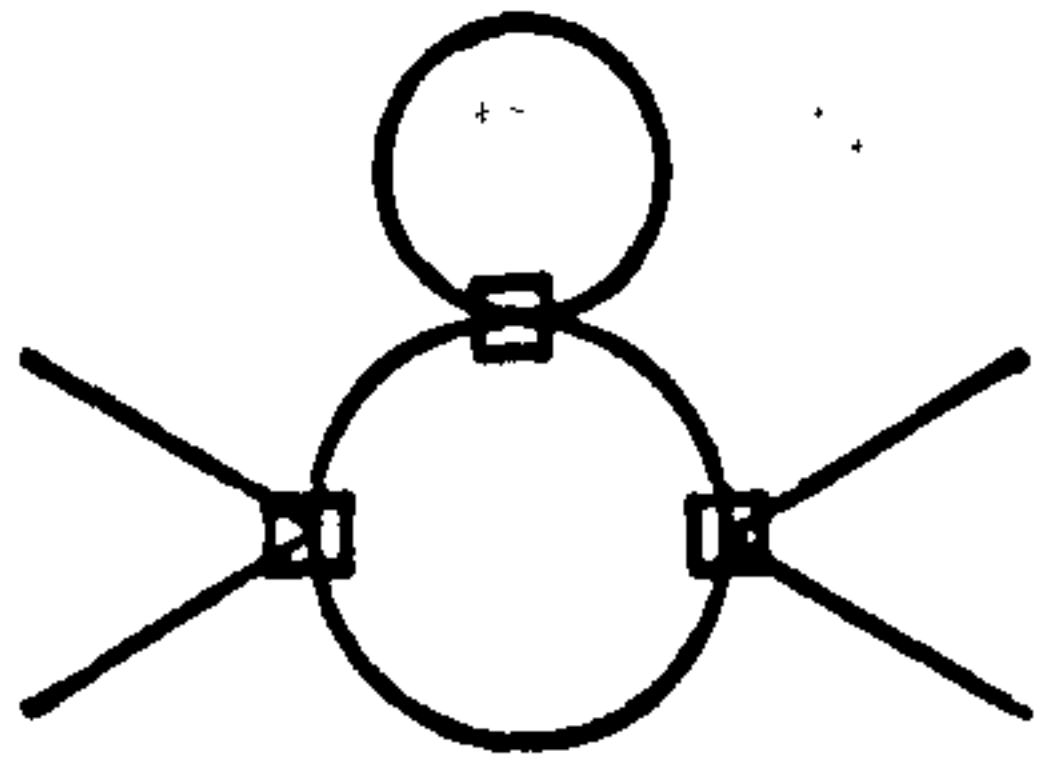
Figure 2-3 (continued)



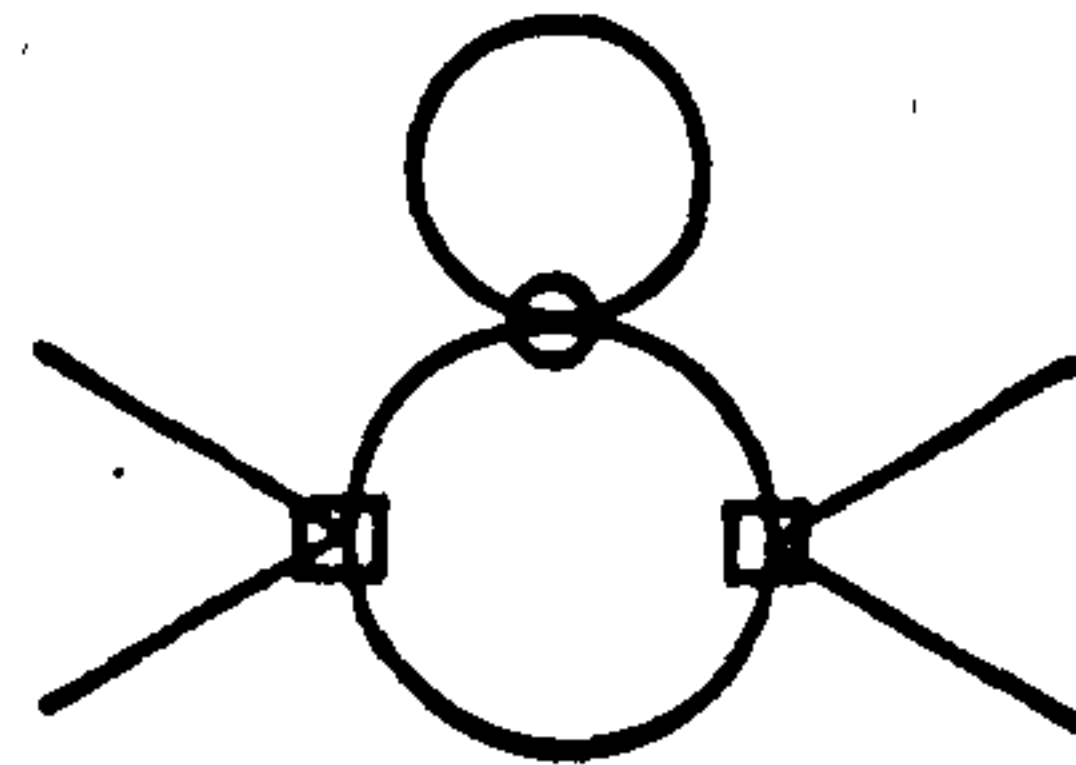
$$u^2v[5S+4F]/3$$



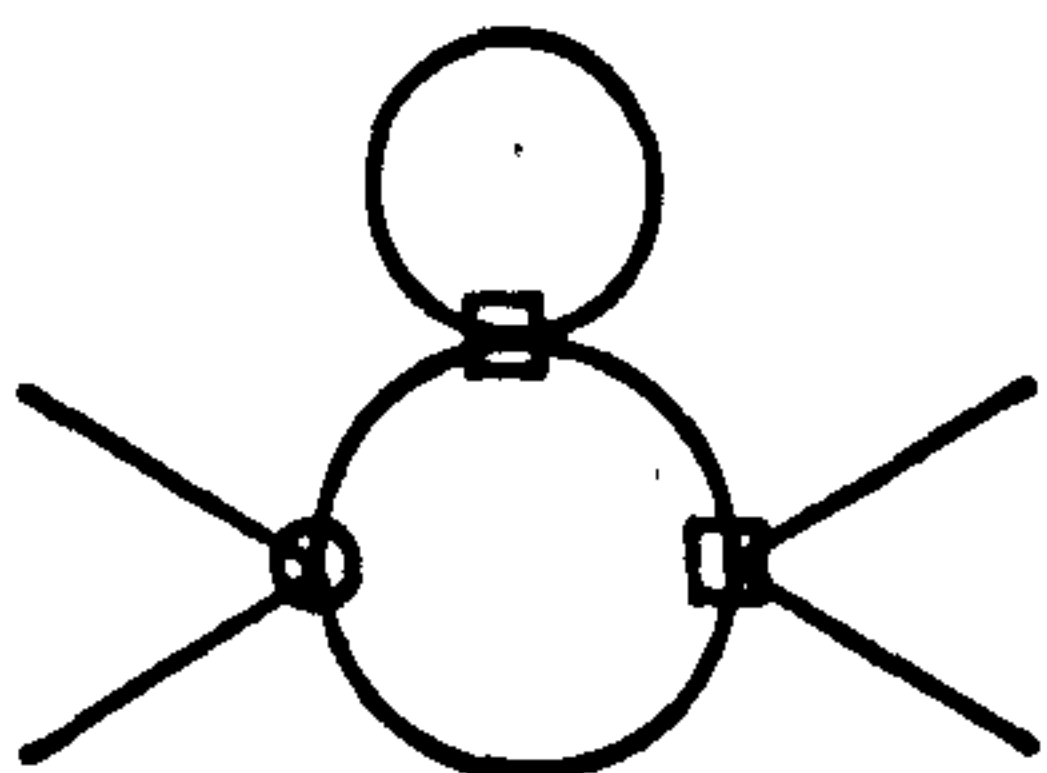
$$u^3(5n+22)S/9$$



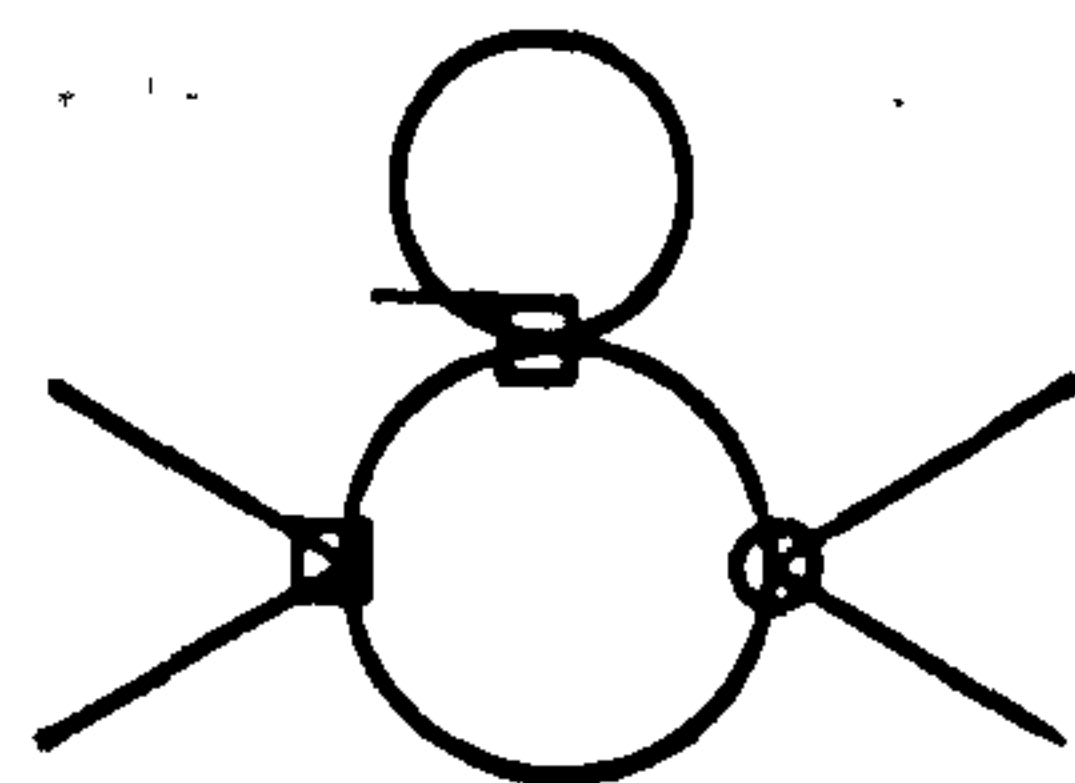
$$3v^3F/2$$



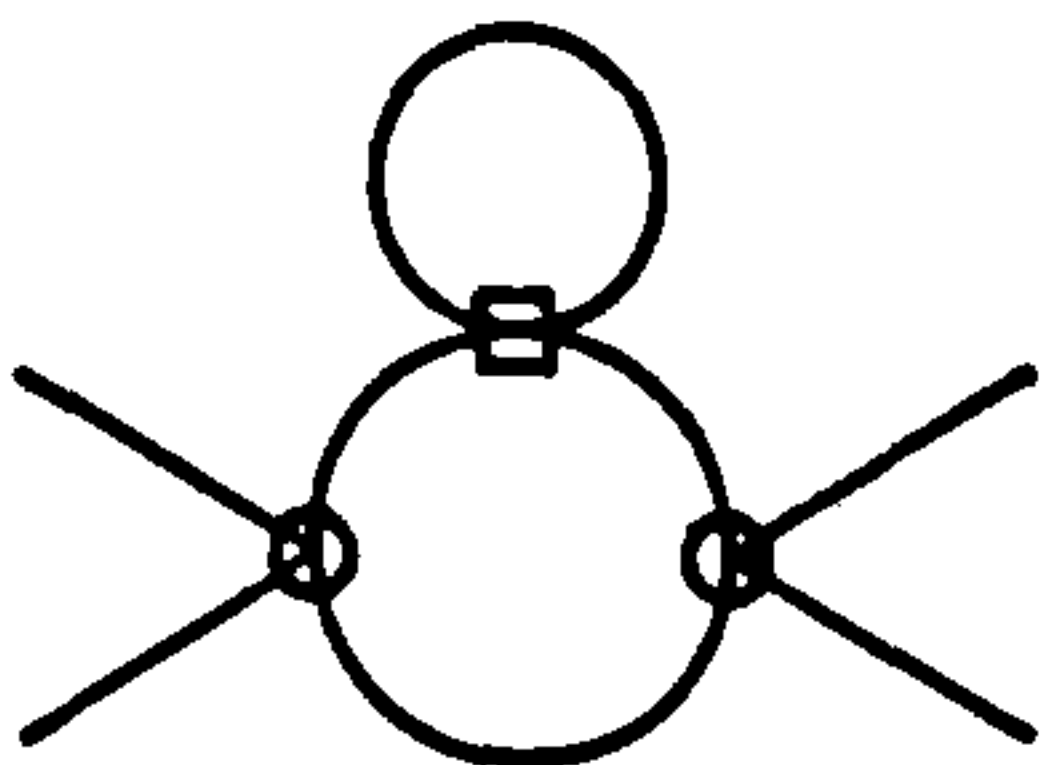
$$uv^2(n+2)F/2$$



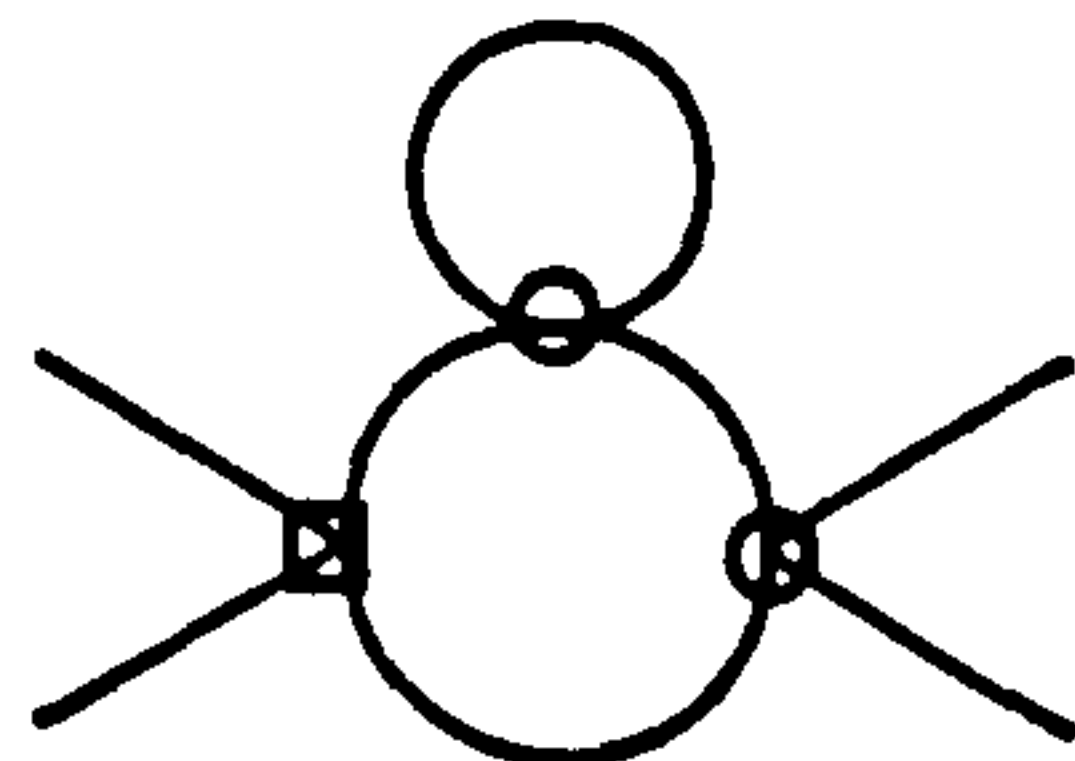
$$uv^2[2S+F]/2$$



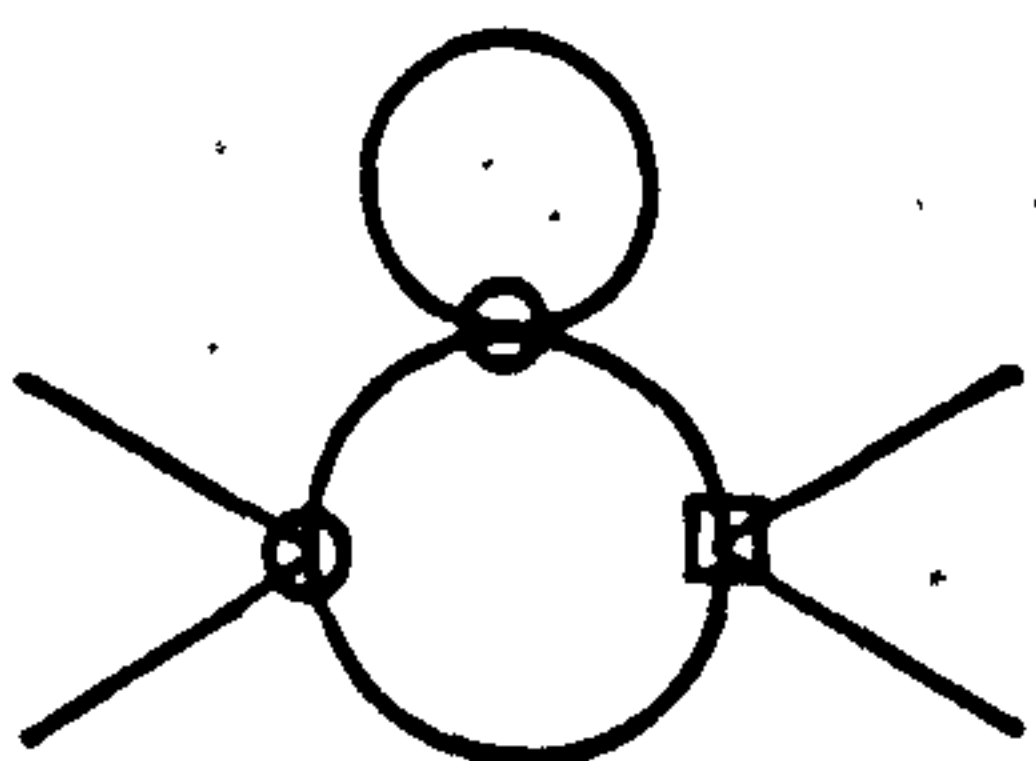
$$uv^2[2S+F]/2$$



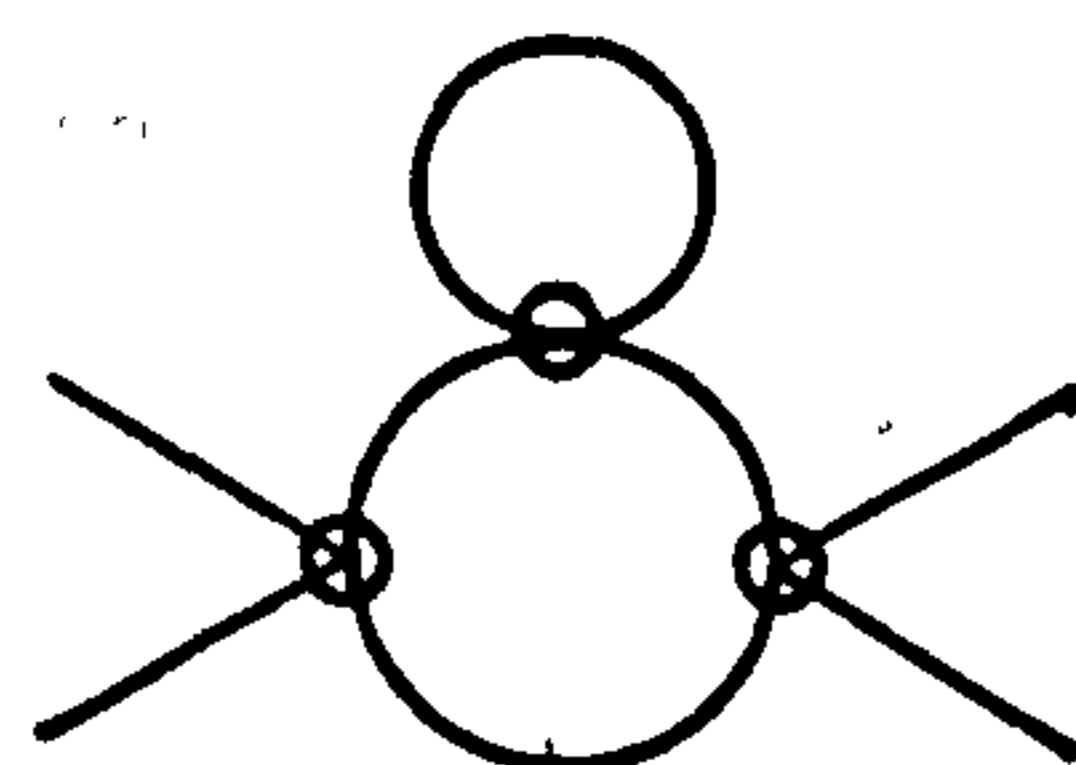
$$u^2v(n+8)S/6$$



$$u^2v(n+2)[S+2F]/6$$



$$u^2v(n+2)[S+2F]/6$$



$$u^3(n+2)(n+8)S/18$$

Figure 2-3 (continued)

u_R and v_R ,

$$u = u_R + b_1 u_R^2 + b_2 u_R v_R \quad (2.63)$$

$$v = v_R + c_1 v_R^2 + c_2 u_R v_R \quad (2.64)$$

substitute these into $\Gamma_b^{(4)}$ and, demanding that the poles in the integrals are minimally subtracted by the coefficients in the expansions of u and v , leads to

$$u = u_R + \frac{(\eta+8)}{6\epsilon} u_R^2 + \frac{1}{\epsilon} u_R v_R \quad (2.65)$$

$$v = v_R + \frac{3}{2\epsilon} v_R^2 + \frac{2}{\epsilon} u_R v_R \quad (2.66)$$

These series may be inverted, order by order in perturbation theory to give the renormalised couplings in terms of the bare, viz.,

$$u_R = u - \frac{(\eta+8)}{6\epsilon} u^2 - \frac{1}{\epsilon} uv \quad (2.67)$$

$$v_R = v - \frac{3}{2\epsilon} v^2 - \frac{2}{\epsilon} uv \quad (2.68)$$

Composite Field Renormalisation

The final renormalisation to be performed is that of the vertex function $\Gamma_b^{(2,1)}$, i.e., the two point function with one ϕ^2 insertion. The divergence associated with this quantity persists after substituting in the renormalised temperature and coupling constants and hence must be removed separately. This is achieved by constructing a function \bar{Z}_ϕ^2 such that the expression

$$\Gamma_R^{(2,1)} = \bar{Z}_\phi^2 \bar{Z}_\phi \Gamma_b^{(2,1)} \equiv \bar{Z}_{\phi^2} \Gamma_b^{(2,1)} \quad (2.69)$$

has a finite limit as $d \rightarrow 4$. The graphs in the expansion of $\Gamma_b^{(2,1)}$ to order one-loop are detailed in Figure 2-4. The resulting expression for $\Gamma_b^{(2,1)}$ to this order is

$$\Gamma_b^{(2,1)} = 1 - \frac{1}{2} \mathcal{I}(k) v - \frac{1}{6} (n+2) \mathcal{I}(k) u \quad (2.70)$$

The integrals entering the loop expansion of $\Gamma^{(2,1)}$ are the same as those in the expansion of $\Gamma^{(4)}$ but the symmetry and combinatoric factors associated with each graph are different.

As before, we write \bar{Z}_{ϕ^2} as a power series in u_R and v_R with unknown coefficients and demand that the poles in ϵ in the vertex function are cancelled. The result is

$$\bar{Z}_{\phi^2} = 1 + \frac{(n+2)}{6\epsilon} u_R + \frac{1}{2\epsilon} v_R \quad (2.71)$$

We now have all the expressions necessary to render any Greens function finite in the limit $d \rightarrow 4$ at one-loop. The strategy we adopt is to calculate the required function as an expansion in terms of bare quantities and only at the end substitute in the renormalised expressions, knowing that we are guaranteed finite results as $\epsilon \rightarrow 0$.

Normally at this stage the next step would be to straightforwardly calculate the integrals in the expansion of $\langle \Phi_{||} \rangle$ using the two distinct propagators involving the longitudinal and transverse masses then, after renormalising the resulting expression, taking the $n \rightarrow 0$ limit. However, to enable us to generalise the method to two loops more easily, we will adopt a different approach and expand the transverse propagator as a Taylor series in n about the longitudinal

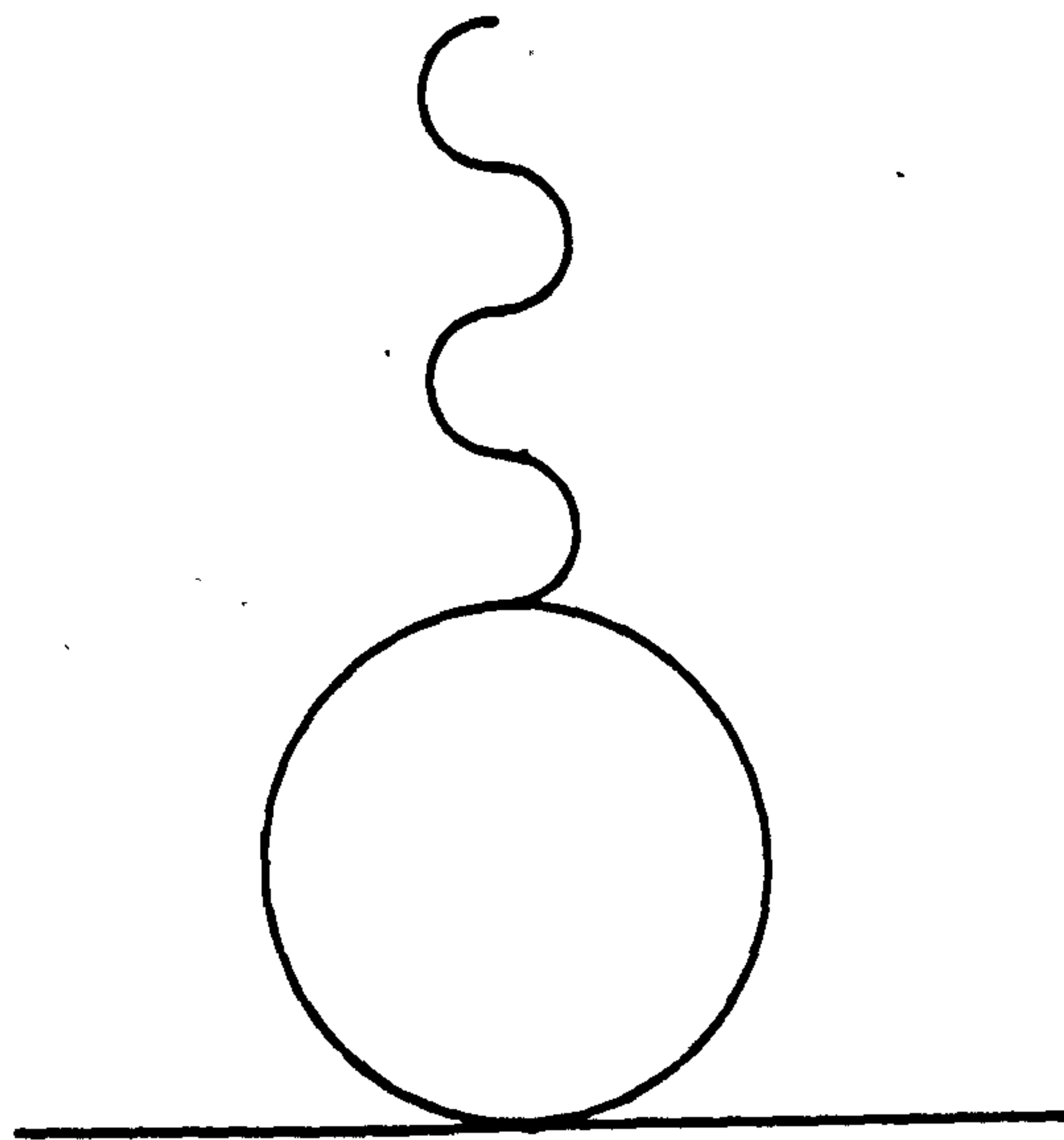
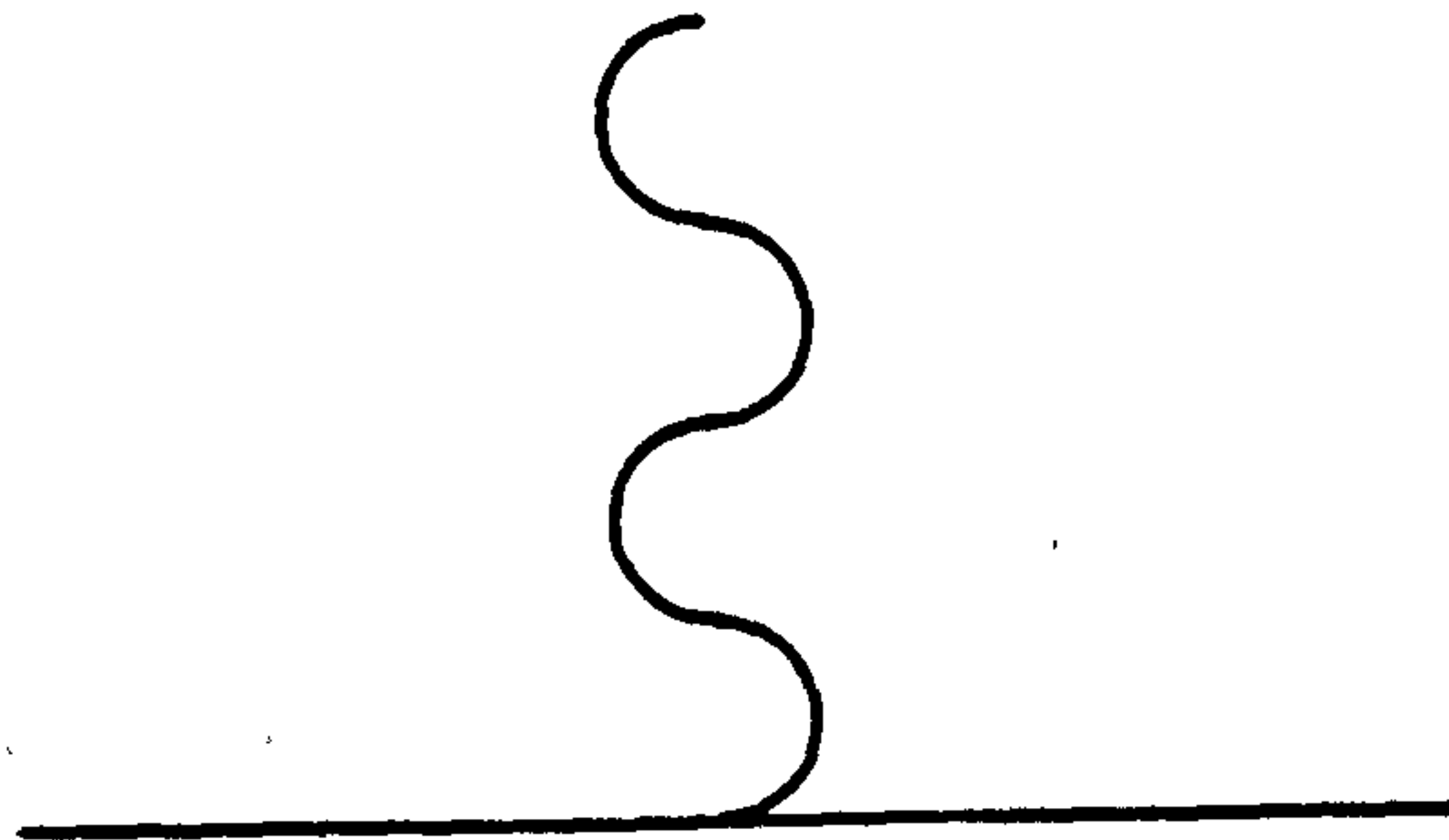


Figure 2-4: Graphs for $\Gamma^{(2,1)}$ to one loop

one. The advantage of this way of calculation is that we can identify terms of order n (which will vanish in the limit $n \rightarrow 0$) from the outset, and we only have one mass in the theory to contend with. The integrals involved in the two loop calculation become practical to do, due to this latter simplification (and other, more remarkable effects!). As a calculational check, the conventional expansion method was carried through to one loop and was found to agree with our method to this order.

In the expansion of $\langle \Phi_{||} \rangle$ the only diagram involving the transverse propagator at one-loop is the lowest one in Figure 2-1. The overall combinatorics are unchanged but the integral associated with the graph is expanded as

$$\int \frac{d^d q}{q^2 + \Gamma_T} = \int \frac{d^d q}{q^2 + \Gamma_{||}} + \frac{1}{3} u_0 n M_0^2 \int \frac{d^d q}{(q^2 + \Gamma_{||})^2} + \frac{1}{9} u_0^2 M_0^4 n^2 \int \frac{d^d q}{(q^2 + \Gamma_{||})^3} \quad (2.72)$$

The integrals

$$\int \frac{d^d q}{(q^2 + \Gamma_{||})^2} \quad (2.73)$$

and

$$\int \frac{d^d q}{(q^2 + \Gamma_{||})^3} \quad (2.74)$$

can be represented diagrammatically as Figure 2-5, in which the notch on the propagator acts as an insertion at zero momentum. It is equivalent to taking a derivative of the internal line with respect to the longitudinal mass - an obvious equivalence once one considers the general form of a Taylor series.

Therefore, to this order, the equation of state is given by

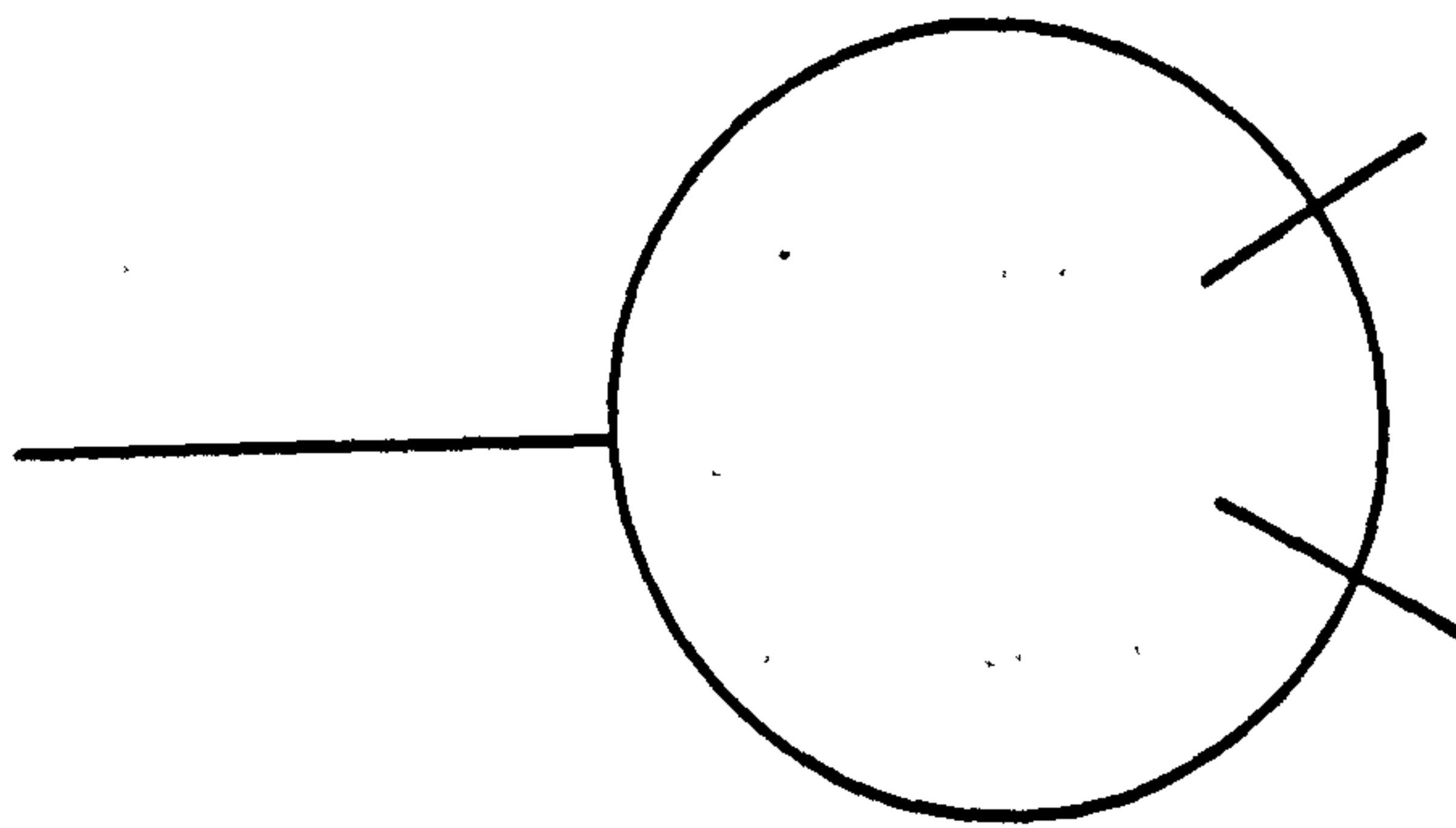
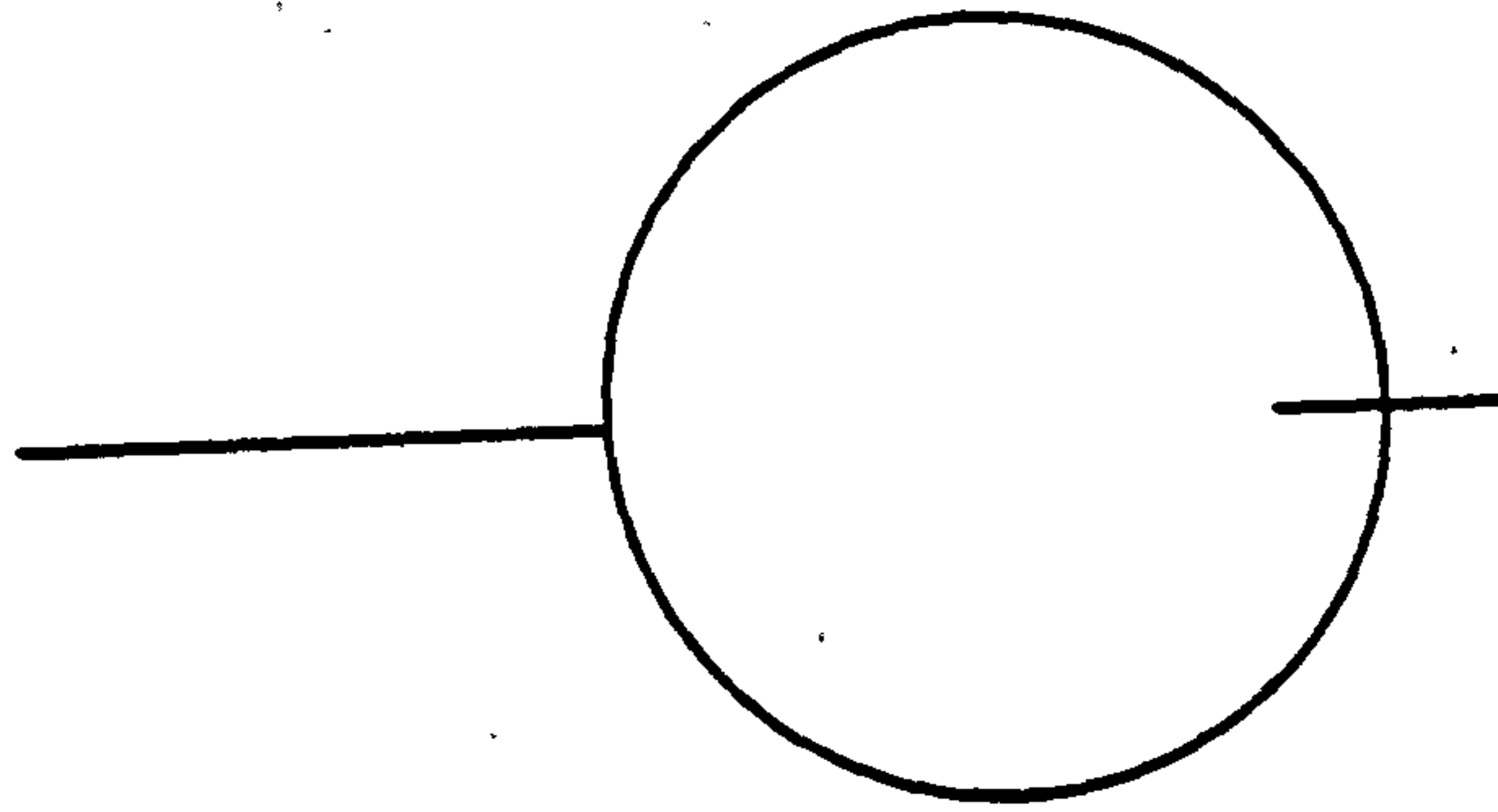


Figure 2-5: Diagrammatic representation of integrals in Taylor expansion

$$\frac{H_0}{M_0} = t_0 + \frac{1}{6} (u_0 n + v_0) M_0^2 + \frac{1}{6} (4u_0 n + 2u_0 + 3v_0) \int \frac{d^d q}{q^2 + \Gamma_n} - \frac{1}{6} u_0 v_0 M_0^2 \int \frac{d^d q}{(q^2 + \Gamma_n)^2} + o(n) \quad (2.75)$$

$$\xrightarrow{n \rightarrow 0} t_0 + \frac{1}{6} v_0 M_0^2 + \frac{1}{6} (2u_0 + 3v_0) I_0^{\circ} - \frac{1}{6} u_0 v_0 M_0^2 I_0^{\prime} \quad (2.76)$$

where

$$I_0^{\circ} = \int \frac{d^d q}{q^2 + b} \quad (2.77)$$

and

$$I_0^{\prime} = \int \frac{d^d q}{(q^2 + b)^2} \quad (2.78)$$

The integrals are easily evaluated and inserting the results into (2.76) leads to the expression

$$\begin{aligned} \frac{H_0}{M_0} = & t_0 + \frac{1}{6} v_0 M_0^2 + \left\{ -\frac{1}{6\epsilon} (t_0 + \frac{1}{2} v_0 M_0^2) (3v_0 + 2u_0) - \frac{1}{6\epsilon} u_0 v_0 M_0^2 \right. \\ & + \frac{1}{12} (t_0 + \frac{1}{2} v_0 M_0^2) \ln (t_0 + \frac{1}{2} v_0 M_0^2) (3v_0 + 2u_0) \\ & \left. + \frac{1}{12} u_0 v_0 M_0^2 \ln (t_0 + \frac{1}{2} v_0 M_0^2) + \frac{1}{12} u_0 v_0 M_0^2 \right\} \quad (2.79) \end{aligned}$$

The renormalised, spontaneous magnetisation is obtained by solving the equation $H=0$ perturbatively for $T < T_c$. Substituting in for the bare quantities in terms of the renormalised expressions we finally obtain a renormalised equation of state to one-loop,

$$\begin{aligned} \frac{H_R}{M_R} = & \mu^2 \left\{ t_R + \frac{1}{6} v_R M_R^2 + \frac{1}{12} (3v_R + 2u_R) (t_R + \frac{1}{2} v_R M_R^2) \ln (t_R + \frac{1}{2} v_R M_R^2) \right. \\ & + \frac{1}{12} u_R v_R M_R^2 \ln (t_R + \frac{1}{2} v_R M_R^2) \\ & \left. + \frac{1}{12} u_R v_R M_R^2 \right\} \quad (2.80) \end{aligned}$$

as previously found by Newlove (1983).



Using the definition of the inverse susceptibility,

$$\chi^{-1} = \frac{\partial H_R}{\partial M_R} \quad (2.81)$$

and the equation for $v_R M_R^2$ below T_c we have

$$\begin{aligned} \mu^{-2} \chi^{-1} &= t_R + \frac{1}{12} (3v_R + 2u_R) t_R \ln t_R, & t_R > 0 \\ \mu^{-2} \chi^{-1} &= (-2t_R) + \frac{1}{12} (3v_R + 2u_R) (-2t_R) \ln(-2t_R) \\ &\quad + \frac{1}{4} (3v_R + 5u_R) (-2t_R), & t_R < 0 \end{aligned} \quad (2.82)$$

At the fixed point there are no corrections to scaling and we may therefore match χ^{-1} to the anticipated power law form to obtain the amplitude ratio

$$\frac{C_+}{C_-} = 2 + \left(\frac{6}{53}\right)^{1/2} \varepsilon^{1/2} \left(\ln 2 - \frac{3}{2}\right) + o(\varepsilon) \quad (2.83)$$

and the exponent

$$\gamma = 1 + \frac{1}{2} \left(\frac{6}{53}\right)^{1/2} \varepsilon^{1/2} + o(\varepsilon) \quad (2.84)$$

This value of γ is in agreement with that obtained by Grinstein and Luther (1976).

As was noted in section 2.4 the universal form of the equation of state may be obtained by rescaling H_R , M_R and t_R and then imposing suitable normalisation conditions on these new fields (Amit, 1984; Aharony and Bruce, 1974). Rescaling the variables so they satisfy the normalisations

$$y = \frac{H_R}{M_R^2} = 1 \quad \text{at} \quad t_R = 0 \quad (2.85)$$

and

$$\chi = \frac{t_R}{M_R^{1/\beta}} = -1 \quad \text{at} \quad H_R = 0, t_R < 0 \quad (2.86)$$

where $\delta = 3 + o(\epsilon)$ and $\beta = \frac{1}{2} + \frac{1}{4} \left(\frac{6}{53}\right)^{1/2} \epsilon^{1/2} + o(\epsilon)$ the equation of state becomes $y = f(x)$ where

$$f(x) = 1 + x + \frac{1}{2} \left(\frac{6}{53}\right)^{1/2} \epsilon^{1/2} x \ln \left\{ \frac{x+3}{2} \right\} + o(\epsilon) \quad (2.87)$$

From this can be obtained the other amplitude ratios for the specific heat and correlation length (Newlove, 1983).

We have therefore obtained a renormalised equation of state in scaling form to one-loop, and extracted the susceptibility amplitude ratio to the same order. In the next section we extend the calculation to obtain the next term in the ϵ -expansion of C_+/C_- .

2.6. Two-Loop expansion of Susceptibility Amplitude Ratio

In the previous section we gave a complete description of a one-loop calculation of the equation of state. There are two motivations for proceeding with a two-loop calculation of the susceptibility amplitude ratio, the one-loop term having been obtained in section 2.5

- as we shall discuss in section 2.7 the $o(\epsilon^{1/2})$ term obtained from the one-loop equation comes in with the "wrong" sign, i.e., the one-loop result is further from the experimental value than the tree approximation. It is relevant to ask whether or not this trend continues at higher order

- it is of inherent interest to explore the feasibility of the analytic calculation to this order.

This latter point is of non-trivial importance. Firstly, in general we would expect to obtain integrals within our expansions involving non-trivial combinations of the two masses, $r_{||}$ and r_{\perp} , present in the Hamiltonian. However, expanding transverse propagators about the longitudinal one as a power series in n and then taking the $n \rightarrow 0$ limit leaves us with pure Ising-like diagrams. Secondly, we avoid the renormalisations of the full equation of state by directly calculating the amplitude ratio in the bare theory. Thirdly, one would expect the finite parts of integrals (the difficult pieces to evaluate) to contribute to the result. Remarkably, this is not so in this case - all that is required are the poles in two integrals. Finally, to obtain the fixed point to $o(\epsilon)$ requires the β -functions to be known to three loops for the $\epsilon^{1/2}$ expansion. These have been calculated by Jayaprakash and Katz (1982) in a different renormalisation scheme. We derive the $o(\epsilon)$ values in our scheme by combining our two-loop β -functions and their values of the exponents ν and η to $o(\epsilon^{3/2})$. The latter part of this work was carried out in collaboration with D.J. Wallace and the following equations summarise the details of this rather lengthy calculation.

As before, our starting point is the Hamiltonian in terms of the shifted fields, Φ , given in equation (2.40). From this Hamiltonian we obtain the equation of state as the graphical expansion of the equation $\langle \Phi_{||} \rangle = 0$; this reads, for the graphs with their weights,

$$\begin{aligned}
\circ &= n^4 M_0 (t_0 + \frac{1}{6} u_0 n M_0^2 + \frac{1}{6} v_0 M_0^2) - n^4 H_0 + n^4 M_0 \left[\frac{1}{2} (u_0 + \frac{v_0}{n}) - \circ \right] + \frac{1}{6} (n-1) (u_0 + 3 \frac{v_0}{n}) - \circ \\
&- n^4 M_0 \left[\frac{1}{6} (u_0 + \frac{v_0}{n})^2 - \circ + \frac{1}{18} (n-1) (u_0 + 3 \frac{v_0}{n})^2 - \circ + \frac{1}{6} (n-1)(n-2) (\frac{v_0}{n})^2 - \circ \right] \\
&+ n^4 M_0 M_0^2 \left[\frac{1}{4} n (u_0 + \frac{v_0}{n})^3 - \circ + \frac{1}{36} n(n-1) (u_0 + \frac{v_0}{n}) (u_0 + 3 \frac{v_0}{n})^2 - \circ \right. \\
&\quad \left. + \frac{1}{54} n(n-1) (u_0 + 3 \frac{v_0}{n})^3 - \circ + \frac{1}{12} n(n-1)(n-2) (\frac{v_0}{n})^2 (u_0 + 3 \frac{v_0}{n}) - \circ \right] \\
&- n^4 M_0 \left[\frac{1}{4} (u_0 + \frac{v_0}{n})^2 - \circ + \frac{1}{12} (n-1) (u_0 + 3 \frac{v_0}{n}) (u_0 + \frac{v_0}{n}) - \circ \right. \\
&\quad \left. + \frac{1}{36} (n-1) (u_0 + 3 \frac{v_0}{n})^2 - \circ \right. \\
&\quad \left. + \frac{1}{36} (n-1) (u_0 + 3 \frac{v_0}{n}) (n+1) u_0 + 3(n+1) \frac{v_0}{n} - \circ \right]
\end{aligned}$$

(2.88)

We now employ the same techniques as outlined in the previous section for the one-loop calculation and expand the transverse propagators in the diagrams as Taylor series in n about the longitudinal and then take the $n \rightarrow 0$ limit (after checking the cancellation of the n^{-1} and n^{-2} factors). The resulting form of the equation of state in graphical notation is

$$\begin{aligned}
\frac{H_0}{M_0} &= t_0 + \frac{1}{6} v_0 M_0^2 + \frac{1}{6} (2u_0 + 3v_0) - \circ - \frac{1}{6} u_0 v_0 M_0^2 - \circ \\
&- \frac{1}{18} (2u_0^2 + 6u_0 v_0 + 3v_0^2) - \circ + \frac{1}{18} u_0 (4u_0 + 3v_0) v_0 M_0^2 - \circ - \frac{1}{18} u_0^2 (v_0 M_0^2)^2 - \circ \\
&+ \frac{1}{36} (14u_0^2 + 24u_0 v_0 + 9v_0^2) v_0 M_0^2 - \circ - \frac{1}{18} u_0 (4u_0 + 3v_0) (v_0 M_0^2)^2 - \circ \\
&- \frac{1}{6} u_0 (2u_0 + v_0) (v_0 M_0^2)^2 - \circ + \frac{1}{9} u_0^2 (v_0 M_0^2)^3 - \circ + \frac{1}{36} u_0^2 (v_0 M_0^2)^3 - \circ \\
&- \frac{1}{36} (2u_0 + 3v_0)^2 - \circ + \frac{1}{36} u_0 (4u_0 + 3v_0) v_0 M_0^2 - \circ \\
&+ \frac{1}{18} u_0 (2u_0 + 3v_0) v_0 M_0^2 - \circ - \frac{1}{18} u_0 (v_0 M_0^2)^2 - \circ
\end{aligned}$$

(2.89)

In the above equation a notched line denotes a zero momentum insertion arising from the expansion of a transverse propagator, and the graphs

represent the integrals arising in the Feynman graph expansion, e.g.,

$$\text{---} \bigcirc = \int \frac{d^d q}{q^2 + b} \quad (2.90)$$

(recall that b is the $n \rightarrow 0$ limit of r_{11}). The integrals appearing in the above equation can be related to one another by differentiating lowest order terms with respect to b . Using the resulting relations, collecting terms and explicitly extracting the factors of b from the integrals we obtain

$$\begin{aligned} \frac{H_0}{M_0} = & b + \frac{1}{6} v_0 M_0^2 + \frac{1}{6} b^{1-\epsilon/2} I_0^0 \{ (2u_0 + 3v_0) + (1-\epsilon/2) u_0 (v_0 M_0^2) b^{-1} \} \\ & - b^{\epsilon/2} I_0^0 \left\{ \frac{1}{18} (2u_0^2 + 6u_0 v_0 + 3v_0^2) + \frac{1}{108} (1-\epsilon) (22u_0^2 + 30u_0 v_0 + 9v_0^2) v_0 M_0^2 b^{-1} \right. \\ & \quad \left. - \frac{1}{108} \epsilon (1-\epsilon) u_0 (4u_0 + 3v_0) (v_0 M_0^2)^2 b^{-2} \right\} \\ & - b I_2^2 \left\{ \frac{1}{6} u_0^2 (v_0 M_0^2)^2 b^{-2} - \frac{1}{36} u_0^2 (v_0 M_0^2)^3 b^{-3} \right\} \\ & + b^{1-\epsilon} (I_0^0)^2 \left\{ \frac{1}{36} (1-\frac{\epsilon}{2}) (2u_0 + 3v_0)^2 + \frac{1}{36} (1-\frac{\epsilon}{2})^2 u_0 (4u_0 + 3v_0) v_0 M_0^2 b^{-1} \right. \\ & \quad \left. - \frac{1}{72} \epsilon (1-\frac{\epsilon}{2}) u_0 (2u_0 + 3v_0) v_0 M_0^2 b^{-1} - \frac{1}{72} \epsilon (1-\frac{\epsilon}{2})^2 u_0^2 (v_0 M_0^2)^2 b^{-2} \right\} \quad (2.91) \end{aligned}$$

where

$$I_0^0 = \int \frac{d^d q}{q^2 + 1} \quad (2.92)$$

$$I_1^0 = \iint \frac{d^d k d^d q}{(q^2 + 1)(k^2 + 1)((k-q)^2 + 1)} \quad (2.93)$$

$$I_2^2 = \iint \frac{d^d k d^d q}{(q^2 + 1)^2 (k^2 + 1)((k-q)^2 + 1)} \quad (2.94)$$

To obtain the susceptibility amplitude ratio from the above expression we go back to the definition of the susceptibility as $\chi = (\partial M / \partial H)$. We require the

ratio

$$R = \frac{\left(\frac{\partial H_0}{\partial M_0}\right)_{H_0=0}^+}{\left(\frac{\partial H_0}{\partial M_0}\right)_{H_0=0}^-} = \frac{\left(\frac{\partial H_0}{\partial M_0}\right)_{H_0=0}^-}{\left(\frac{\partial H_0}{\partial M_0}\right)_{H_0=0}^+} \quad (2.95)$$

where the + (-) denotes $t > 0$ ($t < 0$). The denominator is trivial and is obtained from equation (2.91) by setting $M_0 = 0$ in the right-hand side. For the numerator, where $t_0 < 0$, write $H_0 = M_0 f(t_0, M_0)$. Then

$$\left(\frac{\partial H_0}{\partial M_0}\right)_{H_0=0} = f + M_0 \frac{\partial f}{\partial M_0} \quad (2.96)$$

$$= M_0 \frac{\partial f}{\partial M_0} \quad (2.97)$$

since $f(t_0, M_0) = 0$ in the limit $H_0 \rightarrow 0$. The numerator can therefore be rewritten as

$$\begin{aligned} \left(\frac{\partial H_0}{\partial M_0}\right)_{H_0=0}^- - 2f &= -2t_0 + \frac{1}{6} b^{-\frac{\epsilon}{2}} I_0^0 \left\{ (2u_0 + 3v_0) (-2t_0 - \frac{\epsilon}{2} v_0 M_0^2) + u_0 v_0 M_0^2 b^{-1} (-\frac{\epsilon}{2})(1 - \frac{\epsilon}{2}) \right\} \\ &+ b^{-\epsilon} I_1^0 \left\{ -\frac{1}{18} (2u_0^2 + 6u_0 v_0 + 3v_0^2) (-2t_0 - \epsilon v_0 M_0^2) \right. \\ &\quad \left. + \frac{\epsilon(1-\epsilon)}{108} (v_0 M_0^2)^2 b^{-1} \left[(22u_0^2 + 30u_0 v_0 + 9v_0^2) - (4u_0 + 3v_0) u_0 b^{-1} (-2t_0 + \epsilon v_0 M_0^2) \right] \right\} \\ &+ \frac{1}{36} I_2^2 u_0^2 (v_0 M_0^2)^2 b^{-3} \left[-12b^2 + 10b(v_0 M_0^2) - 2(v_0 M_0^2)^2 \right] \\ &+ (I_0^0)^2 b^{-\epsilon} \left[\frac{1}{36} (2u_0 + 3v_0)^2 (1 - \frac{\epsilon}{2}) (-2t_0 - \epsilon v_0 M_0^2) \right. \\ &\quad - \frac{\epsilon}{36} (1 - \frac{\epsilon}{2})^2 u_0 (4u_0 + 3v_0) (v_0 M_0^2) b^{-1} \\ &\quad + \frac{1}{72} \epsilon^2 (1 - \frac{\epsilon}{2}) u_0 (2u_0 + 3v_0) (v_0 M_0^2) b^{-1} \\ &\quad \left. + \frac{1}{72} \epsilon (1 - \frac{\epsilon}{2})^2 u_0^2 (-2t_0 + \epsilon v_0 M_0^2) (v_0 M_0^2)^2 b^{-2} \right] \quad (2.98) \end{aligned}$$

We now need to know b and $v_0 M_0^2$ to first order. These are obtained by solving the equation $f=0$ perturbatively for $v_0 M_0^2$, giving the results

$$b = (-2t_0) \left\{ 1 - \frac{1}{2} I_0^0 (-2t_0)^{-\frac{\epsilon}{2}} \left[\left(5 - \frac{3\epsilon}{2}\right) u_0 + 3v_0 \right] \right\} \quad (2.99)$$

$$v_0 M_0^2 = 3(-2t_0) \left\{ 1 - \frac{1}{3} I_0^0 (-2t_0)^{-\frac{\epsilon}{2}} \left[\left(5 - \frac{3\epsilon}{2}\right) u_0 + 3v_0 \right] \right\} \quad (2.100)$$

Substituting these expressions back into equation (2.98) gives the numerator

as

$$\begin{aligned} \text{numerator} = & (-2t_0) \left\{ 1 + \frac{1}{6} (-2t_0)^{-\frac{\epsilon}{2}} I_0^0 \left[(2u_0 + 3v_0) \left(1 - \frac{3\epsilon}{2}\right) - \frac{9}{2} u_0 \epsilon \left(1 - \frac{\epsilon}{2}\right) \right] \right. \\ & + \frac{3}{8} \epsilon (-2t_0)^{-\epsilon} (I_0^0)^2 \left[\left(5 - \frac{3\epsilon}{2}\right) u_0 + 3v_0 \right] \left[u_0 + v_0 - \frac{1}{2} \epsilon (2u_0 + v_0) \right] \\ & + (-2t_0)^{-\epsilon} I_1^0 \left[-\frac{1}{18} (2u_0^2 + 6u_0v_0 + 3v_0^2) (1 - 3\epsilon) \right. \\ & \quad \left. + \frac{1}{12} \epsilon (1 - \epsilon) \left\{ (22u_0^2 + 30u_0v_0 + 9v_0^2) - (1 + 3\epsilon) u_0 (4u_0 + 3v_0) \right\} \right] \\ & + (I_0^0)^2 (-2t_0)^{-\epsilon} \left[\frac{1}{36} (2u_0 + 3v_0)^2 \left(1 - \frac{\epsilon}{2}\right) (1 - 3\epsilon) \right. \\ & \quad \left. - \frac{1}{8} \epsilon u_0 (7u_0 + 6v_0 - 3\epsilon [4u_0 + 3v_0]) \right] \left. \right\} \quad (2.101) \end{aligned}$$

and similarly

$$\begin{aligned} \text{denominator} = & t_0 \left\{ 1 + \frac{1}{6} t_0^{-\epsilon/2} I_0^0 (2u_0 + 3v_0) - \frac{1}{18} t_0^{-\epsilon} I_1^0 (2u_0^2 + 6u_0v_0 + 3v_0^2) \right. \\ & \left. + \frac{1}{36} (I_0^0)^2 t_0^{-\epsilon} (2u_0 + 3v_0)^2 \left(1 - \frac{\epsilon}{2}\right) \right\} \quad (2.102) \end{aligned}$$

Remarkably, the finite integral, I_2^0 , in the expansion of the equation of state below T_c has completely cancelled out. Expanding the ratio, R , and replacing $-t_0 \equiv t^*$ in the numerator, $t_0 \equiv t$ in the denominator we find

$$\begin{aligned}
R = 2 & \left[1 + \frac{1}{6} \epsilon^{-\epsilon/2} \mathbb{I}_0^0 \left\{ (2u_0 + 3v_0) \left(2^{-\epsilon/2} \left(1 - \frac{3\epsilon}{2} \right) - 1 \right) - \frac{9}{2} 2^{-\epsilon/2} \epsilon \left(1 - \frac{\epsilon}{2} \right) u_0 \right\} \right. \\
& \quad \times \left. \left\{ 1 - \frac{\epsilon^{-\epsilon/2}}{6} \mathbb{I}_0^0 (2u_0 + 3v_0) \right\} \right. \\
& \quad + \frac{3}{8} \epsilon (2t)^{-\epsilon} (\mathbb{I}_0^0)^2 \left\{ \left(5 - \frac{3\epsilon}{2} \right) u_0 + 3v_0 \right\} \left\{ u_0 + v_0 - \frac{1}{2} \epsilon (2u_0 + v_0) \right\} \\
& \quad + \epsilon^\epsilon \mathbb{I}_1^0 \left\{ -\frac{1}{18} (2u_0^2 + 6u_0v_0 + 3v_0^2) \left(2^{-\epsilon} (1 - 3\epsilon) - 1 \right) \right. \\
& \quad \quad \left. + \frac{1}{4} 2^{-\epsilon} \epsilon (1 - \epsilon) [6u_0^2 + 9u_0v_0 + 3v_0^2 - u_0 \epsilon (4u_0 + 3v_0)] \right\} \\
& \quad + \frac{1}{36} \epsilon^{-\epsilon} (\mathbb{I}_0^0)^2 \left\{ (2u_0 + 3v_0)^2 \left(1 - \frac{\epsilon}{2} \right) \left(2^{-\epsilon} (1 - 3\epsilon) - 1 \right) \right. \\
& \quad \quad \left. - \frac{9}{2} 2^{-\epsilon} \epsilon u_0 \left\{ 7u_0 + 6v_0 - 3\epsilon [4u_0 + 3v_0] \right\} \right\} \left. \right] \quad (2.103)
\end{aligned}$$

This expression must now be renormalised. We shall only introduce renormalised coupling constants as we will find that it is unnecessary to perform any other renormalisations. The one-loop expressions required are

$$u_0 = u_R + \frac{4}{3\epsilon} u_R^2 + \frac{u_R v_R}{\epsilon} \quad (2.104)$$

$$v_0 = v_R + \frac{2}{\epsilon} u_R v_R + \frac{3}{2\epsilon} v_R^2 \quad (2.105)$$

The integrals required are evaluated as (recall that we have absorbed factors of angular integration into a redefinition of the couplings)

$$\mathbb{I}_0^0 = -\frac{1}{\epsilon} + o(\epsilon) \quad (2.106)$$

$$\mathbb{I}_1^0 = -\frac{3}{2\epsilon^2} \left(1 + \frac{\epsilon}{2} + o(\epsilon^2) \right) \quad (2.107)$$

Substituting these into the expression for R , we verify that the poles in ϵ cancel. Now, the fixed point values of u_R and v_R obey the relation $4u_R + 3v_R = o(\epsilon)$. Knowing that the poles in R cancel we can simplify the expression for R by setting $4u_R + 3v_R = 0$ in the terms of second order in u_R and v_R , knowing that corrections are of order three loops. This removes the

need to renormalise the couplings at this order. We also set $t^{-\epsilon/2} \equiv 1$ since these terms are of higher order and are in fact guaranteed to cancel at the fixed point. The result of these manipulations is

$$R = 2 \left\{ 1 + \frac{1}{12} [(2u_R + 3v_R)(\ln 2 + 3) + 9u_R] + u_R^2 \left[\frac{(\ln 2)^2}{72} + \frac{\ln 2}{24} + \frac{5}{16} \right] \right\} \quad (2.108)$$

To obtain the susceptibility amplitude ratio we must evaluate this expression at the fixed point. The values of u_R^* and v_R^* are needed to $o(\epsilon)$ for this to be carried out correctly. However, because the expansion in this model is in terms of $\epsilon^{1/2}$, to obtain the fixed point values to $o(\epsilon)$ requires the β -functions to be known to three loops. Jayaprakash and Katz (1982) have calculated the β -functions to this level but in a different renormalisation scheme from ours; β -functions are only universal up to the two-loop level. Using their results for ν and η to $o(\epsilon^{3/2})$ it is possible to obtain the $o(\epsilon)$ corrections to u_R^* and v_R^* in dimensional regularisation by solving simultaneously the equations

$$\beta_u^* = 0 \quad (2.109)$$

$$\beta_v^* = 0 \quad (2.110)$$

$$\bar{\gamma}_{\phi^2}^* = 2 - \nu^{-1} - \eta \quad (2.111)$$

where

$$\bar{\gamma}_{\phi^2} = -\mu \left(\frac{\partial \ln \bar{Z}_{\phi^2}}{\partial \mu} \right)_{\text{bare}} \quad (2.112)$$

As the right-hand side of (2.112) involves a derivative with respect to the bare functions it is first of all necessary to invert the series for the renormalised

couplings in terms of the bare. The result for $\bar{\gamma}_\phi^2$ is

$$\bar{\gamma}_\phi^2 = \frac{1}{3}u_R + \frac{1}{2}v_R - \frac{1}{6}u_R^2 - \frac{1}{2}u_R v_R - \frac{1}{4}v_R^2 \quad (2.113)$$

(Note: this is independent of ϵ , a result guaranteed by minimal subtraction with dimensional regularisation (Amit, 1984))

Writing

$$u_R^* = -3\left(\frac{6}{53}\right)^{1/2} \epsilon^{1/2} + B\epsilon + o(\epsilon^{3/2}) \quad (2.114)$$

$$v_R^* = 4\left(\frac{6}{53}\right)^{1/2} \epsilon^{1/2} + D\epsilon + o(\epsilon^{3/2}) \quad (2.115)$$

the $o(\epsilon^{3/2})$ terms in both $\beta_u^* = 0$ and $\beta_v^* = 0$ lead to

$$3D + 4B = \frac{72}{53} \quad (2.116)$$

Jayaprakash and Katz (1982) quote the values

$$\nu = \frac{1}{2} + \frac{1}{4}\left(\frac{6}{53}\right)^{1/2} \epsilon^{1/2} + \frac{1}{4} \left\{ \frac{535 - 756\zeta(3)}{5618} \right\} \epsilon + o(\epsilon^{3/2}) \quad (2.117)$$

$$\eta = -\frac{1}{106} \epsilon + \left(\frac{6}{53}\right)^{1/2} \left\{ \frac{756\zeta(3) + 2592}{33708} \right\} \epsilon^{3/2} + o(\epsilon^2) \quad (2.118)$$

and using $\bar{\gamma}_\phi^* = 2 - \nu^{-1} - \eta$ implies

$$3D + 2B = -\left(\frac{6}{53}\right)^2 (4 + 63\zeta(3)) \quad (2.119)$$

Solving (2.116) and (2.119) simultaneously gives the fixed point values to $o(\epsilon)$ as

$$U_R^* = -3 \left(\frac{6}{53}\right)^{1/2} \epsilon^{1/2} + \frac{1}{2} \left(\frac{6}{53}\right)^2 (110 + 63\zeta(3)) \epsilon + o(\epsilon^{3/2}) \quad (2.120)$$

$$V_R^* = 4 \left(\frac{6}{53}\right)^{1/2} \epsilon^{1/2} - 2 \left(\frac{6}{53}\right)^2 (19 + 21\zeta(3)) \epsilon + o(\epsilon^{3/2}) \quad (2.121)$$

Substituting these values into equation (2.108) we finally obtain the universal ratio of susceptibility amplitudes to two loops as

$$\begin{aligned} \frac{C_+}{C_-} = & 2 \left\{ 1 + \left(\frac{6}{53}\right)^{1/2} \left(\frac{1}{2} \ln 2 - \frac{3}{4}\right) \epsilon^{1/2} \right. \\ & + \frac{\epsilon}{12} \left(\frac{6}{53}\right)^2 \left\{ \frac{189}{2} \zeta(3) - 63 \ln 2 \cdot \zeta(3) - 4 \ln 2 + 483 \right\} \\ & \left. + \frac{54}{53} \cdot \epsilon \left\{ \frac{(\ln 2)^2}{72} + \frac{\ln 2}{24} + \frac{5}{16} \right\} \right\} \quad (2.122) \end{aligned}$$

2.7. Conclusions

In this chapter we have obtained an expression for the susceptibility amplitude ratio in the random Ising model to two loops, extending the previous result of Newlove (1983). In Table 2-1 we naively set $\epsilon=1$ in equation (2.122) and tabulate the results for the one-loop and two-loop calculations alongside experimental values obtained for the random system.

	One Loop	Two Loop	Experiment ^(a)
C_+			
--	1.7	3.6	2.45±0.15
C_-			

(a) Birgeneau *et al*, (1986)

Table 2-1: Comparison of results for susceptibility amplitude ratio

The value obtained for C_+/C_- at two loops is considerably higher than the experimental value. The calculation detailed in the previous section confirms that the trend of a negative correction at one-loop is not carried through to the next order in the ϵ -expansion of the ratio in this model. Using a Padé approximant to try and improve the estimate for the ratio yields the value of 1.9.

The strongest statement that can be made about this two-loop result is that the new correction calculated takes the theoretical value "in the right direction", compared to the one-loop result. The practice of setting $\epsilon=1$ in an order $\epsilon^{1/2}$ result to obtain values to compare with experiments in three dimensions is not to be regarded with much seriousness. Since a perturbation expansion parameter should be "small", $\epsilon^{1/2}$ expansions would be expected to give less trustworthy results than an ϵ -expansion to the same order.

STRUCTURE FACTOR IN THE RANDOM ISING MODEL

3.1. Introduction

Experimental data on the critical properties of magnetic systems are in a large part based on neutron scattering measurements of the dynamical structure factor, $S(\mathbf{q}, \omega)$, where \mathbf{q} is the neutron momentum and ω the neutron energy. This is calculated from the scattering cross-section using the relation

$$\frac{d^2\sigma}{d\Omega d\omega} = c \frac{k'}{k} S(\mathbf{q}, \omega), \quad c = \text{constant} \quad (3.1)$$

where

k' = incident wave number

k = scattered wave number

The spin structure factor, defined as the integral over energy of $S(\mathbf{q}, \omega)$, is related to the average Fourier transform of the spin-spin correlation function $[\langle s_\mu(0)s_\mu(\mathbf{x}) \rangle]$ where $\langle \dots \rangle$ implies a thermal average and $[\dots]$ an average over the impurity distribution. Below T_c the longitudinal spin structure factor, i.e., the component of S parallel to the order parameter, M , is

$$S_{\parallel}(\mathbf{q}) = [\langle S_{\parallel}(\mathbf{q}) S_{\parallel}(-\mathbf{q}) \rangle] = \chi_{\parallel}(\mathbf{q}) + C^{(s)}(\mathbf{q}) + M^2 \delta(\mathbf{q}) \quad (3.2)$$

The existence of a term $C^{(s)}(\mathbf{q})$ is a consequence of the non-interchangeability of the thermal and configurational averages and is therefore identically zero for pure systems, and below T_c in the random system; it is a measure of the fluctuations in the local quenched order parameter, and was first pointed out

by Grinstein, Ma and Mazenko (1977) in connection with the dynamics of a random Ising model. These authors proved that in mean field theory,

$$C^{(s)}(q) = \chi_{||}^2(q) \Delta M^2 \quad (3.3)$$

where Δ is the variance of the random distribution (see section 2.3). For the random Ising model this becomes

$$C^{(s)}(q) = \frac{\Delta M^2}{(\chi_{||}(0)^{-1} + Kq^2)^2} \quad (3.4)$$

where K is a constant (Aharony and Pelcovits, 1985). Thus, in mean field theory, this new correlation function exhibits a Lorentzian squared behaviour reminiscent of that found in random field problems. As has been shown by Aharony and Pelcovits (1985) this no longer holds true below the upper critical dimension, and equation (3.4) becomes, for small q ,

$$C^{(s)}(0) = K' \Delta \chi_{||}(0) \quad (3.5)$$

where K' is another constant, i.e., Lorentzian behaviour for small q . Both the general scaling arguments presented in Aharony and Pelcovits, and the explicit calculations of these authors and of the present work show that $C^{(s)}(q=0)$ diverges like $\chi(q=0)$, with an amplitude which is a universal factor times that of $\chi(q=0)$. The appearance of this factor has important consequences for the interpretation of the measured susceptibility amplitude ratio, implying that the experimental results are in fact measuring

$$\frac{C_+}{(1 + K'\Delta)C_-} \quad \text{and not} \quad \frac{C_+}{C_-} \quad (3.6)$$

This also implies that the susceptibility amplitude ratio calculated in the

previous chapter should not be the one compared with the results of neutron scattering experiments. These points are amplified in the discussion at the end of the present chapter.

In this chapter we derive these equations and give a field theoretic derivation of the correlation function, $C^{(s)}(q)$ at $q=0$ to order $\epsilon^{1/2}$, thereby extending the result of Aharony and Pelcovits (1985) to one higher order. This is achieved by utilising an extension of the replica formalism to the case of multiple replica spaces. In section 3.4 we compare experimental results for the susceptibility amplitude ratio with calculated values in the light of this extra term.

3.2. Double Replica Trick

In this section we describe in more detail how the term $C^{(s)}(q)$ arises in the longitudinal structure factor, and introduce a generalisation of the replica trick that allows us to calculate the correlation function in perturbation theory.

As we discussed in section 2.2, the quenched randomness in a disordered system is incorporated by performing a configurational average with respect to the impurity distribution over the free energy, i.e.,

$$\overline{F\{J\}} = \int D\psi P(\psi) \ln Z\{\psi, J\} \quad (3.7)$$

and

$$Z\{\psi, J\} = \int D\phi e^{-\mathcal{H}\{\phi, \psi, J\}} \quad (3.8)$$

where $\mathcal{H}\{\phi, \psi, J\}$ is the random Ising Hamiltonian of equation (2.7). As outlined in section 1.2, correlation functions are generated by appropriate functional

derivatives of the free energy, F , with respect to the source term, J , e.g.,

$$\frac{\delta}{\delta J(x)} \overline{F\{J\}} \Big|_{J=0} = - \int D\psi P(\psi) \frac{1}{Z\{\psi, J\}} \int D\phi \phi(x) e^{-K\{\phi, \psi, J\}} \Big|_{J=0} \quad (3.9)$$

$$= - [\langle \phi(x) \rangle] \quad (3.10)$$

and

$$\frac{\delta^2}{\delta J(x) \delta J(y)} \overline{F\{J\}} \Big|_{J=0} = [\langle \phi(x) \phi(y) \rangle] - [\langle \phi(x) \rangle \langle \phi(y) \rangle] \quad (3.11)$$

Now, in Fourier space

$$C^{(2)}(q) = [\langle \phi(q) \phi(-q) \rangle] - M^2 \delta(q) \quad (3.12)$$

and we are therefore interested in derivatives which generate the first term above. In real space

$$[\langle \phi(x) \rangle \langle \phi(y) \rangle] = \int D\psi P(\psi) \frac{\delta F\{J\}}{\delta J(x)} \Big|_{J=0} \cdot \frac{\delta F\{J\}}{\delta J(y)} \Big|_{J=0} \quad (3.13)$$

$$= \int D\psi P(\psi) \left(\frac{\delta}{\delta J(x)} \ln Z\{\psi, J\} \right) \Big|_{J=0} \left(\frac{\delta}{\delta J(y)} \ln Z\{\psi, J\} \right) \Big|_{J=0} \quad (3.14)$$

In order to calculate the average over the impurity, ψ , we are forced to introduce two sets of replicas, $\phi_{(1)}$ and $\phi_{(2)}$, each with n components. Then, as in section 2.3,

$$[\langle \phi(x) \rangle \langle \phi(y) \rangle] = \lim_{n \rightarrow 0} \frac{1}{n^2} \int D\psi P(\psi) \left\{ \frac{\delta}{\delta J(x)} \int D\phi_{(1)} e^{-K\{\phi_{(1)}, \psi, J\}} \right\} \Big|_{J=0} \\ \times \left\{ \frac{\delta}{\delta J(y)} \int D\phi_{(2)} e^{-K\{\phi_{(2)}, \psi, J\}} \right\} \Big|_{J=0} \quad (3.15)$$

where \mathcal{K} is given by equation (2.17). In the above $\int d\phi$ is shorthand for $\int \Pi d\phi_i$.

Carrying out the functional derivatives and performing the Gaussian integral over ψ (assuming a Gaussian distribution for ψ) we obtain

$$[\langle \phi(x) \rangle \langle \phi(y) \rangle] = \lim_{n \rightarrow 0} \frac{1}{n^2} \int \mathcal{D}\phi_{(1)} \mathcal{D}\phi_{(2)} \left(\sum_{\alpha=1}^n \phi_{(1)}^\alpha \right) \left(\sum_{\beta=1}^n \phi_{(2)}^\beta \right) e^{-[\mathcal{K}\{\phi_{(1)}\} + \mathcal{K}\{\phi_{(2)}\}]} \quad (3.16)$$

If we now construct the vector $\sigma = (\phi_{(1)}^1, \dots, \phi_{(1)}^n, \phi_{(2)}^1, \dots, \phi_{(2)}^n)$ in the direct sum space of the two replica spaces, then

$$[\langle \phi(x) \rangle \langle \phi(y) \rangle] = \lim_{n \rightarrow 0} \frac{1}{n^2} \int \mathcal{D}\sigma \left(\sum_{\alpha=1}^n \sigma^\alpha \right) \left(\sum_{\beta=n+1}^{2n} \sigma^\beta \right) e^{-\mathcal{K}\{\sigma\}} \quad (3.17)$$

where the Hamiltonian is of the form (2.17) but with a 2n-component field.

We therefore apply the same transformation as in Chapter 2, and shift the σ field below T_c ,

$$\underline{\sigma} = (\alpha + (2n)^{1/2} M) \underline{e}_1 + \sum_{j=2}^{2n} \beta_j \underline{e}_j \quad (3.18)$$

where α is the longitudinal field and the β_j are the $2n-1$ transverse fields. The $2n$ vectors $\{\underline{e}_j\}$ are defined by

$$\underline{e}_1 = (2n)^{-1/2} (1, 1, \dots, 1) \quad (3.19)$$

$$\sum_{\alpha=1}^{2n} \underline{e}_i^\alpha \underline{e}_j^\alpha = \underline{e}_i \cdot \underline{e}_j = \delta_{ij} \quad (3.20)$$

$$\sum_{\alpha=1}^{2n} \underline{e}_i^\alpha = 0, \quad i = 2, \dots, 2n \quad (3.21)$$

$$\sum_{j=2}^{2n} \underline{e}_j^\alpha \underline{e}_j^\beta = \delta^{\alpha\beta} - \frac{1}{2n} \quad (3.22)$$

The Hamiltonian obtained is identical to equation (2.40) with the replacements

$$n \rightarrow 2n \quad (3.23)$$

$$(\underline{\Phi}_{\parallel}, \underline{\Phi}_{\perp}) \rightarrow (\underline{\alpha}, \underline{\beta}) \quad (3.24)$$

and the new definitions

$$a_{ijk} = \sum_{\alpha=1}^{2n} e_i^{\alpha} e_j^{\alpha} e_k^{\alpha} \quad (3.25)$$

$$b_{ijkl} = \sum_{\alpha=1}^{2n} e_i^{\alpha} e_j^{\alpha} e_k^{\alpha} e_l^{\alpha} \quad (3.26)$$

In terms of the new, shifted fields the static correlation function under consideration becomes

$$C^{(s)}(q=0) = \lim_{n \rightarrow 0} \frac{1}{2n} \{ \langle \alpha\alpha \rangle - \langle \beta\beta \rangle \} \quad (3.27)$$

where, since the β fields are degenerate, we use

$$\Gamma_{\beta_i \beta_j}^{(2)} = \Gamma_{\beta\beta}^{(2)} \delta_{ij} \quad (3.28)$$

Hence, to calculate $C^{(s)}(q=0)$ we need only calculate the two point functions

$\Gamma_{\alpha\alpha}^{(2)}$ and $\Gamma_{\beta\beta}^{(2)}$. In the next section we proceed with the evaluation of these quantities in perturbation theory.

3.3. Calculation of $C^{(s)}(q=0)$

The calculation of $C^{(s)}(q=0)$ requires us to evaluate the renormalised two-point functions from the $2n$ -component Hamiltonian described in the previous section and in Chapter 2. The basic method is as discussed in Chapter 1 and detailed more fully in the previous chapter. However, we do not expand the transverse propagators about the longitudinal in this case as the calculation to the one-loop order considered here is feasible using the standard methods.

Renormalisation of the theory

The renormalised parameters are the same as in Chapter 2, with the replacement of n by $2n$ wherever it appears. They read

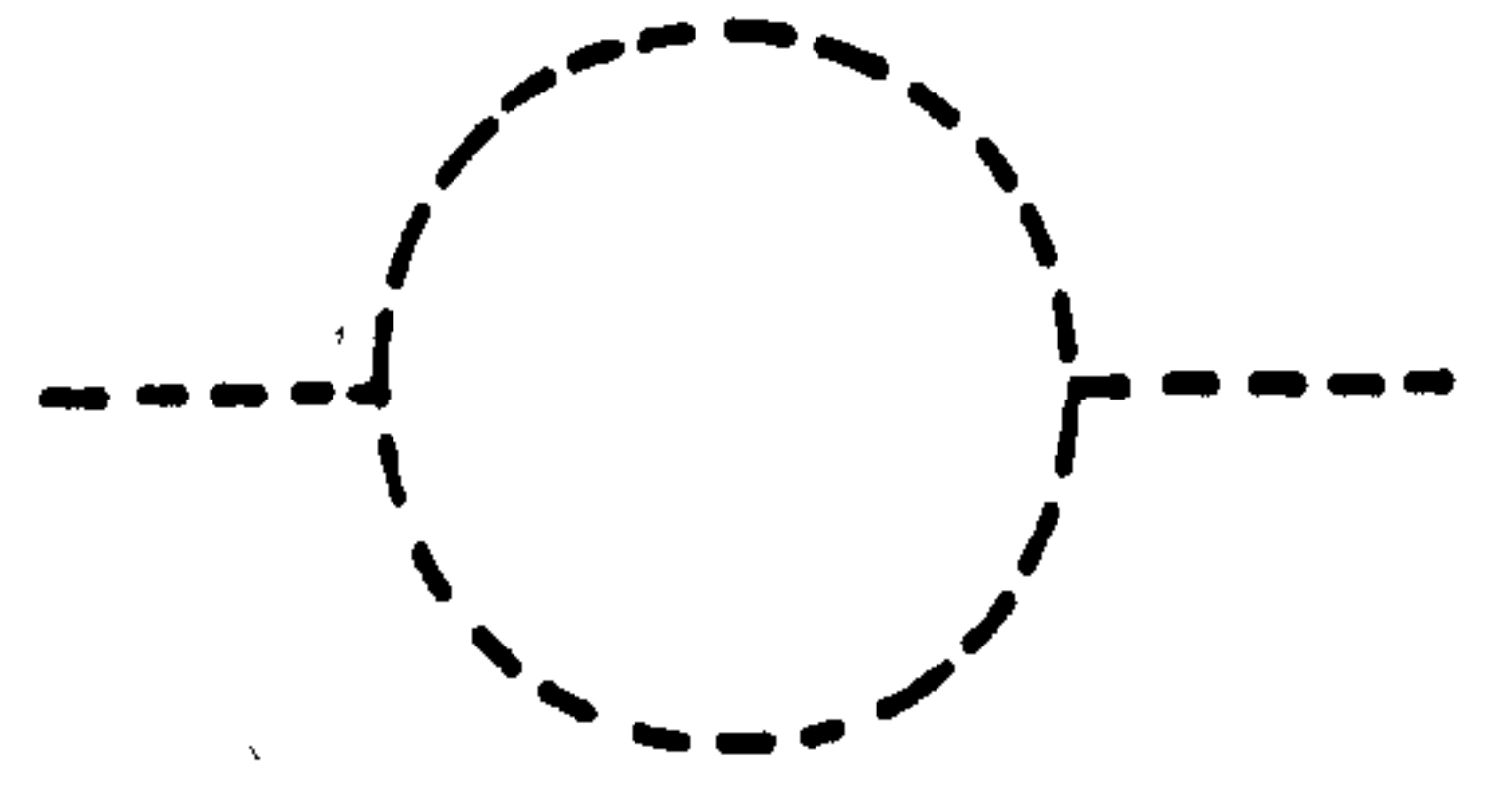
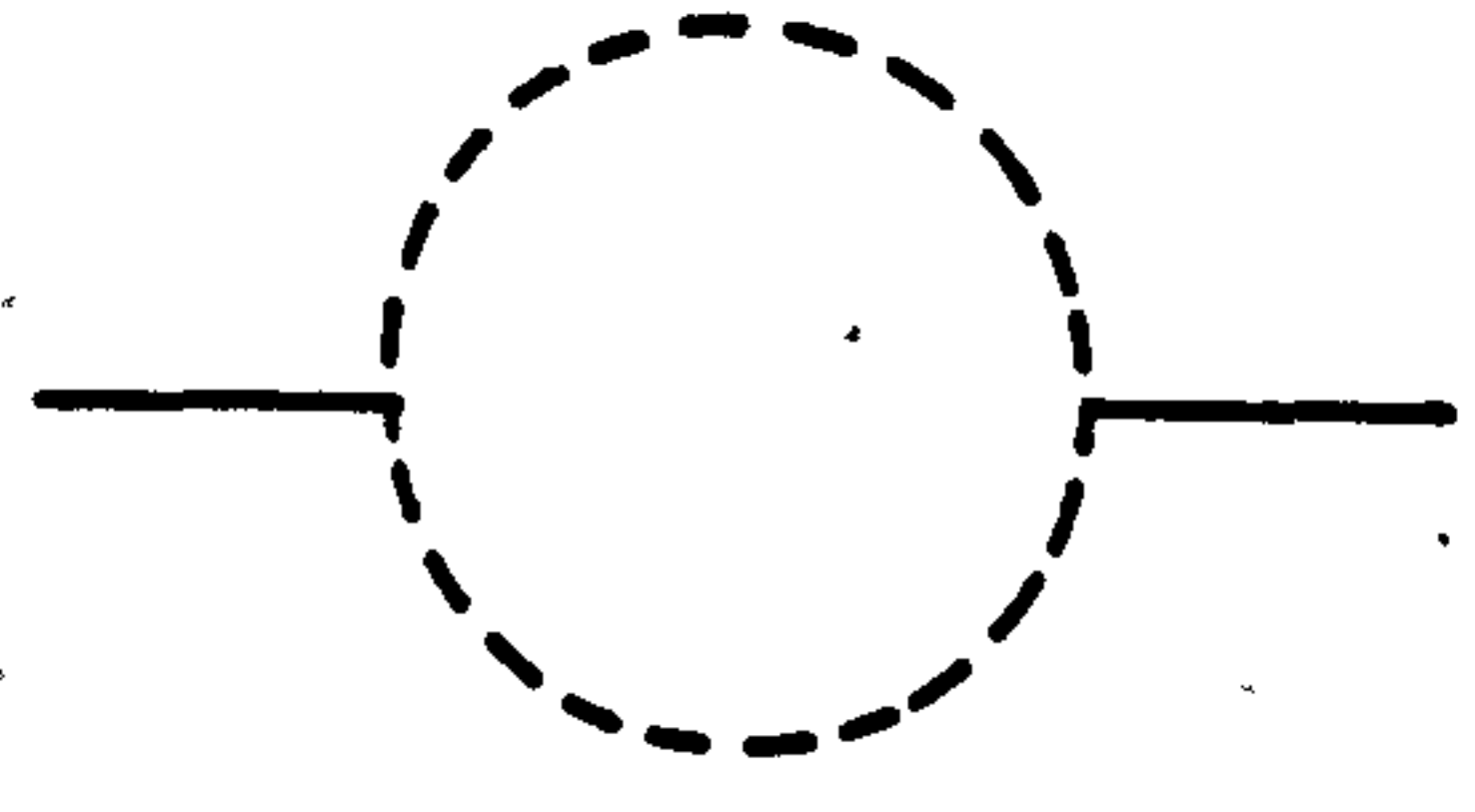
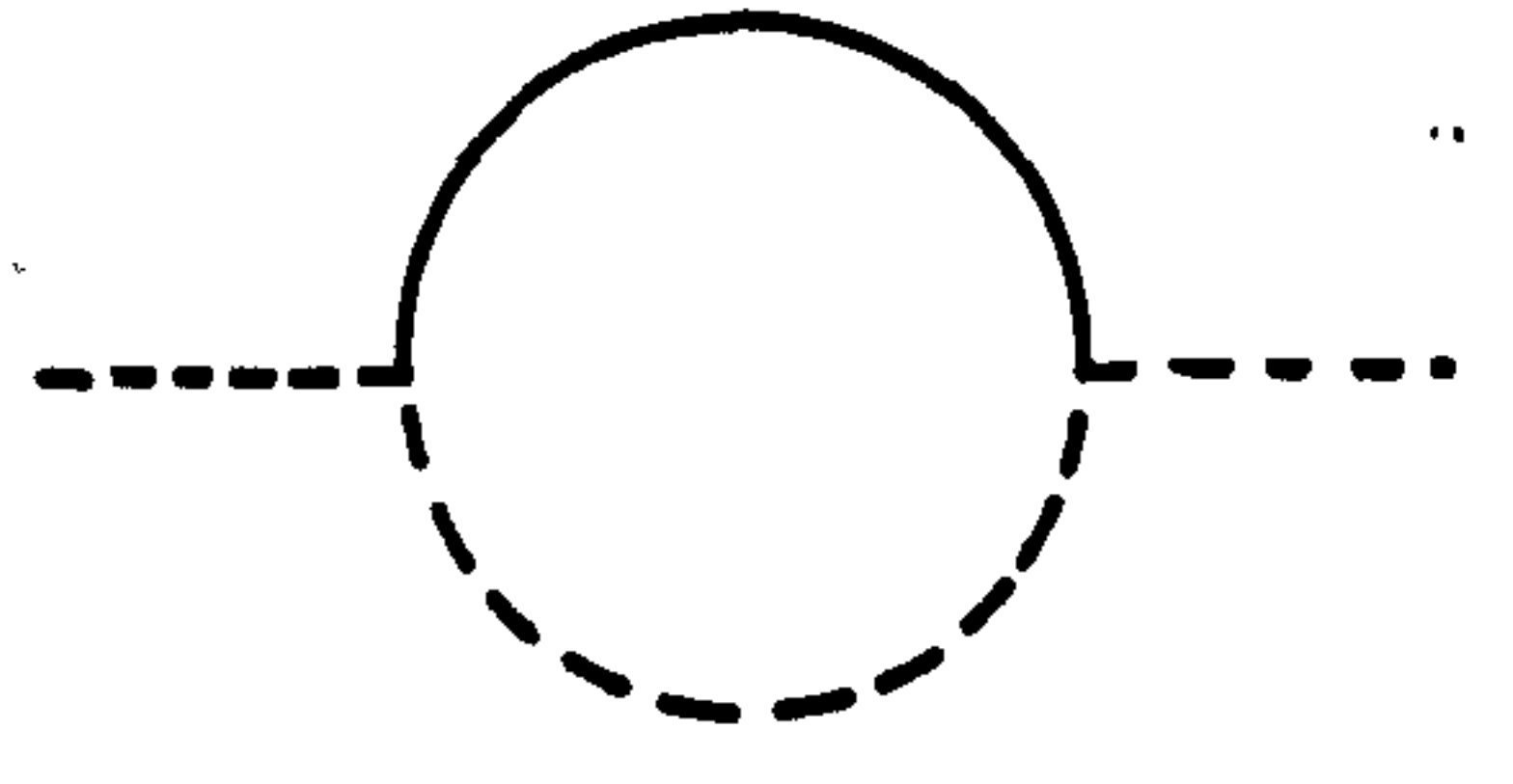
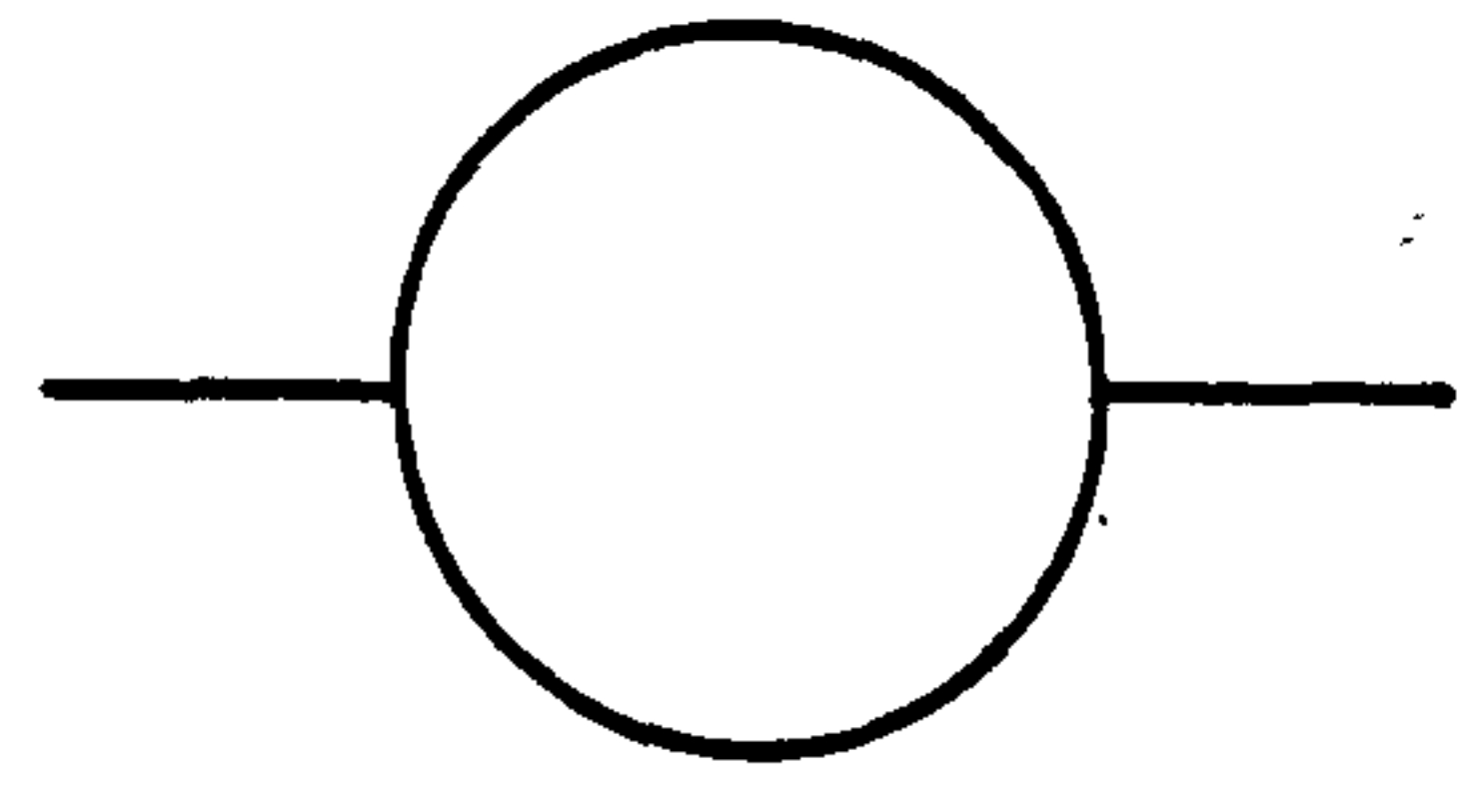
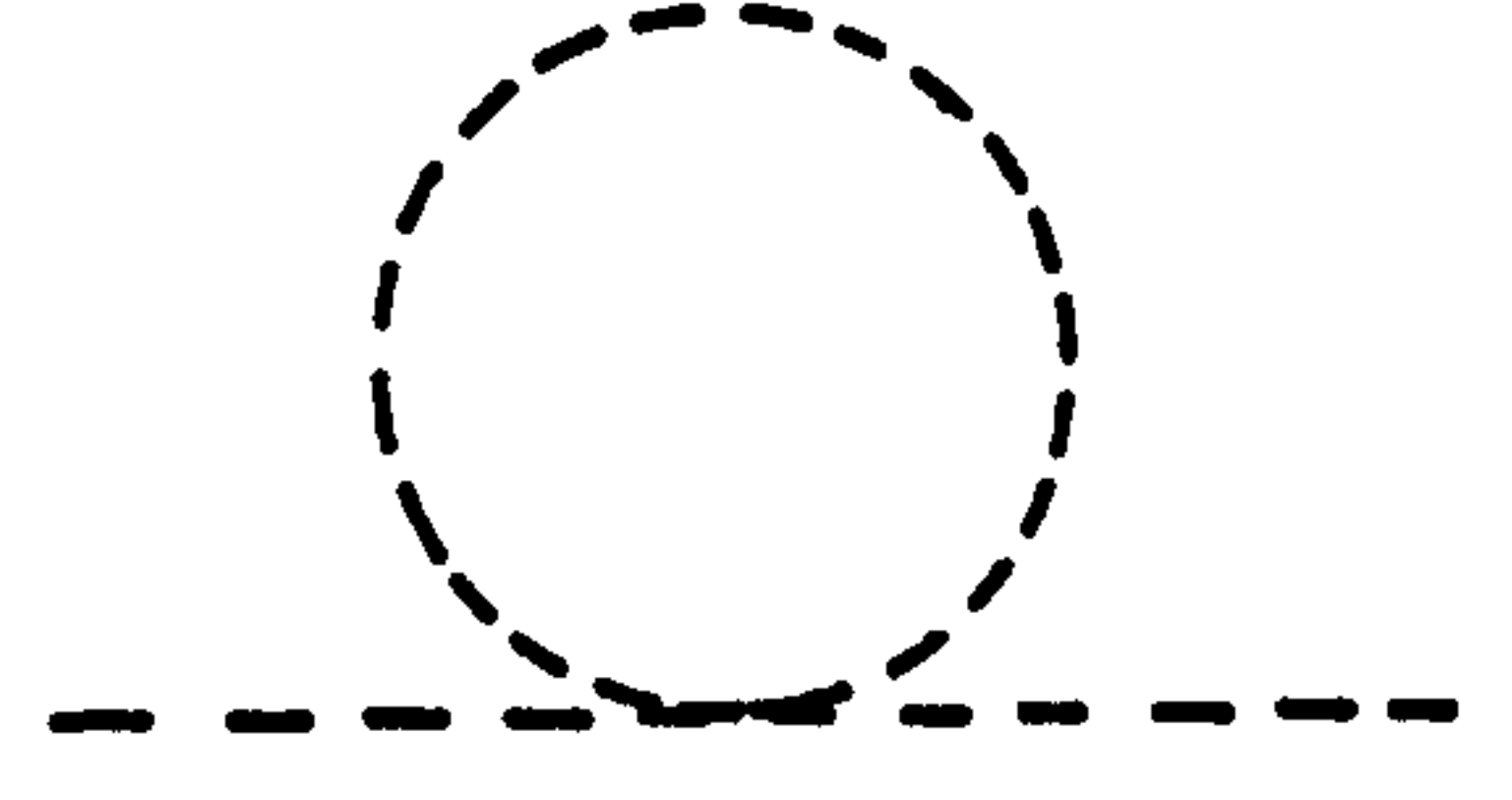
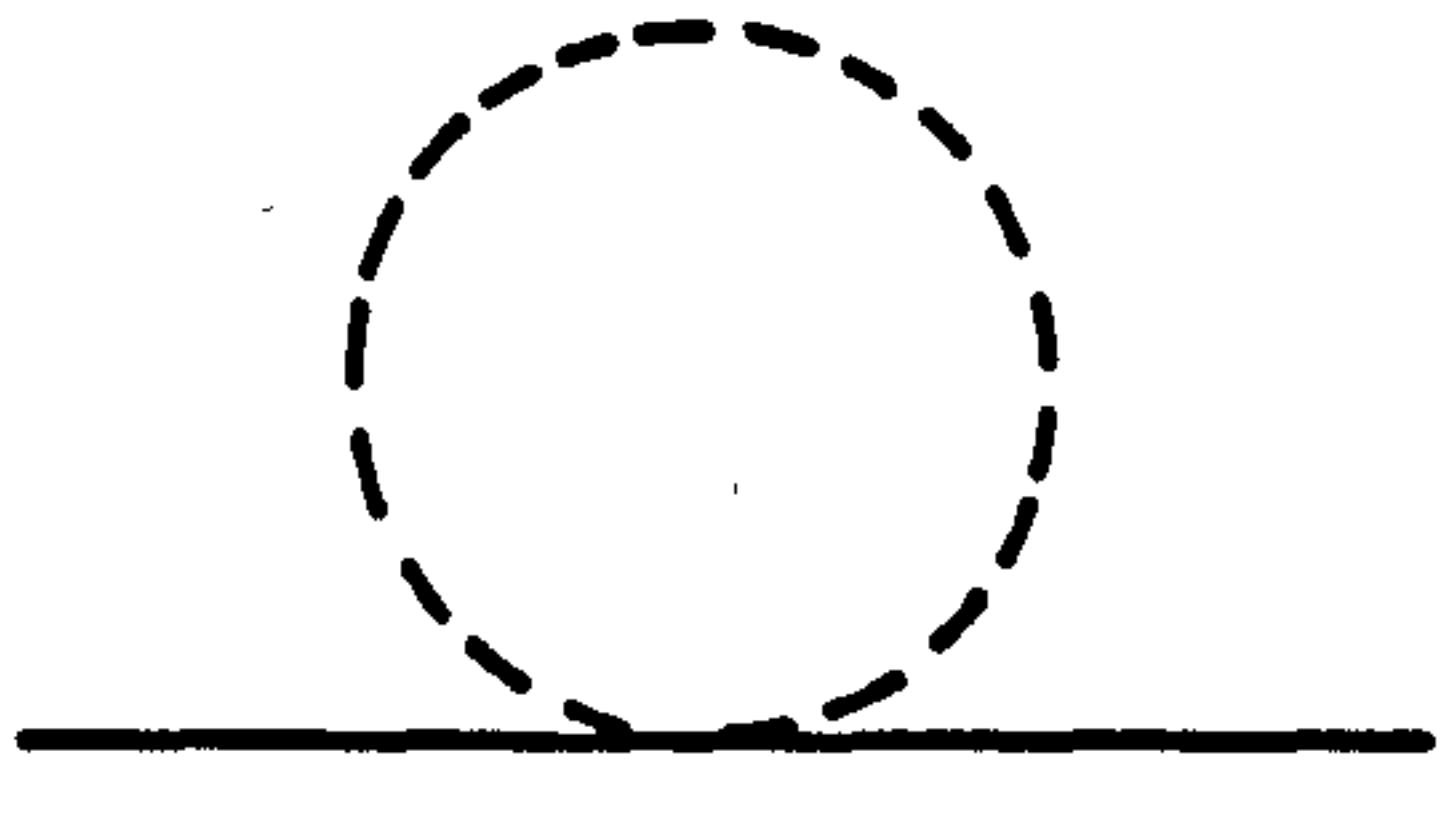
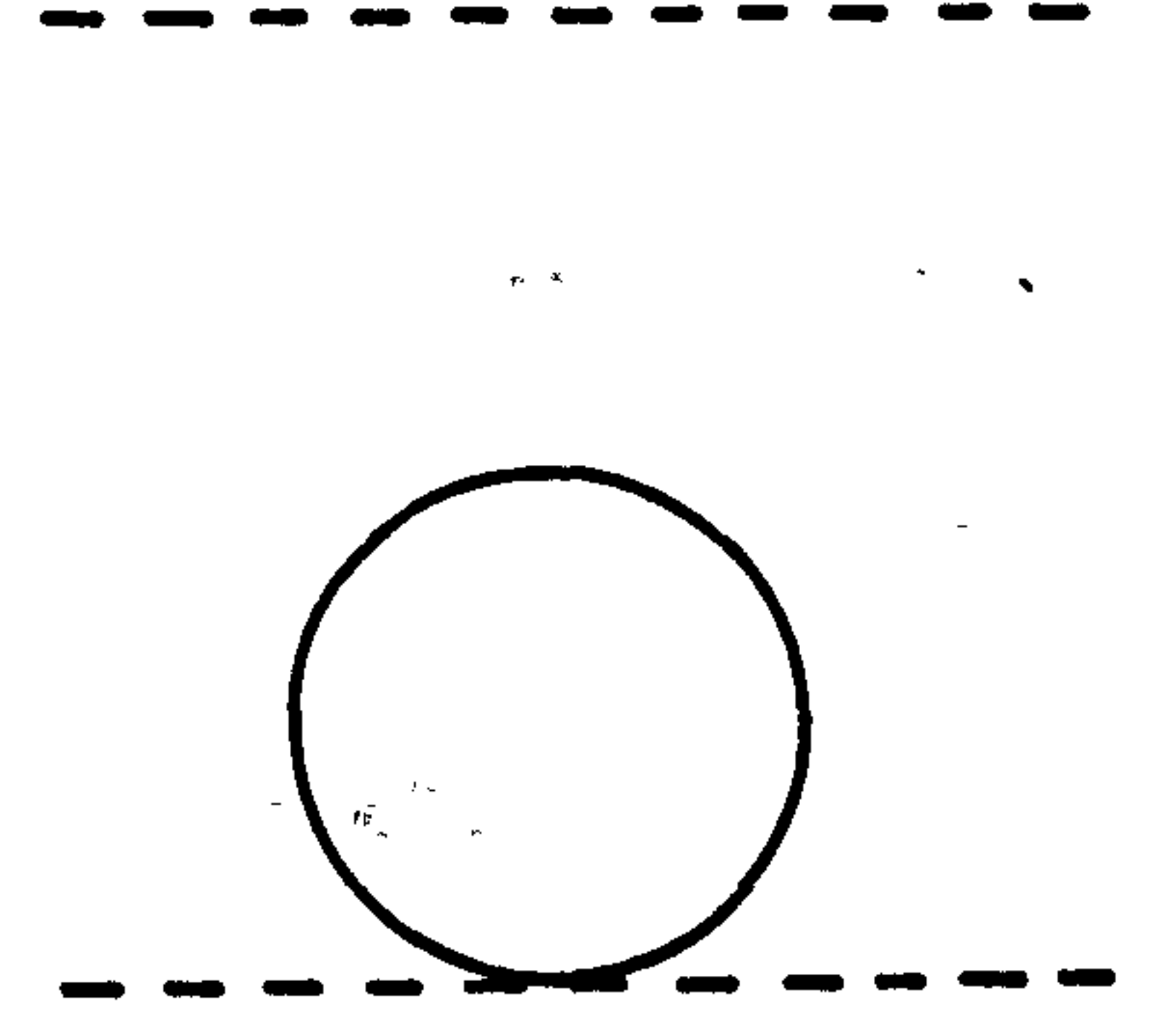
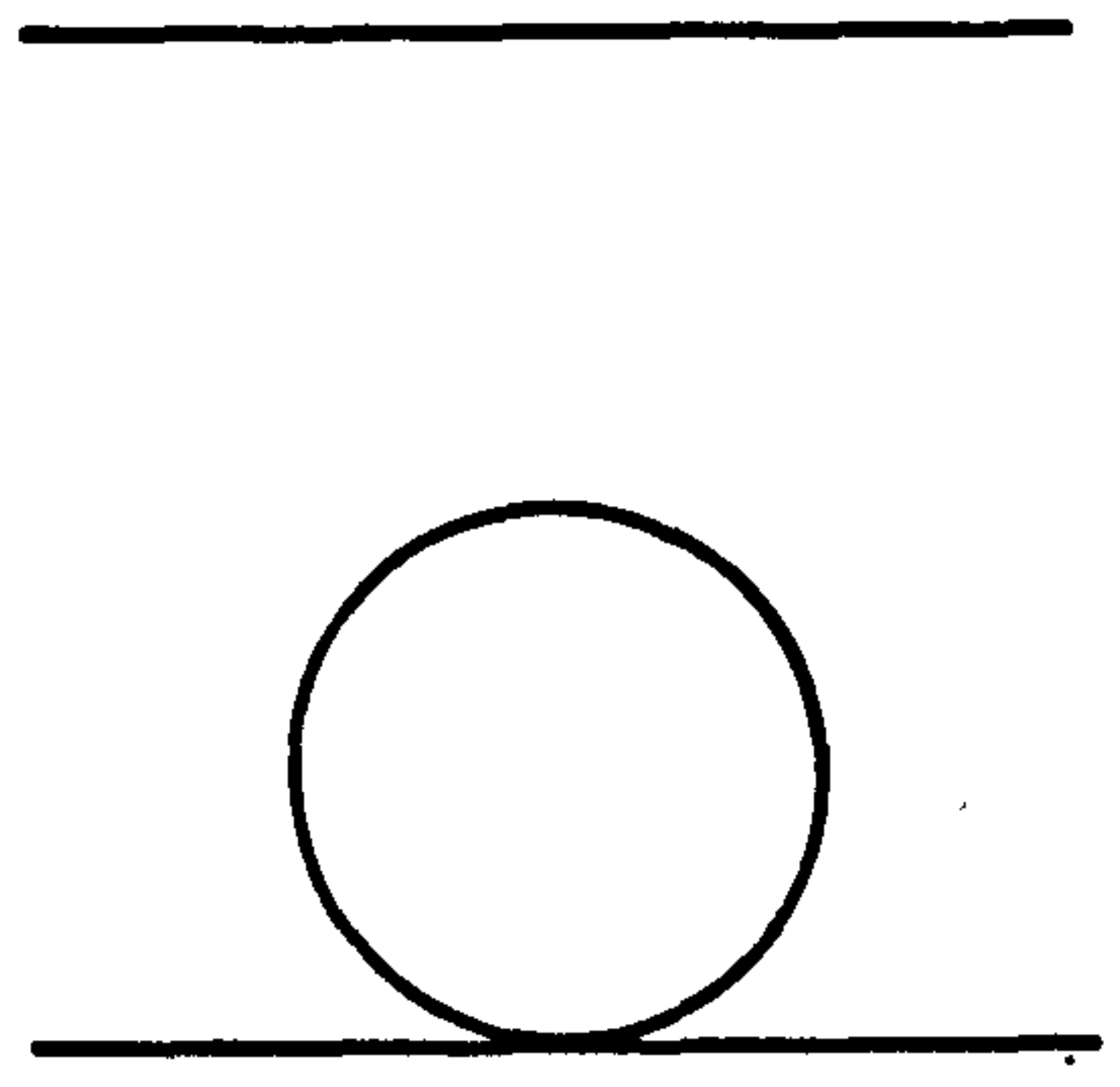
$$t_0 = \mu^2 t_R \left\{ 1 + \frac{1}{2\varepsilon} \frac{S_d}{(2\pi)^d} \left[\frac{2}{3} u_R (n+1) + v_R \right] \right\} \quad (3.29)$$

$$Z_\phi = 1 \quad (3.30)$$

$$u_0 \mu^{-\varepsilon} = u_R + \frac{1}{3\varepsilon} (n+4) u_R^2 \frac{S_d}{(2\pi)^d} + \frac{1}{\varepsilon} u_R v_R \frac{S_d}{(2\pi)^d} \quad (3.31)$$

$$v_0 \mu^{-\varepsilon} = v_R + \frac{3}{2\varepsilon} v_R^2 \frac{S_d}{(2\pi)^d} + \frac{2}{\varepsilon} u_R v_R \frac{S_d}{(2\pi)^d} \quad (3.32)$$

to one-loop. We require $\Gamma_{\alpha\alpha}^{(2)}$ and $\Gamma_{\beta\beta}^{(2)}$ in the ordered state, i.e., for $T < T_c$. The diagrams contributing to each vertex function to one loop are given in Figure 3-1. The diagrammatic series for the function $\Gamma_{\alpha\alpha}^{(2)}$ leads to the expression



$\Gamma_{\alpha\alpha}^{(2)}$

$\Gamma_{\beta\beta}^{(2)}$

Figure 3-1: Graphs in two point functions to one loop

$$\begin{aligned}
\mu^{-2} \Gamma_{ad}^{(2)}(q=0, T < T_c) &= t_R + u_R n M_R^2 + \frac{1}{2} v_R M_R^2 \\
&+ \frac{1}{4} (u_R + \frac{1}{2} v_R n^{-1}) \frac{S_d}{(2\pi)^d} (t_R + u_R n M_R^2 + \frac{1}{2} v_R M_R^2) \ln(t_R + u_R n M_R^2 + \frac{1}{2} v_R M_R^2) \\
&+ \frac{1}{24} (2n-1) (2u_R + 3n^{-1} v_R) \frac{S_d}{(2\pi)^d} (t_R + \frac{1}{3} u_R n M_R^2 + \frac{1}{2} v_R M_R^2) \ln(t_R + \frac{1}{3} u_R n M_R^2 + \frac{1}{2} v_R M_R^2) \\
&+ \frac{1}{2} n M_R^2 (u_R + \frac{1}{2} n^{-1} v_R)^2 \frac{S_d}{(2\pi)^d} \ln(t_R + u_R n M_R^2 + \frac{1}{2} v_R M_R^2) \\
&+ \frac{1}{18} (2n-1) n M_R^2 (u_R + \frac{3}{2} n^{-1} v_R)^2 \frac{S_d}{(2\pi)^d} \ln(t_R + \frac{1}{3} u_R n M_R^2 + \frac{1}{2} v_R M_R^2) \\
&+ \frac{1}{2} n M_R^2 (u_R + \frac{1}{2} v_R n^{-1})^2 \frac{S_d}{(2\pi)^d} + \frac{1}{18} (2n-1) n M_R^2 (u_R + \frac{3}{2} n^{-1} v_R)^2 \frac{S_d}{(2\pi)^d} \quad (3.33)
\end{aligned}$$

and, for $\Gamma_{\beta\beta}^{(2)}$,

$$\begin{aligned}
\mu^{-2} \Gamma_{\beta\beta}^{(2)}(q=0, T < T_c) &= t_R + \frac{1}{3} u_R n M_R^2 + \frac{1}{2} v_R M_R^2 \\
&+ \frac{1}{24} (2u_R + 3n^{-1} v_R) \frac{S_d}{(2\pi)^d} (t_R + u_R n M_R^2 + \frac{1}{2} v_R M_R^2) \ln(t_R + u_R n M_R^2 + \frac{1}{2} v_R M_R^2) \\
&+ \frac{1}{4} \left[\frac{1}{3} (2n+1) u_R + \frac{2n-1}{2n} v_R \right] \frac{S_d}{(2\pi)^d} (t_R + \frac{1}{3} u_R n M_R^2 + \frac{1}{2} v_R M_R^2) \ln(t_R + \frac{1}{3} u_R n M_R^2 + \frac{1}{2} v_R M_R^2) \\
&+ \frac{1}{6 u_R} \left[u_R + \frac{3}{2} n^{-1} v_R \right]^2 \frac{S_d}{(2\pi)^d} \left\{ (t_R + u_R n M_R^2 + \frac{1}{2} v_R M_R^2) \ln(t_R + u_R n M_R^2 + \frac{1}{2} v_R M_R^2) \right. \\
&\quad \left. - (t_R + \frac{1}{3} u_R n M_R^2 + \frac{1}{2} v_R M_R^2) \ln(t_R + \frac{1}{3} u_R n M_R^2 + \frac{1}{2} v_R M_R^2) \right\} \\
&+ \frac{1}{4} \left(\frac{n-1}{n} \right) v_R^2 M_R^2 \frac{S_d}{(2\pi)^d} \ln(t_R + \frac{1}{3} u_R n M_R^2 + \frac{1}{2} v_R M_R^2) \\
&+ \frac{1}{4} \left(\frac{n-1}{n} \right) v_R^2 M_R^2 \frac{S_d}{(2\pi)^d} \quad (3.34)
\end{aligned}$$

We now require the $n \rightarrow 0$ limit of these expansions. To carry out this limiting procedure we first expand the logarithms as power series in n using

$$\begin{aligned}
(e n^{-2} + c n^{-1} + d + f n) (a n + b) \ln(a n + b) &= e \left\{ n^{-2} b \ln b + a (\ln b + 1) n^{-1} + \frac{a^2}{2b} - \frac{a^3}{6b^2} n \right\} \\
&+ \ln b \{ b c n^{-1} + b d + a c \} + a c + n \left\{ (a d + b f) \ln b + a d + \frac{a^2 c}{2b} \right\} \\
&+ o(n^2) \quad (3.35)
\end{aligned}$$

The results of this expansion procedure are (throughout $b = t_R + \frac{1}{2} v_R M_R^2$)

$$\mu^{-2} \Gamma_{\alpha\alpha}^{(2)} = t_R + \frac{1}{2} v_R M_R^2 + u_R M_R^2 \eta + \frac{S_d}{(2\pi)^d} \left\{ \right.$$

$$\begin{aligned} & \ln b \left[b \left(\frac{1}{6} u_R + \frac{1}{4} v_R \right) + \frac{5}{12} u_R v_R M_R^2 + \frac{1}{4} v_R^2 M_R^2 \right] \\ & + \frac{5}{12} u_R v_R M_R^2 + \frac{1}{4} v_R^2 M_R^2 + \frac{1}{b} \cdot \frac{1}{12} u_R v_R^2 M_R^4 \\ & + n \left[\ln b \left(\frac{2}{3} u_R^2 M_R^2 + \frac{5}{12} u_R v_R M_R^2 + \frac{1}{6} u_R b \right) + \frac{2}{3} u_R^2 M_R^2 + \frac{5}{12} u_R v_R M_R^2 \right. \\ & \left. + \frac{1}{b} \left(\frac{1}{2} u_R^2 v_R M_R^4 + \frac{1}{12} u_R v_R^2 M_R^4 \right) + \frac{1}{b^2} \left(-\frac{1}{18} u_R^2 v_R^2 M_R^6 \right) \right] \left. \right\} \\ & + O(n^2, \epsilon) \end{aligned} \quad (3.36)$$

and

$$\mu^{-2} \Gamma_{\beta\beta}^{(2)} = t_R + \frac{1}{2} v_R M_R^2 + \frac{1}{3} u_R M_R^2 \eta + \frac{S_d}{(2\pi)^d} \left\{ \right.$$

$$\begin{aligned} & \ln b \left[b \left(\frac{1}{6} u_R + \frac{1}{4} v_R \right) + \frac{5}{12} u_R v_R M_R^2 + \frac{1}{4} v_R^2 M_R^2 \right] \\ & + \frac{5}{12} u_R v_R M_R^2 + \frac{1}{4} v_R^2 M_R^2 + \frac{1}{b} \cdot \frac{1}{12} u_R v_R^2 M_R^4 \\ & + n \left[\ln b \left(\frac{2}{9} u_R^2 M_R^2 + \frac{1}{12} u_R v_R M_R^2 + \frac{1}{6} u_R b \right) + \frac{2}{9} u_R^2 M_R^2 + \frac{1}{12} u_R v_R M_R^2 \right. \\ & \left. + \frac{1}{b} \left(\frac{5}{18} u_R^2 v_R M_R^4 + \frac{1}{12} u_R v_R^2 M_R^4 \right) + \frac{1}{b^2} \left(-\frac{5}{108} u_R^2 v_R^2 M_R^6 \right) \right] \left. \right\} \\ & + O(n^2, \epsilon) \end{aligned} \quad (3.37)$$

(Note that all factors of n^{-1} have vanished identically).

Recalling that the universal behaviour in a system is obtained by studying the correlation functions evaluated with the coupling constants set equal to their fixed point values, $u_R^* = -3 \left(\frac{6}{53} \right)^{1/2} \epsilon^{1/2}$ and $v_R^* = 4 \left(\frac{6}{53} \right)^{1/2} \epsilon^{1/2}$, we have

$$C^{(2)}(q=0) = \lim_{n \rightarrow 0} \frac{1}{2n} \left\{ \left[\Gamma_{\alpha\alpha}^{(2)}(q=0) \right]^{-1} - \left[\Gamma_{\beta\beta}^{(2)}(q=0) \right]^{-1} \right\}_{\text{fixed point}} \quad (3.38)$$

$$= \lim_{n \rightarrow 0} \frac{1}{2n} \cdot \frac{\Gamma_{\beta\beta}^{(2)} - \Gamma_{\alpha\alpha}^{(2)}}{\Gamma_{\alpha\alpha}^{(2)} \Gamma_{\beta\beta}^{(2)}} \Big|_{\text{fixed point}} \quad (3.39)$$

To lowest order in the $\epsilon^{1/2}$ -expansion this gives

$$C^{(S)}(q=0) = \mu^2 \lim_{n \rightarrow 0} \frac{1}{2n} \left\{ \frac{1}{t_R + \frac{1}{2} v_R M_R^2 + u_R n M_R^2} - \frac{1}{t_R + \frac{1}{2} v_R M_R^2 + \frac{1}{3} u_R M_R^2 n} \right\} \quad (3.40)$$

$$= \mu^2 \frac{-\frac{1}{3} u_R^* M_R^2}{(t_R + \frac{1}{2} v_R^* M_R^2)^2} \quad (3.41)$$

$$= \mu^2 \frac{\Delta_R^* M_R^2}{(t_R + \frac{1}{2} v_R^* M_R^2)^2} \quad (3.42)$$

$$= \mu^2 \Delta_R^* M_R^2 \chi(0)^2 \quad (3.43)$$

As in the equation of state calculation the condition $\langle \alpha \rangle = 0$ gives M_R for $T < T_c$, in an analogous way to the calculation of the two-point functions. The expression obtained reads, in the $n \rightarrow 0$ limit,

$$v_R M_R^2 = -6t_R - \frac{S_d}{(2\pi)^d} \frac{1}{2} (3v_R + 2u_R) (-2t_R) \ln(-2t_R) - \frac{S_d}{(2\pi)^d} \frac{3}{2} u_R (-2t_R) \ln(-2t_R) - \frac{S_d}{(2\pi)^d} \frac{3}{2} u_R (-2t_R) \quad (3.44)$$

(This provides a useful check on $\Gamma_{\alpha\alpha}^{(2)}$ and $\Gamma_{\beta\beta}^{(2)}$ - substituting in for $v_R M_R^2$ and taking the $n \rightarrow 0$ limit we recover $\chi(0)$ as in Newlove (1983) and Chapter 2).

At the fixed point there are no corrections to scaling and the magnetisation behaves as

$$M_R \sim |1 - t_R|^\beta \quad (3.45)$$

Using (3.44) with u_R and v_R put equal to u_R^* and v_R^* we find

$$V_R^* M_R^2 = 3 \left\{ 2 + \frac{S_d}{(2\pi)^d} (\ln 2 + 3) \left(\frac{6}{53}\right)^{1/2} \epsilon^{1/2} \right\} t_R^{1 + \frac{1}{2} \left(\frac{6}{53}\right)^{1/2} \epsilon^{1/2}} + o(\epsilon) \quad (3.46)$$

i.e.,

$$\beta = \frac{1}{2} + \frac{1}{4} \left(\frac{6}{53}\right)^{1/2} \epsilon^{1/2} + o(\epsilon) \quad (3.47)$$

For $\chi(0)$ we have at the fixed point

$$\chi \sim C_+ |t_R|^{-\gamma}, \quad t_R > 0 \quad (3.48)$$

and this gives

$$\gamma = 1 + \frac{1}{2} \left(\frac{6}{53}\right)^{1/2} \epsilon^{1/2} + o(\epsilon) \quad (3.49)$$

Hence, to this order $\gamma = 2\beta$ and, therefore, $M_R^2 \chi(0)$ is constant at the fixed point. Thus,

$$C^{(s)}(q=0) = \mu^2 \Delta_R^* M_R^2 \chi(0)^2 \{1 + o(\epsilon^{1/2})\} \quad (3.50)$$

$$= \mu^2 \frac{\Delta_R^*}{V_R^*} \chi(0) \{1 + o(\epsilon^{1/2})\} \quad (3.51)$$

$$= \frac{3}{4} \chi(0) \{1 + o(\epsilon^{1/2})\} \quad (3.52)$$

Therefore the amplitude ratio measured in $S(q)$ is not C_+/C_- , but is in fact

$$\frac{C_+}{C_- \left\{ \frac{7}{4} + o(\epsilon^{1/2}) \right\}}$$

(3.53)

in agreement with the lowest-order calculation reported by Aharony and Pelcovits (1985).

Using the two-loop results which were derived in Chapter 2 for the fixed point values of the couplings we can extend this result to obtain the $o(\epsilon^{1/2})$ term. Writing the coupling constant ratio at the fixed point as

$$-\frac{3\Delta_R^*}{V_R^*} = \frac{u_R^*}{v_R^*} = \frac{a\epsilon^{1/2} + b\epsilon + c\epsilon^{3/2}}{d\epsilon^{1/2} + e\epsilon + f\epsilon^{3/2}} \quad (3.54)$$

$$= \frac{a}{d} + \frac{1}{d^2} (bd - ae)\epsilon^{1/2} + \text{3 loop corrections} \quad (3.55)$$

and putting in the fixed point couplings to the two-loop level obtained in the previous chapter we find

$$\frac{\Delta_R^*}{V_R^*} = \frac{1}{4} \left\{ 1 - \left(\frac{53}{6}\right)^{1/2} \epsilon^{1/2} \right\} + o(\epsilon) \quad (3.56)$$

This is sufficient to obtain the next order term in the expansion of $C^{(s)}(q=0)$ since all corrections are of order ϵ and we have included all graphs which contribute to the expansion at $o(\epsilon^{1/2})$. Therefore

$$C^{(s)}(q=0) = \mu^2 \frac{3}{4} \left\{ 1 - \left(\frac{53}{6}\right)^{1/2} \epsilon^{1/2} \right\} \chi(0) \left\{ 1 - \frac{21}{9} \left(\frac{6}{53}\right)^{1/2} \epsilon^{1/2} \right\} \\ \times \frac{\left\{ 2 + (\ln 2 - 3) \left(\frac{6}{53}\right)^{1/2} \epsilon^{1/2} \right\} \{-t\epsilon\}^{2\beta}}{\left\{ 2 + (\ln 2 - 3/2) \left(\frac{6}{53}\right)^{1/2} \epsilon^{1/2} \right\} \{-t\epsilon\}^{\beta}} \quad (3.57)$$

and carrying out the algebra we arrive at the expression

$$C^{(s)}(q=0) = \mu^2 \chi(0) \left\{ \frac{3}{4} - \frac{293}{32} \left(\frac{6}{53}\right)^{1/2} \epsilon^{1/2} \right\} + o(\epsilon) \quad (3.58)$$

3.4. Conclusions

In this chapter we have calculated the correction to the ratio of critical amplitudes of the susceptibility above and below T_c to order $\epsilon^{1/2}$ and have confirmed the findings of Aharony and Pelcovits (1985) that the experimental measurements of the structure factor must be reinterpreted to take account of the static correlation functions contribution. This was carried out in a different formalism to their work and enabled the result to be extended to the next order in the $\epsilon^{1/2}$ -expansion.

To enable this calculation to be carried out an extension of the replica trick was developed in which two sets of replica spins were introduced. This is easily extendable to allow more complicated correlation functions than the one detailed here to be studied in a field theoretic framework. In the table displayed in Table 3-1 we list the various quantities of interest. In the ϵ -expansion results we have naively set $\epsilon=1$ to extrapolate to three dimensions.

Experiment ^(a)	Random Ising one loop	Pure Ising ^(b) one loop	Present calculation
2.45±0.15	1.7	3.2	-1.28

(a) Birgeneau *et al* (1986)
(b) Brézin *et al* (1974)

Table 3-1: Comparison of results for susceptibility amplitude ratio

Recent results of a neutron scattering experiment (Birgeneau *et al*, 1986) designed to study the critical behaviour of the site random Ising model $Mn_xZn_{1-x}F_2$ for two different dilutions give the value of the susceptibility amplitude ratio as 2.45 ± 0.15 . A search for a contribution to this ratio from a $C^{(s)}(q=0)$ term was conducted but no evidence of such a contribution was found.

4.1. Introduction

With the advent of more powerful digital computers numerical simulations have become an important tool in the theoretical physicists bag. A large range of physical models (and unphysical ones!) have been subjected to analysis using this technique - everything from classical liquids through to galactic dynamics. A review of general techniques and models considered can be found in Binder (1979) and for the more relevant area of phase transition physics we refer the reader to the book by Mouritsen (1984). In the following discussion we will concentrate our attention on simulations designed to explore the area of statistical mechanics and phase transitions.

The two main types of computer simulation which have contributed significantly to the field of critical phenomena are **molecular dynamics** and **Monte Carlo** methods. In the case of a molecular dynamics simulation the classical equations of motion are integrated numerically to calculate the time evolution of a system. In a Monte Carlo simulation, stochastic elements are introduced to allow the simulation to sample phase space via a random walk to enable the estimation of the phase space integrals in thermodynamic averages. It is this latter method which was employed in the current work.

In considering problems in statistical mechanics it is soon obvious that a simple, random sampling of points in phase space is not the best way to estimate the required integrals in the average of an observable, $O(x)$,

$$O(x) = \frac{\int dx O(x) e^{-H/kT}}{\int dx e^{-H/kT}} \quad (4.1)$$

- the exponential in the partition function varies over too large a range near the critical temperature. The solution is to use a sampling method which collects statistical information according to its importance - this means that the phase space points are chosen with a probability which reflects the size of their contribution to the integrals in (4.1). The most common of these sampling methods is the Metropolis algorithm (Metropolis *et al*, 1953) in which the random walk is defined by specifying a probability of transition from phase space point x to phase space point y , $W(x \rightarrow y)$, such that detailed balance is satisfied, i.e.,

$$P_{eq}(x) W(x \rightarrow y) = P_{eq}(y) W(y \rightarrow x) \quad (4.2)$$

where

$$P_{eq}(x) \propto e^{-H(x)/kT} \quad (4.3)$$

This implies that the change in energy alone governs the ratio of transition probabilities

$$\frac{W(x \rightarrow y)}{W(y \rightarrow x)} = e^{-\Delta H/kT} \quad (4.4)$$

A realisation of the above Markov process that is commonly used is

1. generate a random initial configuration, C_1
2. choose a trial state, C_2 , according to the probability $W(C_1 \rightarrow C_2)$
3. if the change in energy, $\Delta H = H(C_2) - H(C_1)$, is negative, C_2 is taken as the next element in the Markov chain.
4. If ΔH is positive, take C_2 as the next element in the chain with probability, $\exp(-\Delta H/kT)$. Else, duplicate C_1 as the next element
5. go to 2

If the matrix of transition probabilities is such that the Markov chain is ergodic the above sequence will, in the long (Monte Carlo) time limit, generate a distribution of states constituting the equilibrium ensemble at temperature T .

A variation of the above procedure is to repeat steps 2 to 4 a number of times with the same trial state C_2 (multiple hits). In the limit of the number of hits tending to infinity we produce a distribution of states which is correctly thermalised. This is the heat-bath algorithm and is the technique adopted here; however, it is not implemented by "hitting" an infinite number of times! In the random site-diluted Ising model a spin variable at lattice site i , s_i , can be in one of three states, "up", "down" or "vacant". As the vacancies are quenched we need only consider "updating" the occupied lattice sites. The heat-bath algorithm is implemented in this case by posing the question, "what is the probability, P_i , of the spin s_i being up, given its' configuration of neighbouring spins?" A pseudo-random number, ζ , in the range $[0,1]$ is then

chosen and, if $\zeta < P_i$, then s_i is set up, else s_i is set down.

The simulations described herein were executed on an ICL Distributed Array Processor (DAP), part of the Edinburgh Regional Computing Centre (ERCC) hardware available to the University of Edinburgh's computer users. We shall now briefly describe this machine and explain why it is particularly suited to the problem under consideration.

The ICL Distributed Array Processor

The DAP is a single-instruction-stream, multiple-data-stream (SIMD) parallel processor (Hockney and Jesshope, 1981; Bowler, 1983) consisting of a square array of 4096 processing elements (PE's), each with an associated 4kbit store of local memory. The DAP treats its contents as 4096 bit planes, all the elements in one bit-plane being operated on simultaneously. The PE's are joined together in the topology of a two-dimensional square grid, with a PE located at each node (each having four neighbours; north, south, east and west), giving an ideal geometry for the simulation of two-dimensional, square lattice Ising models. The array edges can be connected in either of two geometries - planar or cyclic - allowing the effects of boundary conditions to be studied. Planar geometry corresponds to setting all the undefined neighbours surrounding the array to zero, whereas cyclic geometry identifies the north edge with the south, and the east with the west, thereby forming a 2-torus.

All the PE's in the DAP have a set of three hardware registers. Two of these, forming the Q plane and the C plane, are simply an accumulator and a carry store, whereas the third, the activity or A plane, is used to selectively mask out processing elements during certain operations. This feature allows

the addition of impurities into our model in a natural and computationally efficient manner.

Since the DAP has no input/output facilities incorporated in its design, it is necessarily parasitic on a host machine which is used to control its operation. This function is provided by an ICL 2900 series mainframe. The DAP is then used as follows

- a 'host' Fortran program is run on the 2900
- this calls a subroutine written in DAP Fortran to run on the DAP
- data is passed to and from the DAP via Fortran common areas
- the DAP performs computations on its local store
- control is passed back to the host
- results are output from the common areas

The Fortran variant, DAP Fortran, is an extended version of Fortran 4 designed to exploit the parallel nature of the machine by allowing operations to be performed simultaneously on 64x64 arrays. This, combined with the speed with which the DAP performs logical operations (i.e., operations on bits), provides an ideal environment for performing Ising model simulations. The current best estimate for the critical temperature in a three-dimensional Ising simulation was obtained using the DAP in Edinburgh (Pawley *et al*, 1984).

The random, spin- $\frac{1}{2}$, Ising model is implemented on the DAP by using

logical `.true.` to represent spin up, logical `.false.` to represent spin down, and using the A plane to mask off sites which contain non-magnetic impurities. This, coupled with a central updating routine written in the DAP assembler language, APAL, allowed the simulation to update at a rate of approximately 9 million spin update trials per second.

We now turn our attention to methods of analysing the results obtained from simulations performed using the Monte Carlo method.

Scaling Analysis of Finite System Results

In most Monte Carlo simulations we are faced with the problem of extrapolating our measurements of an observable on finite size systems to extract the infinite system behaviour. The method most commonly used is to apply the ansatz of finite-size scaling introduced by Fisher (1971)-which rests on the realisation that the size of a system is itself a variable in terms of which thermodynamic quantities scale (Fisher and Barber,1972; Nightingale,1976; Suzuki,1977; Derrida,1981). A modern review of finite-size scaling can be found in the article by Barber (in Domb and Green,1983), and Amit (1984) gives a field theoretic explanation of the important ideas underpinning the technique.

Consider a finite system with characteristic size L . Let $Q_L(t)$ be some thermodynamic quantity which becomes singular in the limit $L \rightarrow \infty$, $t \rightarrow 0$, and define

$$\frac{Q_L(t)}{Q_\infty(t)} = g(L,t) \tag{4.5}$$

Then, the finite-size scaling hypothesis is introduced by asserting that

$$g(L, t) = f(L/\xi(t)) \quad (4.6)$$

where $\xi(t)$ is the correlation length in the finite system, defined by

$$\xi^2 = \frac{\int r^2 G(r) dr}{\int G(r) dr} \quad (4.7)$$

where $G(r)$ is the two-point, spatial correlation function (Amit, 1984). This gives, for the free energy of a finite system of N particles,

$$F(N, t) = L^{-\frac{(2-\alpha)}{\nu}} \bar{F}(tL^{1/\nu}) \quad (4.8)$$

where α and ν are the specific heat and correlation length exponents respectively, and t is the reduced temperature. The function f is a universal scaling function of the variable $tL^{1/\nu}$.

Since we are dealing with a finite system the model cannot undergo a genuine second order phase transition. However, Fisher (1971) has suggested that a "transition temperature" for a finite system, $T_c(L)$, can be defined as the temperature at which the specific heat has its maximum value. Finite-size scaling then gives, for the shift in the critical temperature,

$$\delta T_c = T_c(\infty) - T_c(L) \sim L^{-1/\nu} \quad (4.9)$$

For systems of size L which are outwith the asymptotic region corrections to finite-size scaling must be introduced, e.g.,

$$\delta T_c \sim L^{-1/\nu} (1 + aL^{-\omega}) \quad (4.10)$$

where ω is the correction-to-scaling exponent (Wegner,1972; Aharony and Fisher,1983). The system is simulated on different sizes of lattice and the above is used to extrapolate to the bulk behaviour, $L \rightarrow \infty$, since it can be shown that the exponents implied by the finite-size scaling ansatz are those of the bulk system (Barber,1983).

In the work presented here this we are study the scaling behaviour of the block variable, s_L , defined by

$$s_L = L^{-d} \sum_{L \text{ block}} \sigma_i \quad (4.11)$$

as the block size, L , is varied. In this case, an extension of the finite-size formalism leads us to make the ansatz that the probability distribution function, $P_L(s)$, of the block variable has the scaling form

$$P_L(s) = L^{-\beta/\nu} \rho(sL^{\beta/\nu}, tL^{1/\nu}, yL^{-\omega}) \quad (4.12)$$

where t and y are the leading thermal and irrelevant scaling fields present. The method of analysis of sub-blocks of a larger system does not incorporate the length scale provided by the finite system size. Standard finite-size scaling analysis studies the behaviour of quantities as the system size is changed; here, we study the scaling of variables defined on blocks of a larger system as we vary the block size. To refer to this as finite-size scaling in the conventional sense is a misnomer given this distinction. Binder (1981) has suggested a method by which the transition temperature can be located accurately using an analysis of the distribution function of the magnetisation of sub-blocks of a larger lattice; the ideas of the real-space renormalisation group, coarse-graining and universality lead one to believe that for large

system size, and at criticality, the distributions should tend to universal scaling forms (Bruce, 1981). For a detailed description of a finite-size scaling analysis of block distribution functions in the pure Ising model we refer the reader to the previously cited paper by Binder. Here we will only quote the salient results.

To define a block variable in the Ising Model we partition the lattice into sub-blocks of side L and define, e.g., the block magnetisation, by performing the spatial average over the spin variables, σ_j , within the block, i.e., in d dimensions

$$S_i = \frac{1}{L^d} \sum_{j \in i^{\text{th}} \text{ block}} \sigma_j \quad (4.13)$$

where

$$\sigma_j = \begin{cases} +1 & \text{if spin at site } j \text{ is up} \\ 0 & \text{if site is unoccupied} \\ -1 & \text{if spin at site } j \text{ is down} \end{cases} \quad (4.14)$$

The block distribution function is then the analogue of the Boltzmann probability factors for the spin variables σ_j , giving the probability distribution for the block variables, s_i , for sub-blocks of side L ,

$$P_L(s_i) = Z^{-1} \exp[-\mathcal{H}_{\text{coarse}}(\{s_i\})] \quad (4.15)$$

Here, $\mathcal{H}_{\text{coarse}}$ is the coarse-grained Hamiltonian arising from the blocking procedure. If we define the moments of the distribution through

$$\langle s^k \rangle_L = \int ds s^k P_L(s) \quad , \quad k \text{ even} \quad (4.16)$$

and the cumulant ratio

$$G_L = \frac{3\langle s^2 \rangle_L^2 - \langle s^4 \rangle_L}{2\langle s^2 \rangle_L} \quad (4.17)$$

it can be shown (Binder, 1981) that, as $L \rightarrow \infty$, $G_L \rightarrow 0$ for $T > T_c$, $G_L \rightarrow 1$ for $T < T_c$, and for $T = T_c$, $G_L \rightarrow G_L^*$, a non-trivial "fixed point". The behaviour of the cumulant ratio as a function of L can be visualised as a renormalisation group flow diagram, with G_L flowing to fixed point values under the change of length scale, L . This can therefore be used as a means of locating the transition temperature, T_c . However, to obtain a good estimate for T_c , L^{-1} must be small. The criteria of having a sub-block L large enough to probe close to the fixed point values and simultaneously small enough compared to the overall system size not to see the effects of the finite system it is embedded in, are not realisable for the system sizes currently feasible for simulation, even in two dimensions. Binder suggests using the ratio of cumulant values for different block sizes. In this case the critical temperature, T_c , is obtainable from the relationship

$$\left(\frac{G_L}{G_{L'}} \right)_{T=T_c} = 1 \quad (4.18)$$

The fact that the cumulants for different sub-block sizes, L , are measured during the same simulation run, and are therefore correlated, can be exploited to reduce the statistical errors in an estimate for T_c . If we take the difference between the cumulant values for different L values then the effect of the correlations between the moments will be to give a smaller statistical error in this result than in the G 's individually. We therefore used the relationship

$$\left(\frac{G_{L_1} - G_{L_2}}{G_{L_3} - G_{L_4}} \right)_{T=T_c} = 0 \quad (4.19)$$

to obtain our estimate for T_c .

The following section presents the results of the application of the above to the case of the pure Ising model.

4.2. Critical Behaviour in the Pure Ising Model

Introduction

As a preliminary to any study of a dilute Ising model it is wise to check the accuracy and veracity of the method on the pure model since comparison with exact results is possible for the two-dimensional case. In this section we give details of the simulation and analysis used to obtain the transition temperature and exponent values for the pure Ising model.

Simulation Details

The simulation reported in this section was carried out in two dimensions on a 128^2 lattice of Ising spins with periodic boundary conditions. A cold start, with all the spins aligned, was used, and before data were collected 100,000 lattice updates were discarded to allow for equilibration of the system. Measurements were subsequently taken every 100 lattice updates and results binned over every 10 measurements. Each complete run collected 500 results and took approximately 17 minutes of DAP time. The quantities calculated in the measuring phase were the second moment, $\langle s^2 \rangle_L$, the fourth moment, $\langle s^4 \rangle_L$, the energy (nearest-neighbour correlation function), the total magnetisation, M , and the absolute magnetisation $|M|$ (this quantity is the absolute value of the magnetisation averaged over 10 measurements, not the average of the absolute values). Results for the moments were obtained on

sub-block sizes 2, 4, 8, 16, 32 and 64, although not all these sizes were subsequently used in the analysis due to finite-size and correction-to-scaling effects - see the discussion accompanying the data analysis for details. After the moments had been collected, from their average values the cumulant ratio G_L was calculated.

The test used for equilibration was subjective in character and involved studying the behaviour of coarse-grained averages along the Markov chain of configurations generated by the simulations. Mouritsen (1984) suggests the following procedure for obtaining an estimate of the length of the Markov chain, M , required to obtain a reliable approximation to the equilibrium ensemble. If we define the n^{th} coarse-grained average of an observable O by

$$\langle O \rangle_n = \frac{1}{\Delta M} \sum_{i=(n-1)\Delta M+1}^{n\Delta M} O(C_i) \quad (4.20)$$

where ΔM = number of statistically independent configurations, C_i , averaged over, then the function

$$A_m = (m+1)^{-1} \sum_{\lambda=0}^m \langle O \rangle_{\frac{M}{\Delta M} - \lambda} \quad (4.21)$$

provides us with information on the reliability of our data. If A_m settles down to a reasonably stable value over a large range of m values, this value can be taken as an estimate of the required equilibrium average, $\langle O \rangle$. The number of sweeps discarded for equilibration purposes was chosen by studying long simulation run data for T near the known exact value of T_c and picking, by eye, a value of M in excess of the equilibration time indicated by the function A_m . The stability of the data thereafter showed up in the low standard deviations in the values measured during the run.

We now present the results of the simulation of the pure two-dimensional Ising model on a square lattice of 128^2 spins.

Results

The pure model was simulated for a range of temperatures from $T=1$ to $T=3$, measured in units of coupling strength/Boltzmann's constant. The total amount of DAP time used for this set of runs was of the order of 50 hours, with initially 5 runs at each temperature. The second and fourth moment values were then averaged over these runs and an error assigned to their average values on the basis of the standard deviations in the statistically independent results obtained from the different runs. From these average values the cumulant ratio was calculated for block sizes differing by a factor of 2, e.g.,

$$\frac{G_8 - G_4}{G_4 - G_2}, \quad \frac{G_{16} - G_8}{G_8 - G_4}, \quad \&c. \quad (4.22)$$

The value of T_c was then estimated from the point at which the above functions changed sign. The resulting estimates are tabulated in Table 4-1. Additional results carried out for a few selected temperatures confirmed that the sign of the ratio was well-determined by the number of runs considered here.

Exact Value	$\frac{G_8 - G_4}{G_4 - G_2}$	$\frac{G_{16} - G_8}{G_8 - G_4}$	$\frac{G_{32} - G_{16}}{G_{16} - G_8}$	$\frac{G_{64} - G_{32}}{G_{32} - G_{16}}$
2.2691853	2.2651(1)	2.2701(3)	2.272(2)	2.27(3)

Table 4-1: Estimates of T_c for Pure Ising Model

The cumulant values for different sub-block sizes are plotted as a function of temperature as Figure 4-1. Clearly, as $L \rightarrow \infty$, the cumulant assumes a step-function behaviour as predicted at a value of $T=T_c$. An "eyeball" estimation of T_c from the graph by the point where the lines cross gives a value of 2.27.

The magnetisation and energy of the pure system are displayed in Figures 4-2 and 4-3. The magnetisation shows the step-function characteristic of a transition from a disordered to an ordered state as we pass through the critical temperature. Again, an "eyeball" estimate of T_c from the magnetisation plot produces the value of 2.25; this value should be taken as just an indication of the region in which the critical temperature lies. The graph of energy versus temperature contains evidence of the divergence of the specific heat at criticality; since the specific heat is the derivative of the energy with respect to temperature, at T_c this divergence will be apparent as a vertical gradient in the E v T plot. Due to the finite size of the system simulated the gradient does not actually achieve the vertical, but it does come quite close. As $T \rightarrow 0$, the energy tends to the value of -2 and the magnetisation tends to 1, as expected in the fully-ordered state.

Finite-size scaling predictions for the behaviour of the moments studied can also be utilised to locate the critical temperature and to extract values for the critical exponents, β and ν . It can be shown (Binder,1981) that the moments have the scaling form

$$\langle S^2 \rangle_L = a_0 L^{-2\beta/\nu} (1 + a_1 (T-T_c) L^{1/\nu} + a_2 L^{-\omega}) \quad (4.23)$$

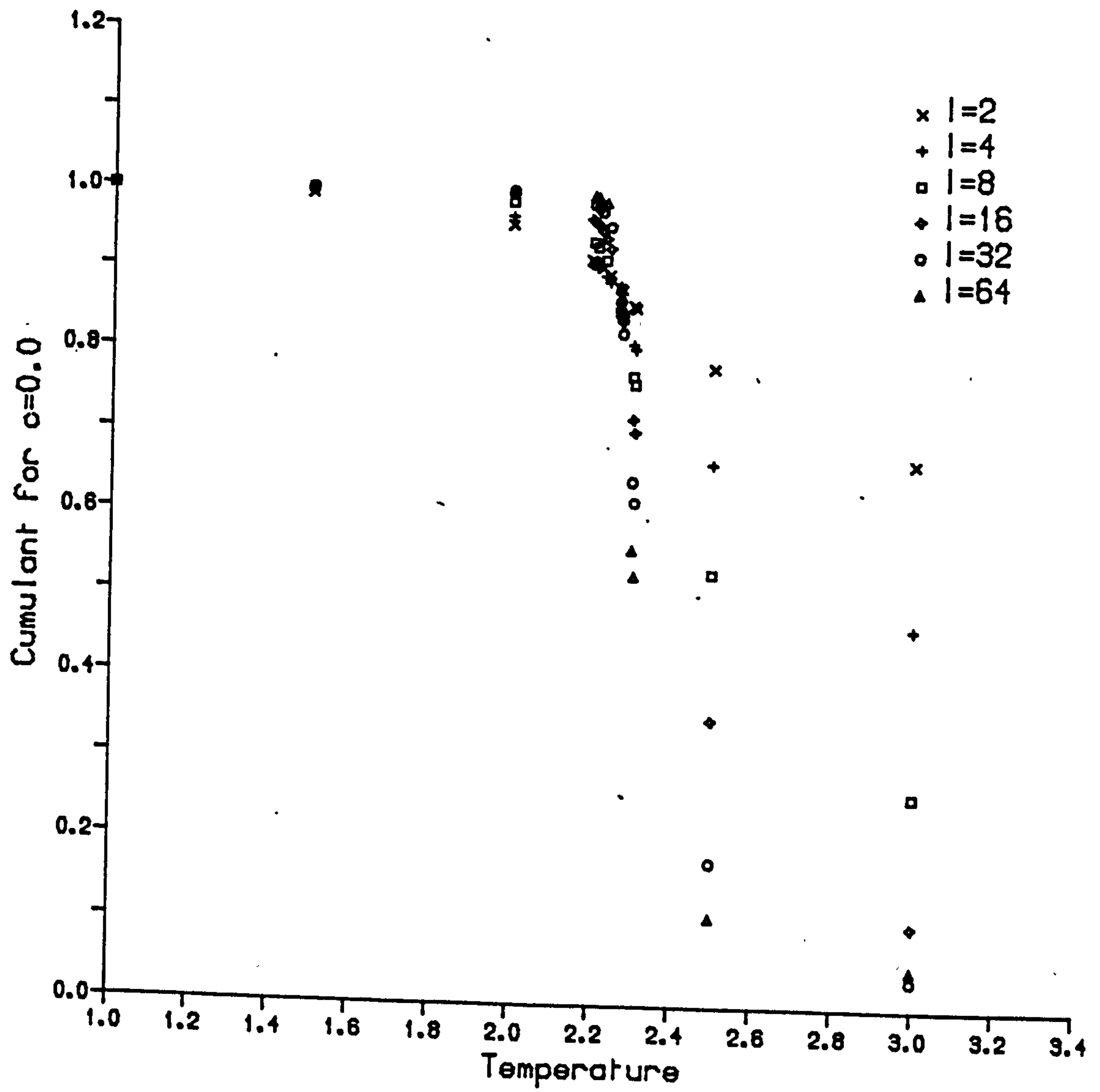


Figure 4-1: Cumulant versus Temperature for the pure system

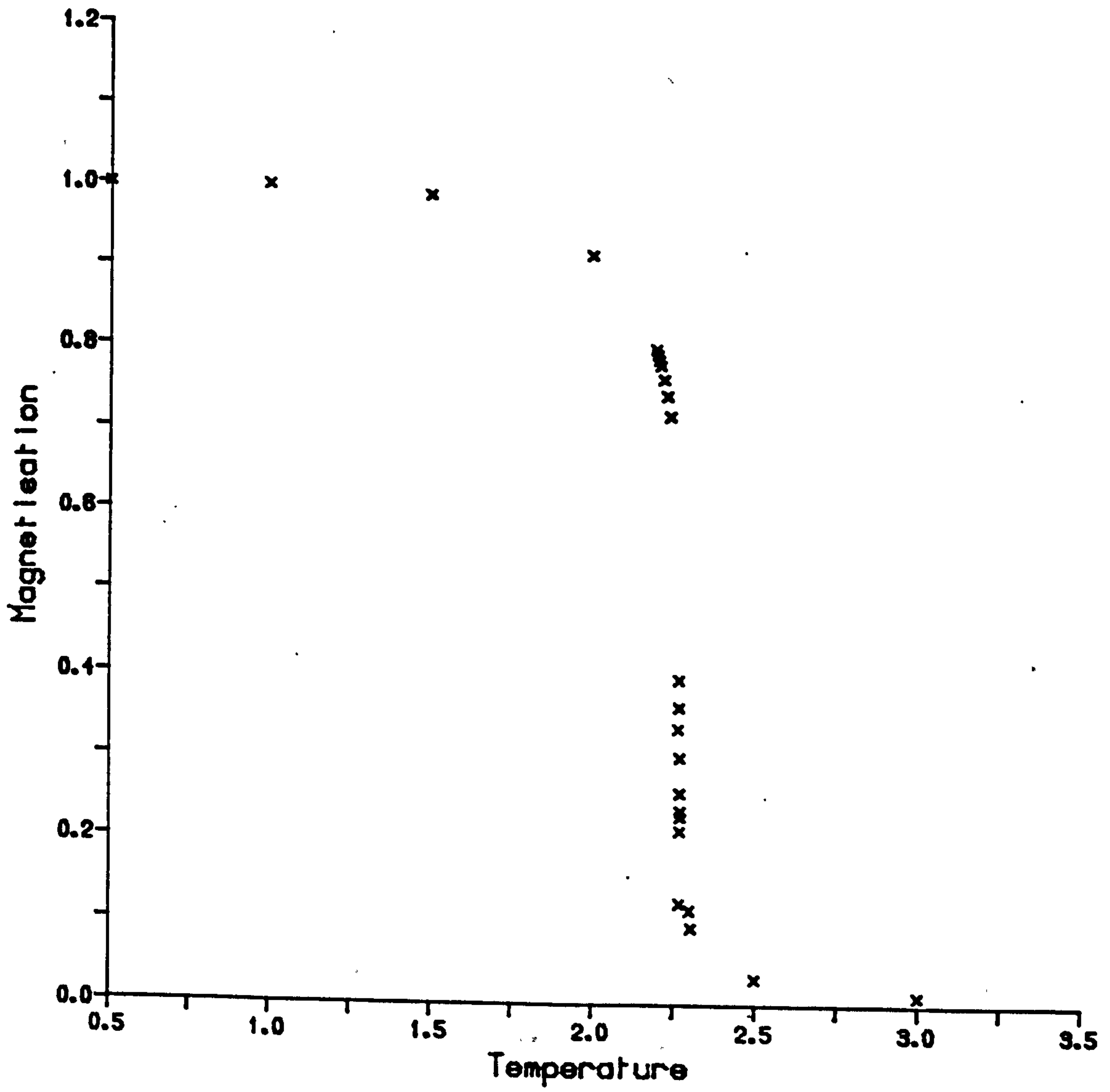


Figure 4-2: Magnetisation versus Temperature for the pure system

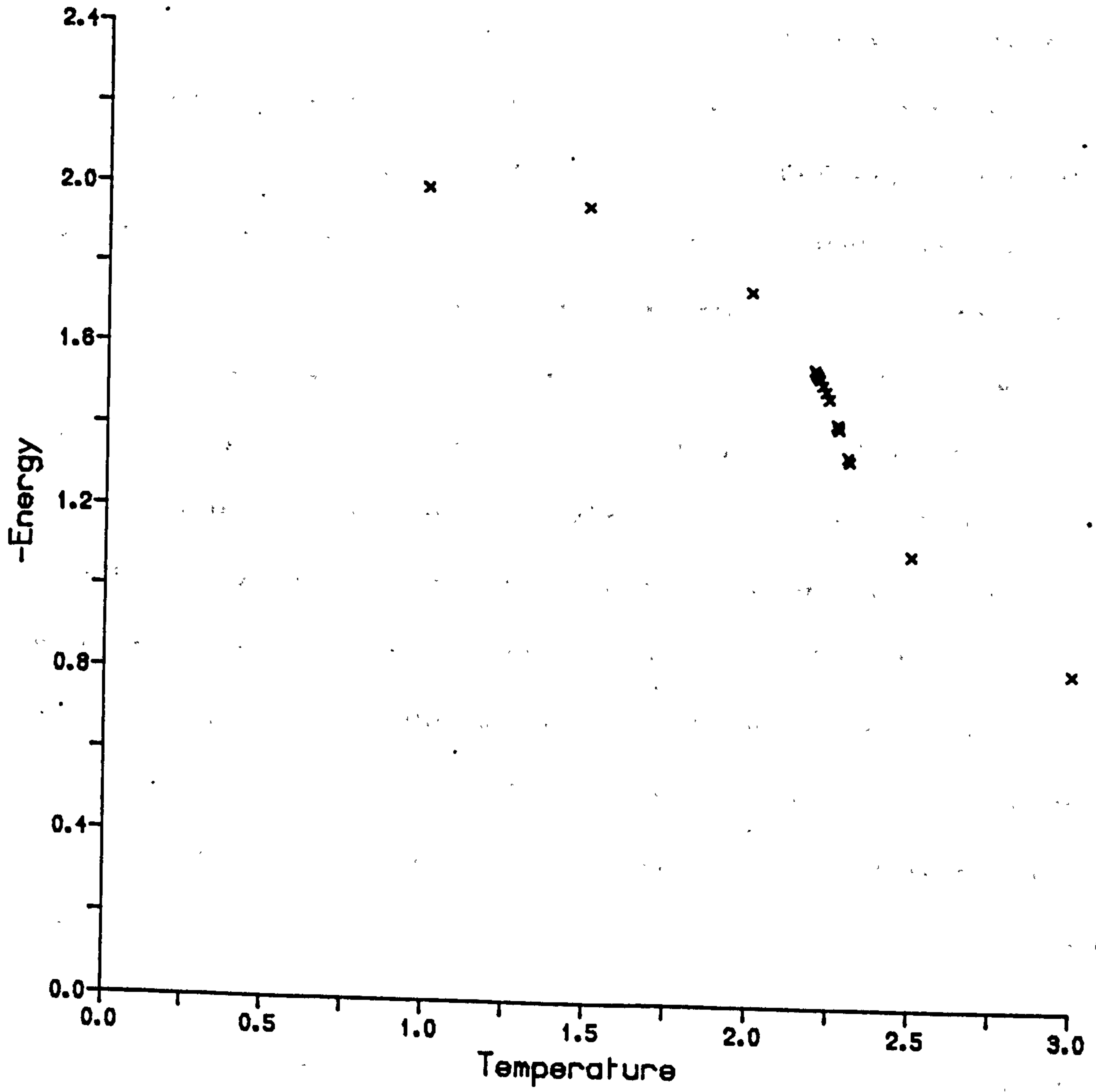


Figure 4-3: Energy versus Temperature for the pure system

and

$$\langle s^4 \rangle_L = a_0' L^{-4\beta/\nu} (1 + a_1' (\tau - \tau_c) L^{1/\nu} + a_2' L^{-\omega}) \quad (4.24)$$

where we have included a correction-to-scaling term, with exponent ω . We have explicitly set α to zero in these scaling relations since we are working in two dimensions. The scaling relation, $\nu d = 2 - \alpha$, then implies that $\nu=1$ in this case. In the fits whose results are quoted the exponent ν was left as a free parameter to check consistency with this prediction. The vanishing of the specific heat exponent implies a logarithmic divergence of the specific heat in the two-dimensional Ising model and the above fitting form should be modified from a power law singularity of the reduced temperature to a logarithmic divergence. Some fits were performed to the data with this type of scaling form but no improvement in the quality of the fits over the power law case was found. For the reasons stated for examining the cumulant ratio, fitting the (dimensional) ratio $\langle s^4 \rangle_L / \langle s^2 \rangle_L$ is expected to give better results than fitting to the individual moments. Comparing the values obtained in this manner (see below) to the exact values for the critical temperature, $T_c=2.2691853\dots$, and exponents, $\beta=0.125$ and $\nu=1.0$, the much improved results from using the ratio of the moments rather than the individual moments themselves stand out clearly. The scaling form of the ratio is the same as that for the second moment given in equation (4.23). Fits were performed to all three of the above quantities, the two moments and the ratio, for all possible ranges of L values between 4 and 64 which could be included. This was to enable us to make a prediction as to the best range of L values to be used in the later studies of the diluted model. Initial attempts at fitting the

data produced very high χ^2 values. On examining the major contributions to the χ^2 it was found that spuriously low standard deviations for temperatures at which only a few runs had been performed contributed disproportionately. Therefore, the standard deviations for sets of three adjacent temperatures were averaged to produce a more representative contribution to the χ^2 . This procedure was to be preferred to discarding the data completely for these temperatures. Data at the extreme ends of the temperature range considered were discarded as these are expected to lie outside the asymptotic regime in which the above scaling forms are assumed to be valid. The results from the fitting procedure are tabulated as Tables 4-2, 4-3 and 4-4. The correction-to-scaling exponent, ω , was found to be ill-determined by this fitting procedure, as found by Binder in his analysis of the three dimensional case. The belief is that the two-dimensional Ising model is a special case in which there are no non-analytic corrections-to-scaling (Barma and Fisher, 1985). The tabulated results for the range of L values of L=4 to L=32, combined with the values of T_c obtained from considering the cumulant ratios involving G's measured on these sub-block sizes leads us to use this range of L for the later analysis of the dilute Ising case.

Since $\langle s^k \rangle_L = L^{-k\beta/\nu} a_0 f_k(\xi/L)$ in the sub-block case, we can find the exponent ratio $2\beta/\nu$ by analysing the function (Binder, 1981)

$$W_\beta = -\ln \left\{ \frac{\langle s^2 \rangle_{bL}}{\langle s^2 \rangle_L} \right\} \cdot (\ln b)^{-1} \quad (4.25)$$

At T_c , $\langle s^2 \rangle_L = L^{-2\beta/\nu} a_0 f_2(\infty)$ and hence the corresponding value of W_β , W_β^* , is an estimate for the exponent ratio $2\beta/\nu$. The results obtained for different values of the scale factor, b, are then extrapolated as a function of $(\ln b)^{-1}$ to

Table 4-2:Results of fits to second moments for pure system

L	T_c	β	ν
4-8	2.25(1)	0.12(3)	1.2(1)
4-16	2.277(4)	0.17(2)	1.20(6)
4-32	2.273(3)	0.19(7)	1.24(4)
4-64	2.28(2)	0.17(4)	1.44(4)
8-16	2.270(2)	0.19(5)	1.3(2)
8-32	2.23(2)	0.25(3)	1.12(2)
8-64	2.266(4)	0.19(9)	1.54(6)
16-32	2.25(2)	0.3(2)	1.1(5)
32-64	2.22(3)	0.22(2)	2.02(4)

Table 4-3:Results of fits to fourth moments for pure system

L	T_c	β	ν
4-8	2.28(1)	0.16(1)	0.99(6)
4-16	2.276(3)	0.161(9)	1.10(4)
4-32	2.276(3)	0.17(6)	1.2(4)
4-64	2.34(5)	0.2(2)	1.41(3)
8-16	2.278(3)	0.16(5)	1.5(2)
8-32	2.235(3)	0.19(5)	1.3(2)
8-64	2.272(2)	0.20(7)	1.6(3)
16-32	2.22(3)	0.16(6)	3.1(9)
16-64	2.28(3)	0.23(6)	1.5(2)
32-64	2.29(2)	0.265(7)	1.6(4)

Table 4-4: Results of fits to ratios of moments for pure system

L	T_c	β	ν
4-8	2.255(7)	0.073(4)	0.98(5)
4-16	2.266(1)	0.12(4)	1.0(3)
4-32	2.2701(3)	0.126(3)	1.02(2)
4-64	2.2711(3)	0.113(4)	1.10(2)
8-16	2.286(1)	0.168(6)	0.982(5)
8-32	2.2706(3)	0.125(5)	1.10(4)
8-64	2.272(1)	0.112(4)	1.18(2)
16-32	2.267(3)	0.13(2)	1.14(9)
16-64	2.268(5)	0.13(9)	1.22(8)
32-64	2.276(3)	0.13(2)	1.3(1)

the limit $(\ln b)^{-1} \rightarrow 0$ to obtain the infinite system value. The results of this procedure are shown in Figure 4-4. Similarly, the function Y_β defined as

$$Y_\beta = - \ln \left\{ \frac{\langle S^4 \rangle_{bL}}{\langle S^4 \rangle_L} \right\} \cdot (\ln b)^{-1} \quad (4.26)$$

gives estimates for $4\beta/\nu$ at criticality. The values obtained are plotted as a function of $(\ln b)^{-1}$ in Figure 4-5. If the two sets of estimates for the ratio obtained from the second and the fourth moments are plotted on the same diagram the estimates are found to be entirely consistent, with the fourth moment results having the smaller spread at the low b values. From this we estimate a final β/ν value,

$$\frac{\beta}{\nu} = 0.122 \pm 0.002 \quad (4.27)$$

consistent with the exact value of 0.125.

We now turn our attention to the simulation of the diluted Ising model.

4.3. Critical Behaviour in the Diluted Ising Model

In this section we present the results obtained from the simulation described in the previous section of this chapter, when the model was modified by the addition of quenched impurities. The details of the data collection and analysis are the same as for the pure case, apart from the important addition of the configurational average over the vacancy distribution.

Recently, Binder and Landau (1985) have used the technique of sub-block scaling to locate the phase boundary in two dimensional Ising models with nearest-, next-nearest- and third-nearest-neighbour couplings. The first

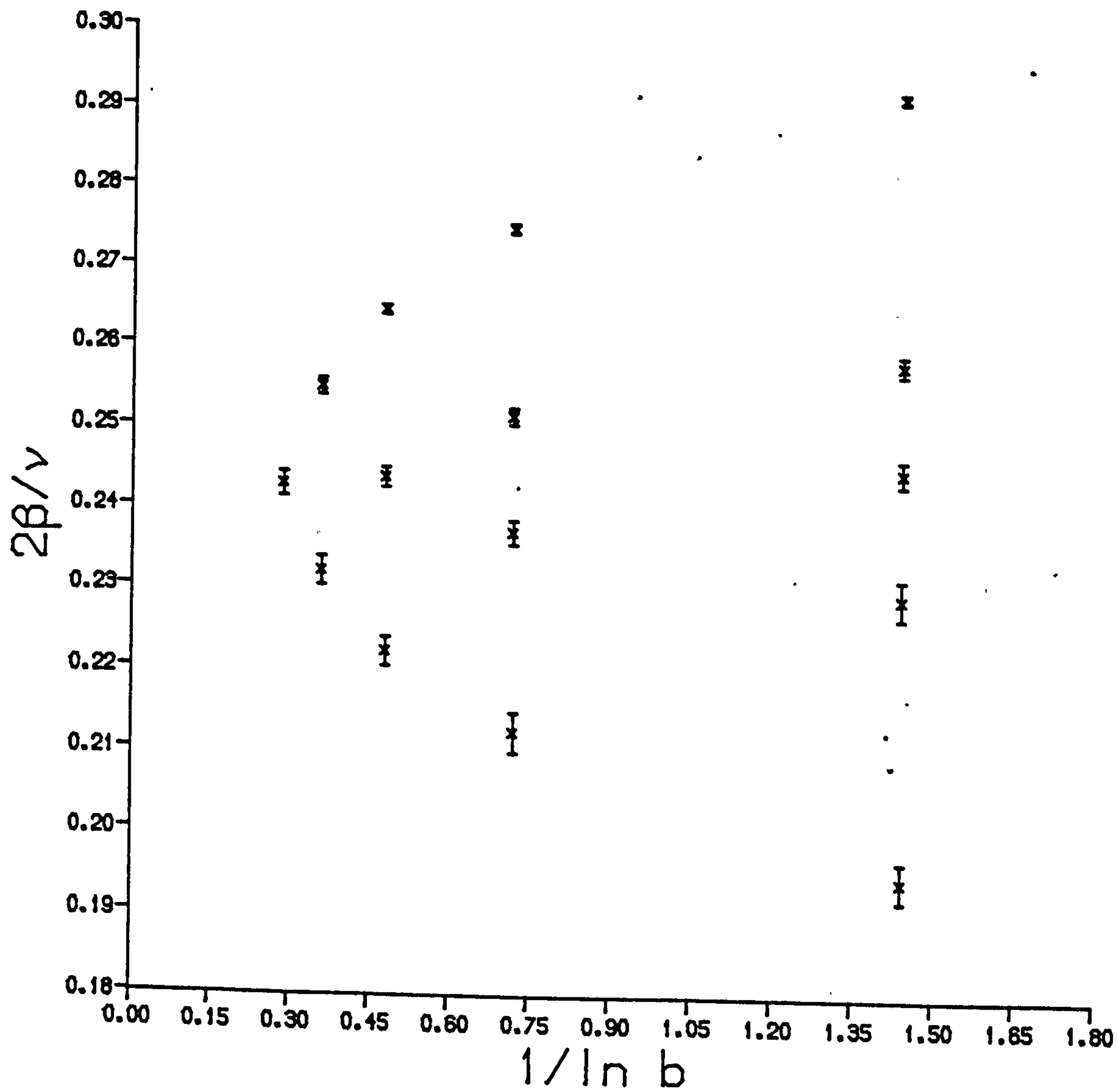


Figure 4-4: Pure system $2\beta/v$ estimates plotted against $(\ln b)^{-1}$

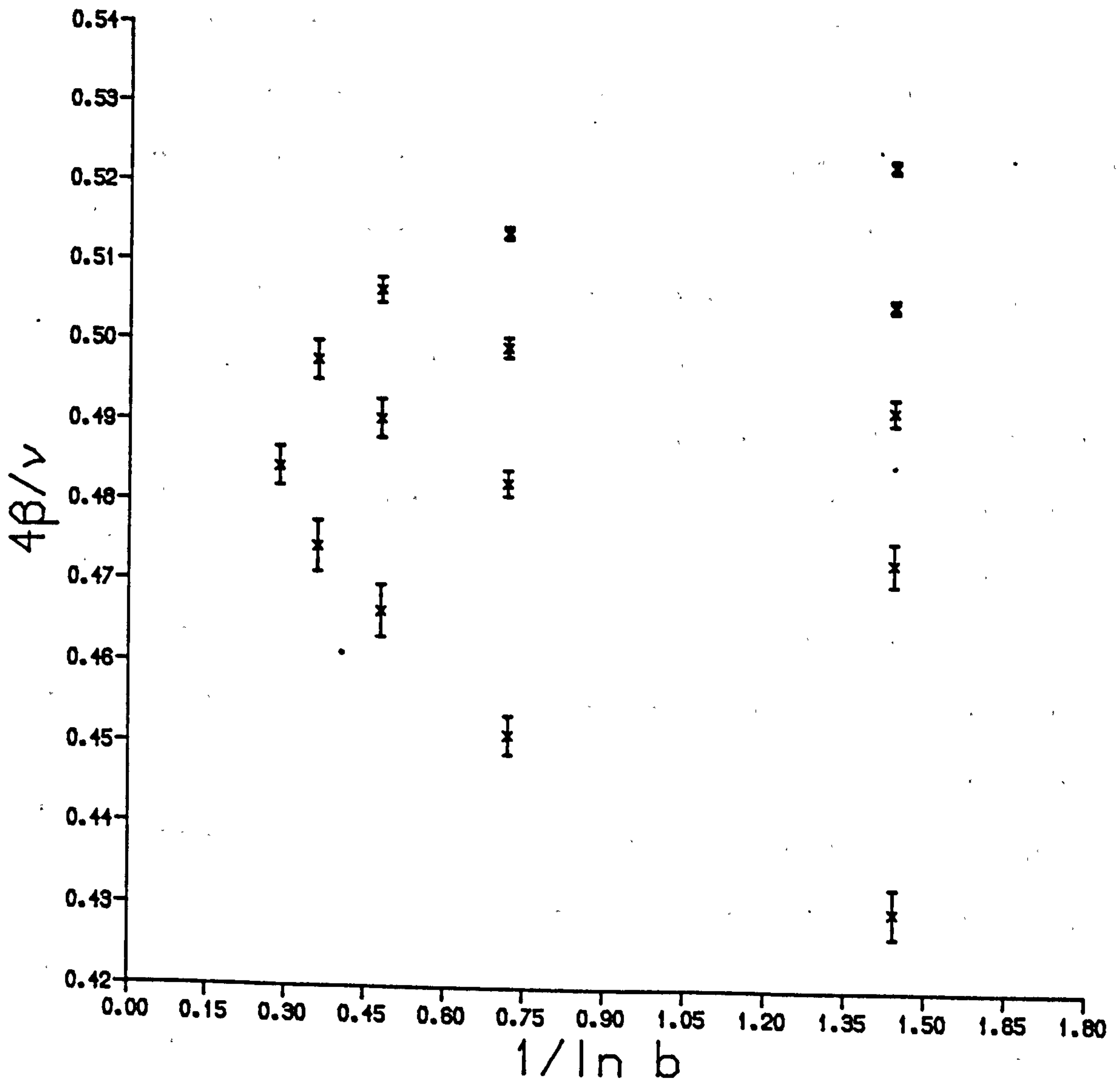


Figure 4-5: Pure system $4\beta/v$ estimates plotted against $(\ln b)^{-1}$

objective of the current study was to locate and map out the critical curve as a function of the dilution in the two-dimensional, site-diluted Ising model. The cumulant, G_L , described in the previous section is modified by the presence of a configurational average over the moments, i.e., $\langle s^2 \rangle_L$ is replaced by $[\langle s^2 \rangle_L]$, where the [...] represent the average over the impurities. This was incorporated into the simulation by repeating runs for a given temperature and dilution with different vacancy distributions and then averaging over the results. Usually, about 5 runs were incorporated into these averages, utilising, on average, about one-and-a-half hours of DAP time per temperature. For the site-diluted two-dimensional Ising model on a square lattice the percolation concentration is, approximately, $p_c=0.59$. Ten different values of p were used in the following work, ranging from $p=0.6$ to $p=1.0$ (the pure case). As one approaches the critical point the effects of critical slowing down become manifest, where changes in the values being measured occur over longer (Monte Carlo) timescales. Equilibration time increases as we increase the amount of dilution introduced into the system, due to the reduction in the number of possible paths by which the effect of spin flips can be propagated. This constrained us to study values of p in the range quoted above, and not to probe closer to the percolation threshold. As mentioned in the previous section concerning the pure Ising case, the time for equilibration was estimated from "eyeballing" coarse-grained averages over long runs for various dilutions. Overall about 300 hours of DAP time were needed to complete the data collection for the diluted case. As for the pure model, the energy and magnetisation were also measured. These quantities as a function of temperature for different dilutions are presented as Figures 4-6 and 4-7. The energy plots reveal the expected inflection point which can be used as an estimate for T_c ; in the limit of the system size $\rightarrow \infty$ the energy as a function of

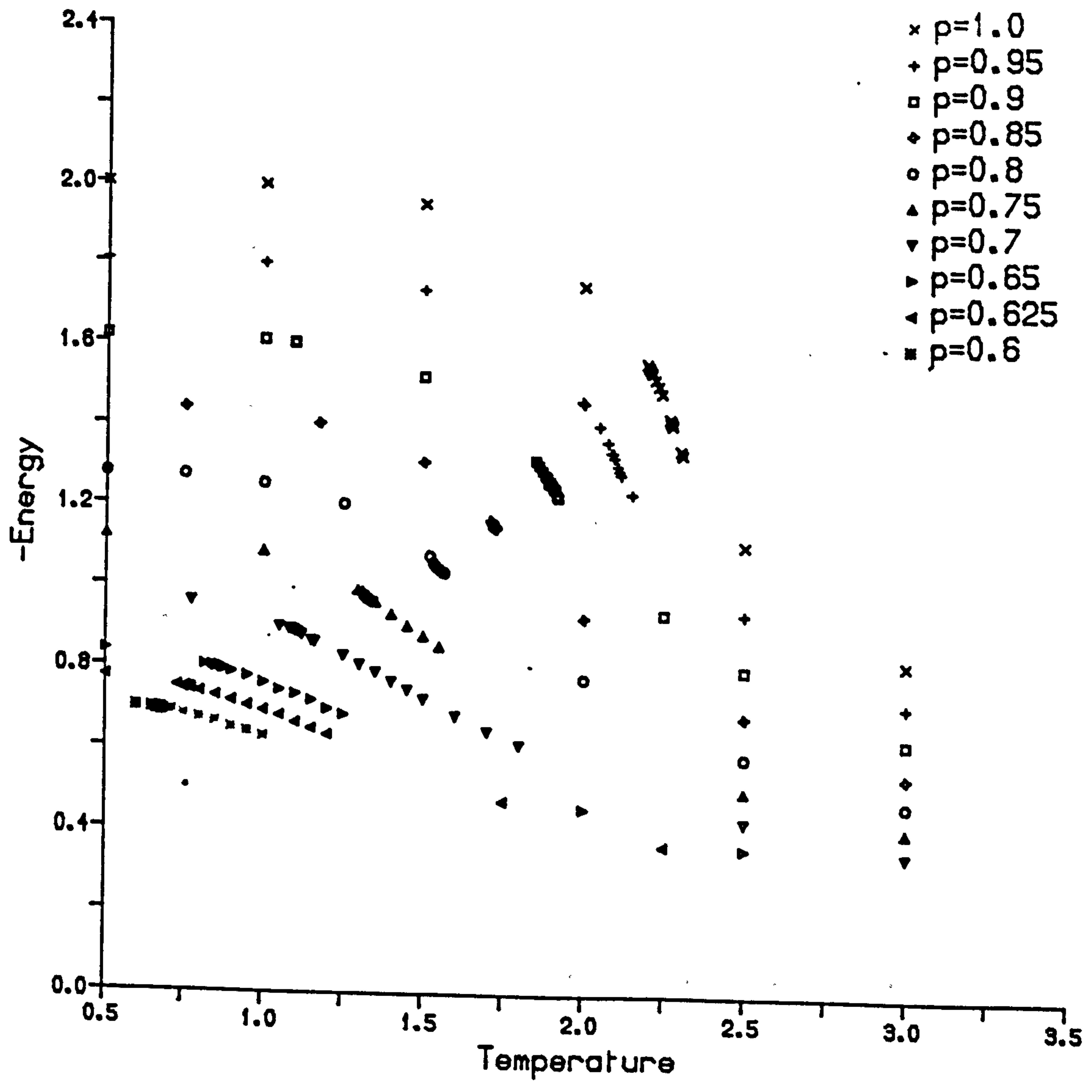


Figure 4-6: Energy versus Temperatures for the different dilutions

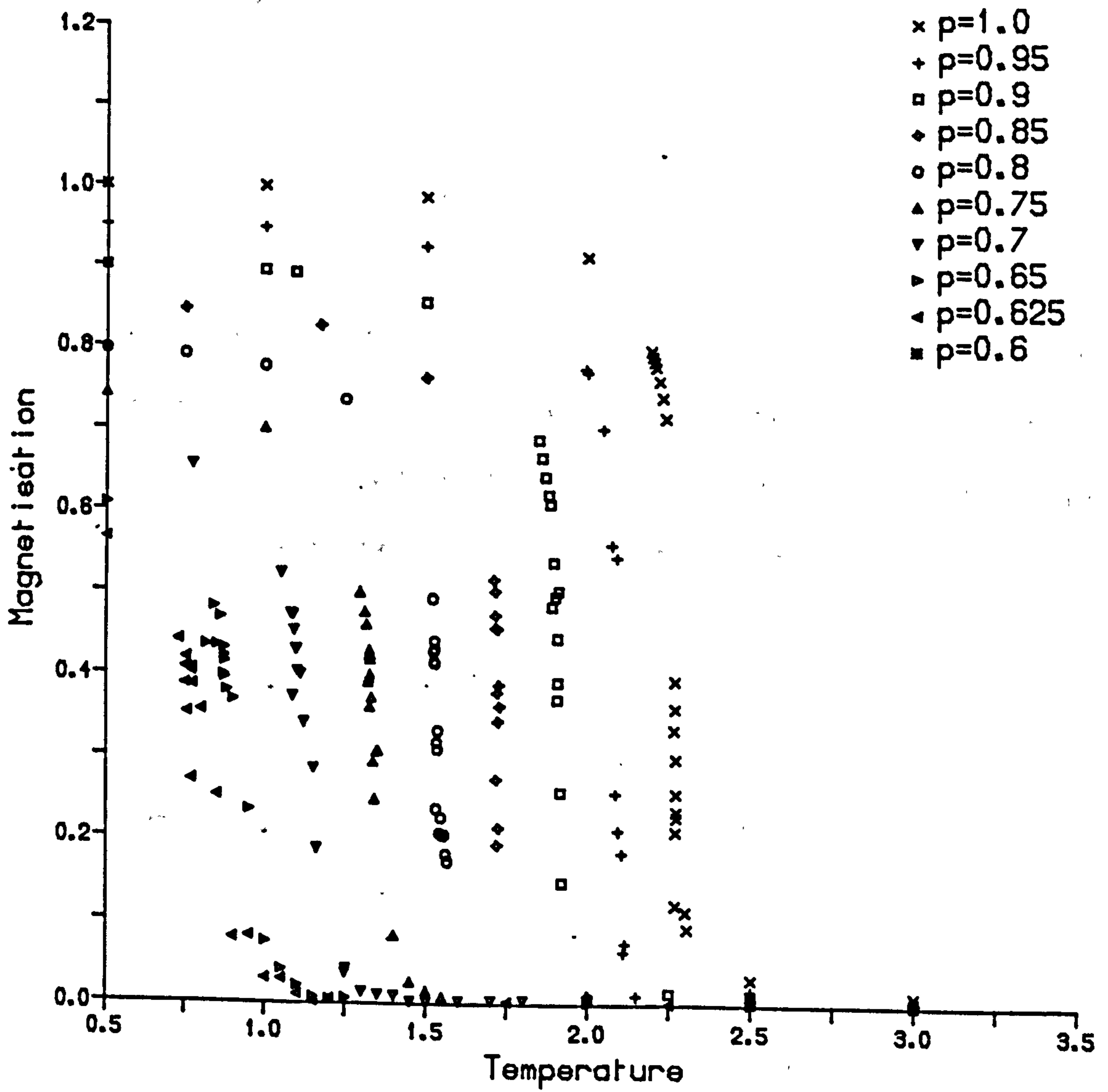


Figure 4-7: Magnetisation versus Temperatures for the different dilutions

temperature has infinite slope at T_c giving rise to the divergence in the specific heat at $T=T_c$. The plots of the magnetisation against temperature shows the expected transition to the (thermally) disordered state at the same value of T . The cumulant values measured were assigned an error according as the standard deviation in the (statistically independent) runs with different distributions of vacancies. As in the pure case, the criterion used as a signal for the phase transition was

$$\left(\frac{\overline{G}_L - \overline{G}_{L'}}{\overline{G}_L - \overline{G}_{L''}} \right)_{T=T_c} = 0 \quad (4.28)$$

where the bar over the G_L indicates they are calculated from impurity averaged moments. As we are running on a 128^2 system, to minimise the influence of finite-size effects (large L) and corrections-to-scaling (small L), the ratio which is expected to produce the most accurate results is

$$\frac{G_{32} - G_{16}}{G_{16} - G_8} \quad (4.29)$$

The results of these measurements are presented as the phase diagram given in Figure 4-8. Measuring the reduced limiting slope

$$S = \frac{1}{T_c} \left. \frac{dT_c}{d\rho} \right|_{\rho=1} \quad (4.30)$$

from the graph, we obtain the value of 1.578 ± 0.012 , in good agreement with the exact result of 1.565 (Stinchcombe, in Domb and Lebowitz, 1983).

The ratio of the moments measured during the simulations was analysed, as in the pure case, by fitting the data to a predicted scaling form to extract the critical temperature and exponent values. The range of L values included

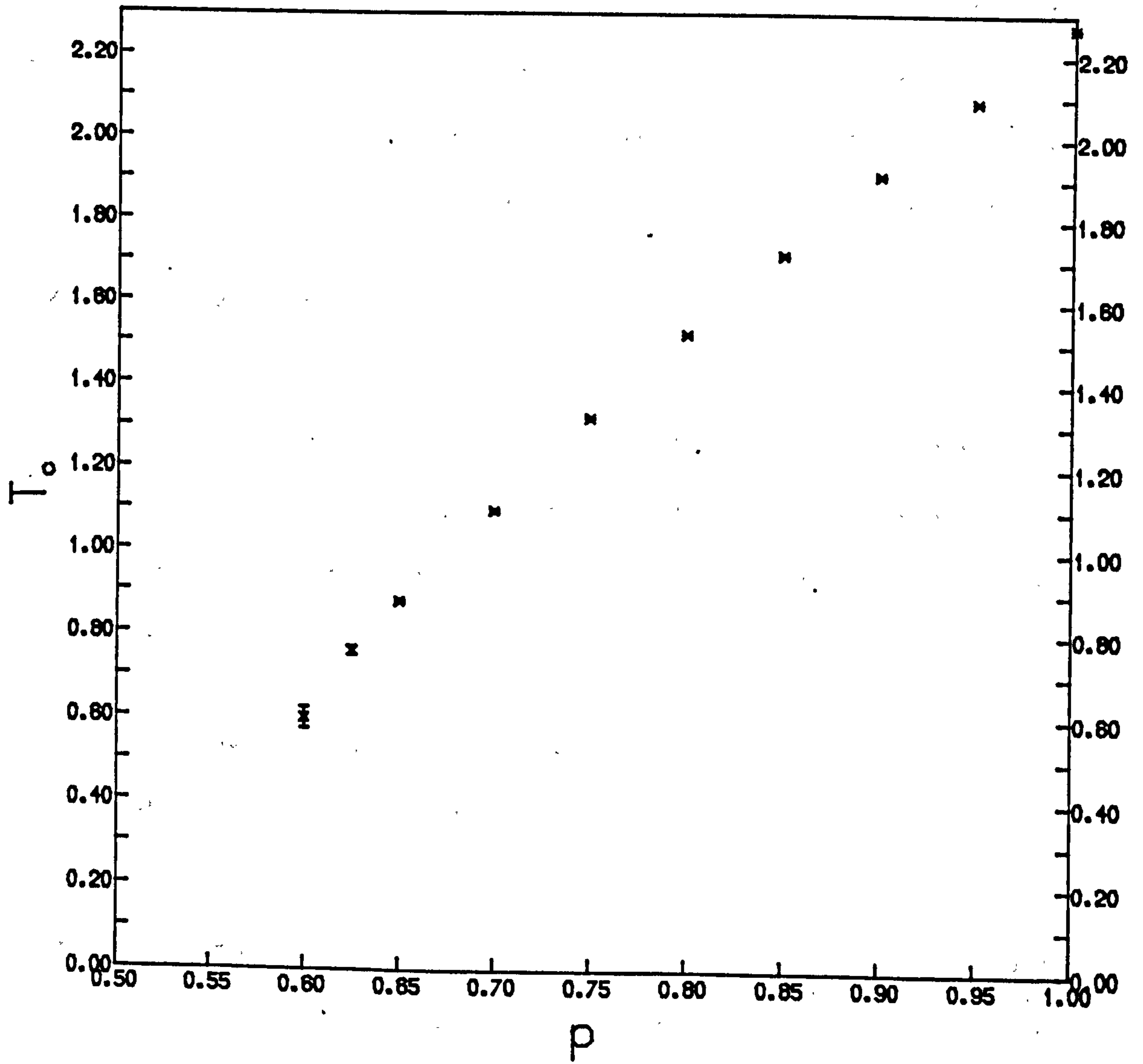


Figure 4-8: Phase Diagram of random, site-diluted Ising model

for this analysis was taken as $L=4$ to $L=32$, the choice being guided by the results of the pure system analysis. The results obtained are tabulated as Table 4-5.

Again, as for the pure system, the function Y_{β} was used to produce a series of estimates for the exponent $4\beta/\nu$ for varying values of dilution. The smaller spread in the Y_{β}^* values makes it easier to estimate the limiting value as $(\ln b)^{-1} \rightarrow 0$ and hence is used in preference to W_{β}^* . From this function we obtain estimates as to the value of $4\beta/\nu$, as plotted in Figures 4-9 (a)-(i).

4.4. Discussion of results

In this section we discuss the results for the exponent ratio β/ν obtained from the simulation performed on the site-diluted Ising model and presented in the previous section. Reference should be made to the figures at the end of that section.

To estimate the value of the exponent ratio in the limit $(\ln b)^{-1} \rightarrow 0$, the wedge of points contained within the outer curves in the plots of the function Y_{β} is expected to be the best indicator of any trend. The reason for this is that the upper curve consists of points involving block size 2 compared to the other sizes. As may clearly be seen from the graphs these points detach themselves from the others when dilution is introduced. This is to be expected, due to the introduction of a new, random fixed point, since the system will then be affected by a correction-to-scaling exponent wherever it lies in phase space and it is the small block sizes which are most affected by correction-to-scaling effects. The points along the bottom curve are those which involve a moment calculated on a block size of 64. These values are most affected by finite-size effects. For dilutions of 0.05 and 0.1 the data are

Table 4-5: Results of fits to ratio of moments for diluted system

p	χ^2	T_c	β	ν
0.95	1500/80	2.076(1)	0.15(2)	1.005(7)
0.9	106/100	1.88(2)	0.17(2)	0.93(3)
0.85	54/92	1.713(7)	0.14(3)	1.1(2)
0.8	80/160	1.520(2)	0.11(2)	0.92(4)
0.75	104/124	1.045(3)	0.176(3)	0.881(9)
0.7	1335/124	0.9(3)	0.25(4)	1.02(2)
0.65	260/92	0.97(8)	0.180(5)	0.90(2)
0.625	380/88	0.82(2)	0.17(2)	0.93(3)
0.6	218/84	0.64(1)	0.08(7)	1.02(3)

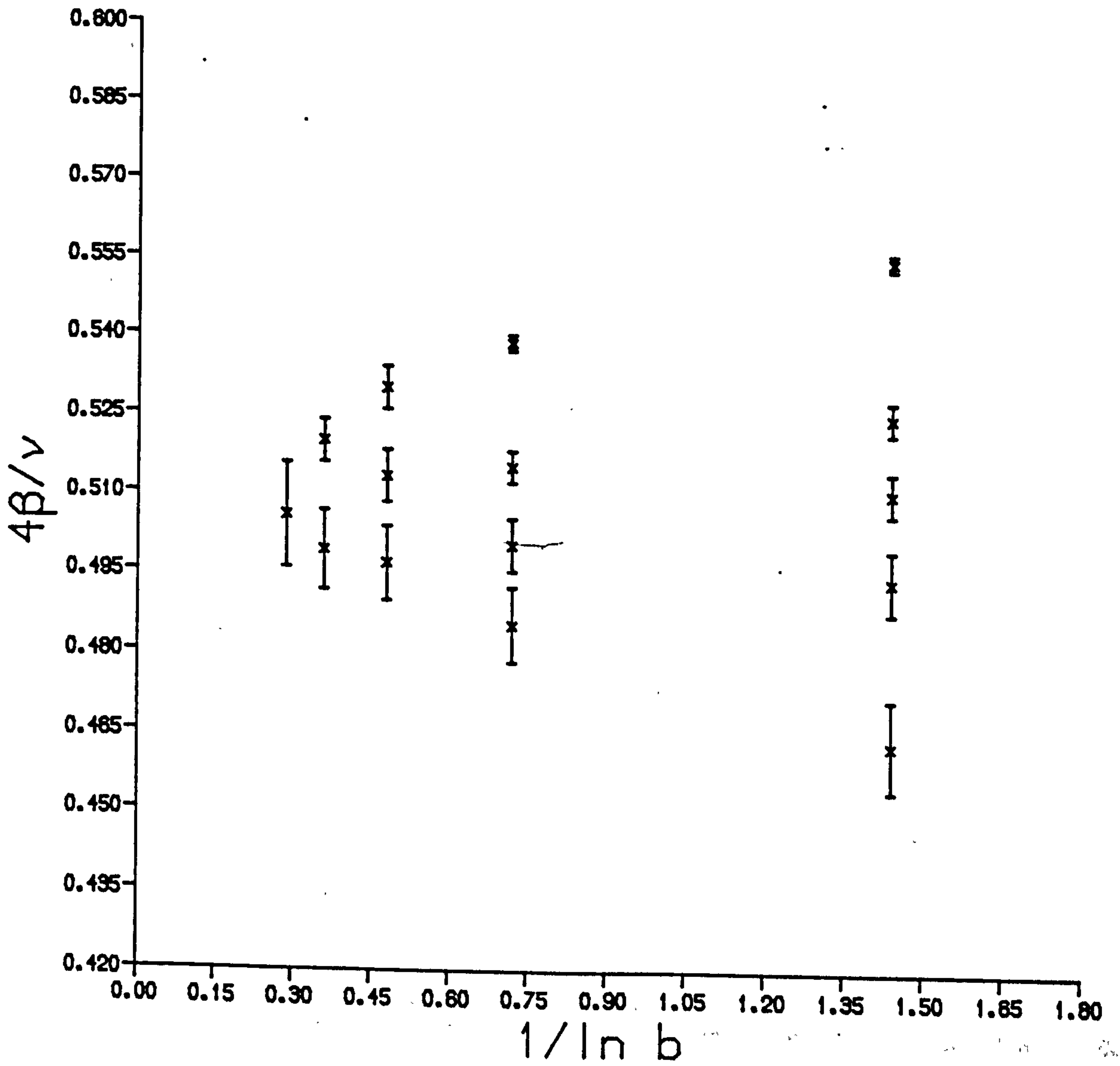


Figure 4-9a: $4\beta/v$ estimates for $p=0.95$

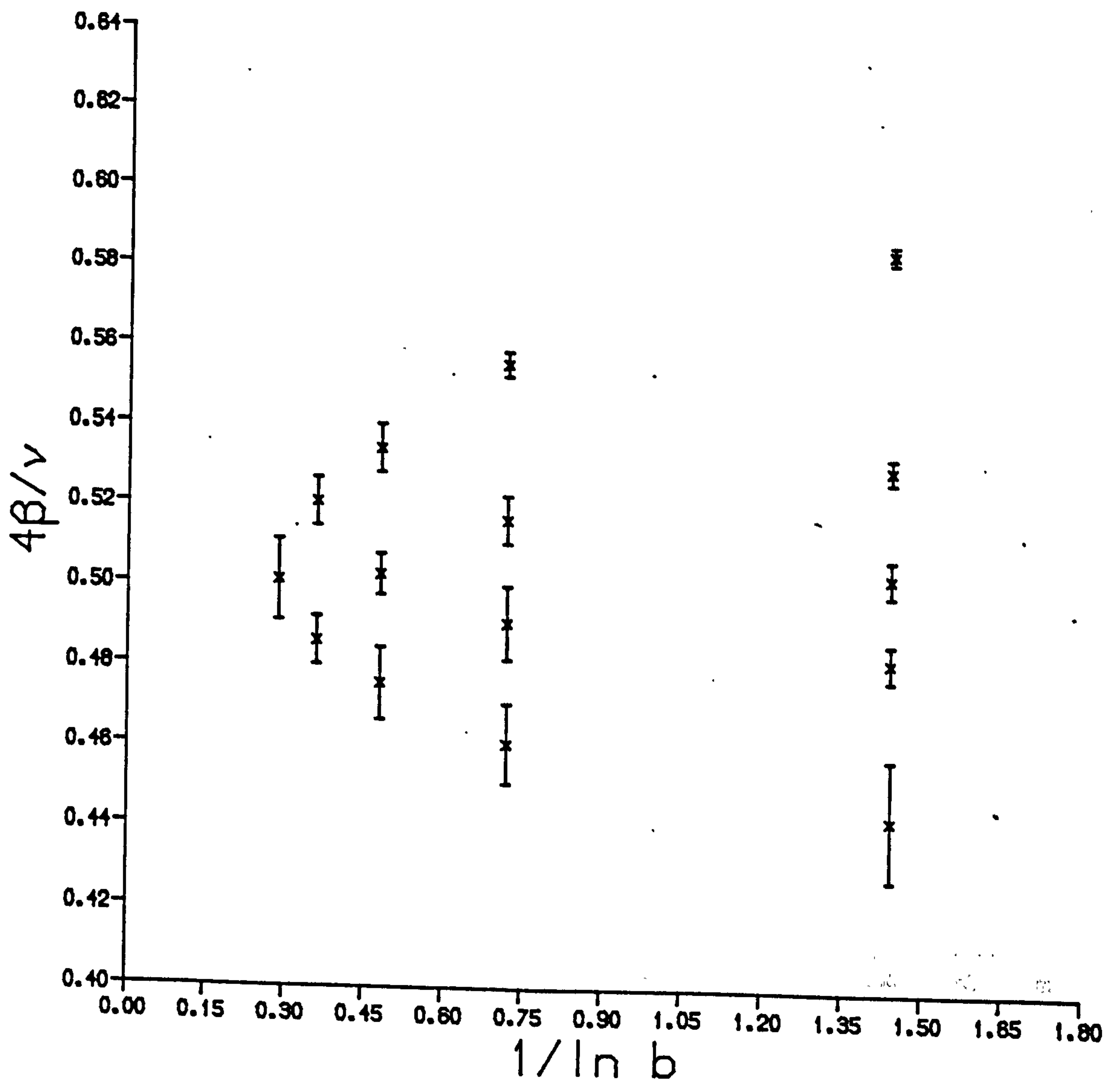


Figure 4-9b: $4\beta/v$ estimates for $p=0.9$

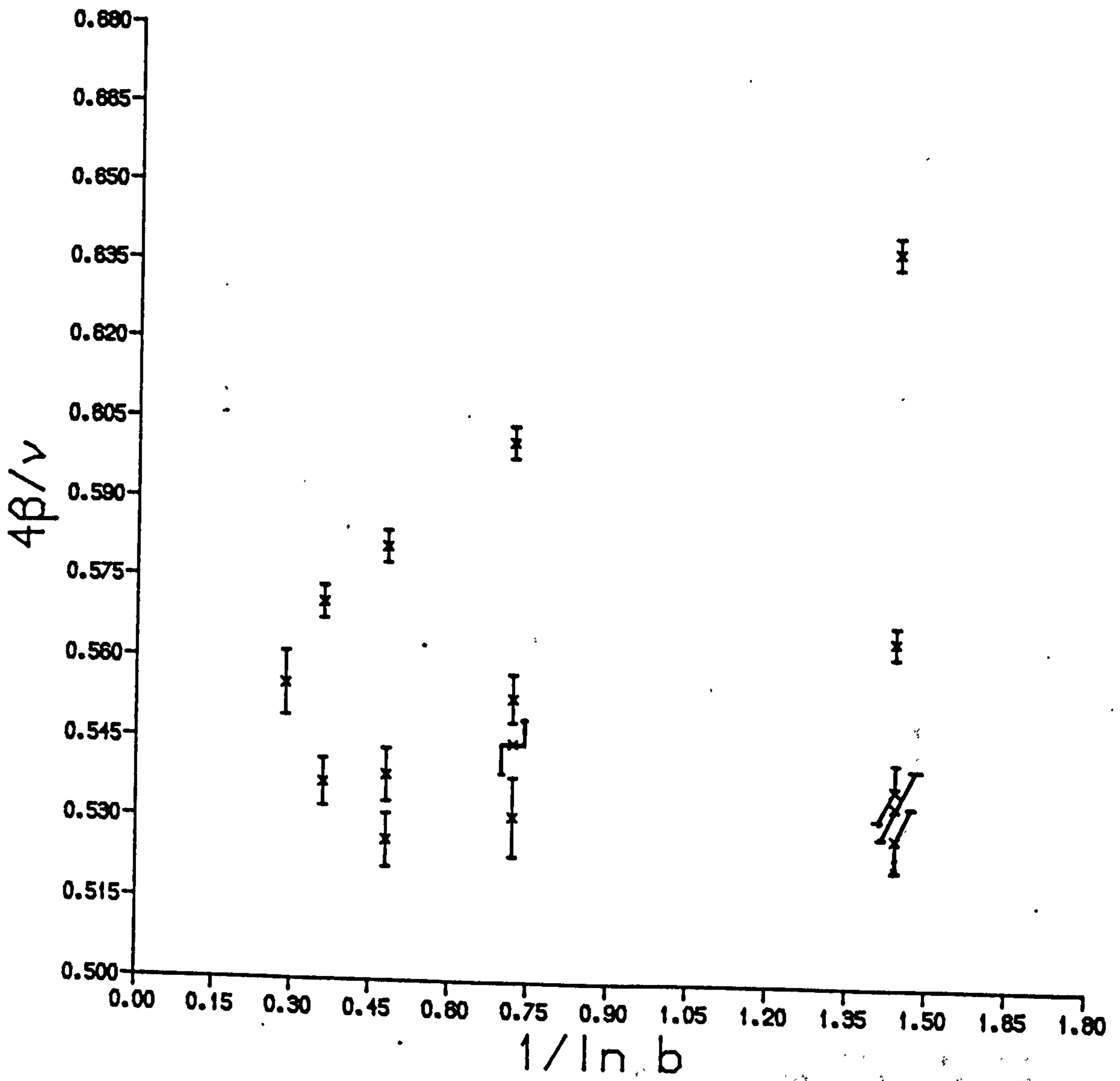


Figure 4-9c: $4\beta/v$ estimates for $p=0.85$

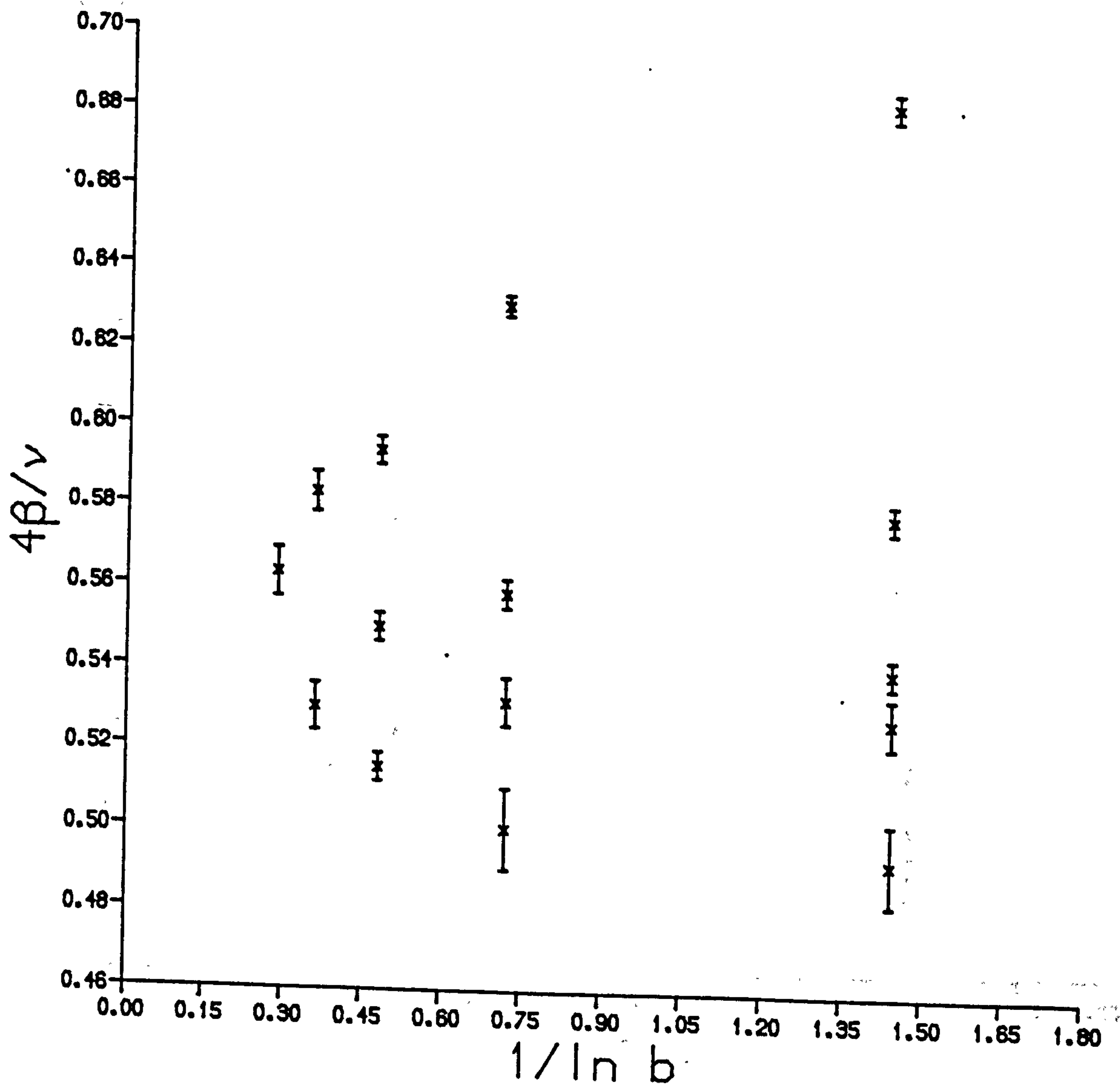


Figure 4-9d: $4\beta/v$ estimates for $p=0.8$

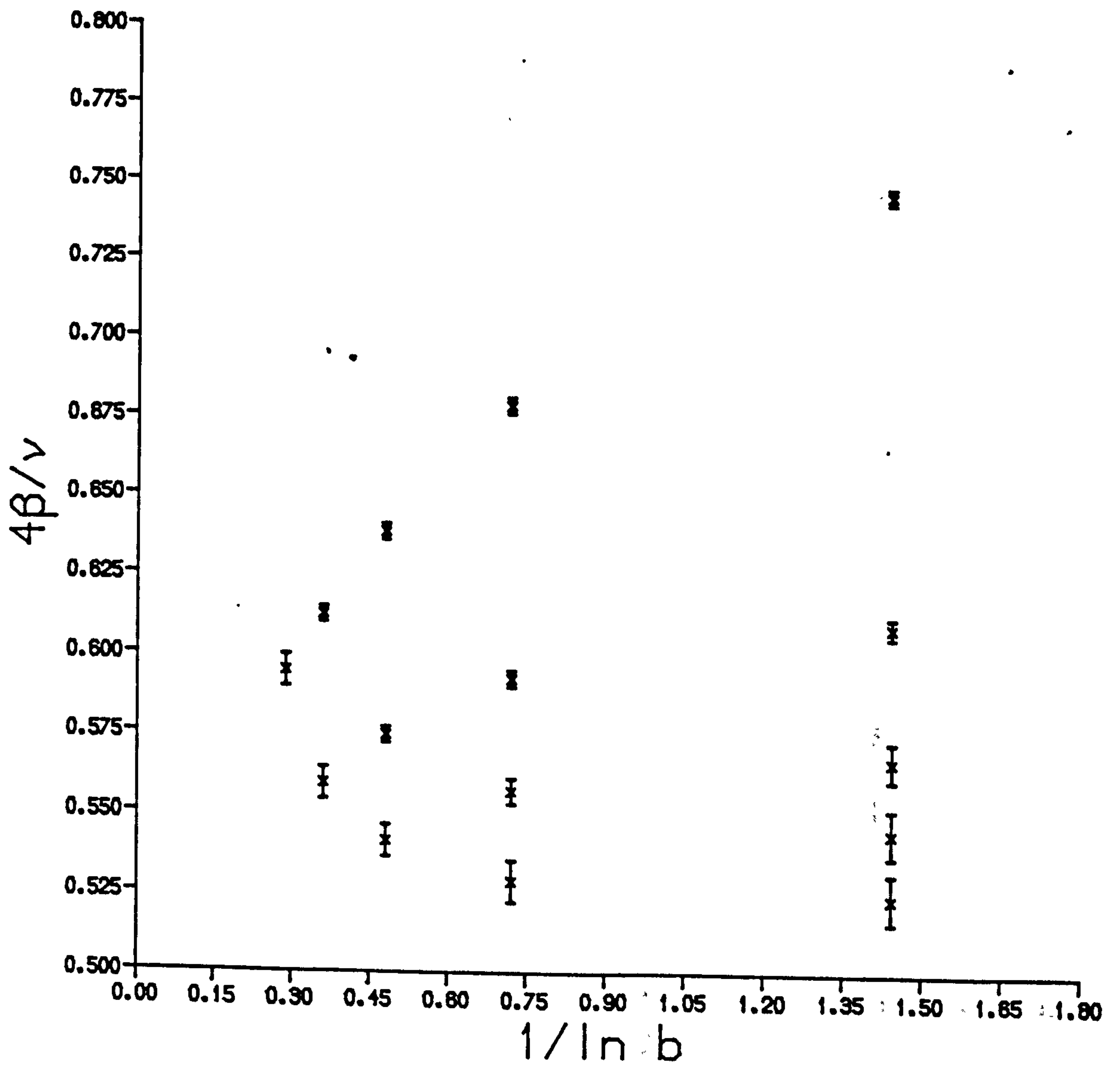


Figure 4-9e: $4\beta/v$ estimates for $p=0.75$

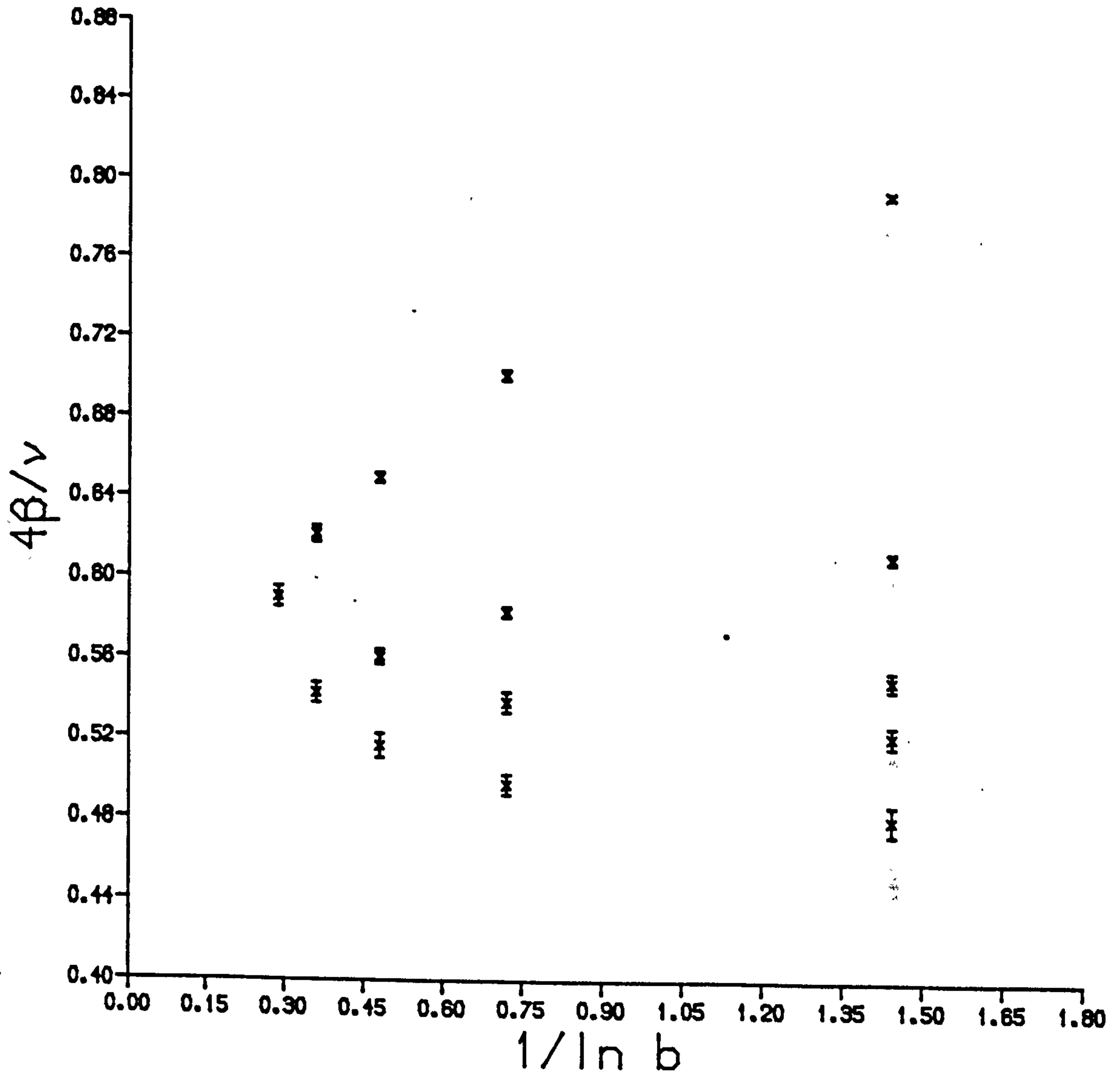


Figure 4-9f: $4\beta/v$ estimates for $p=0.7$

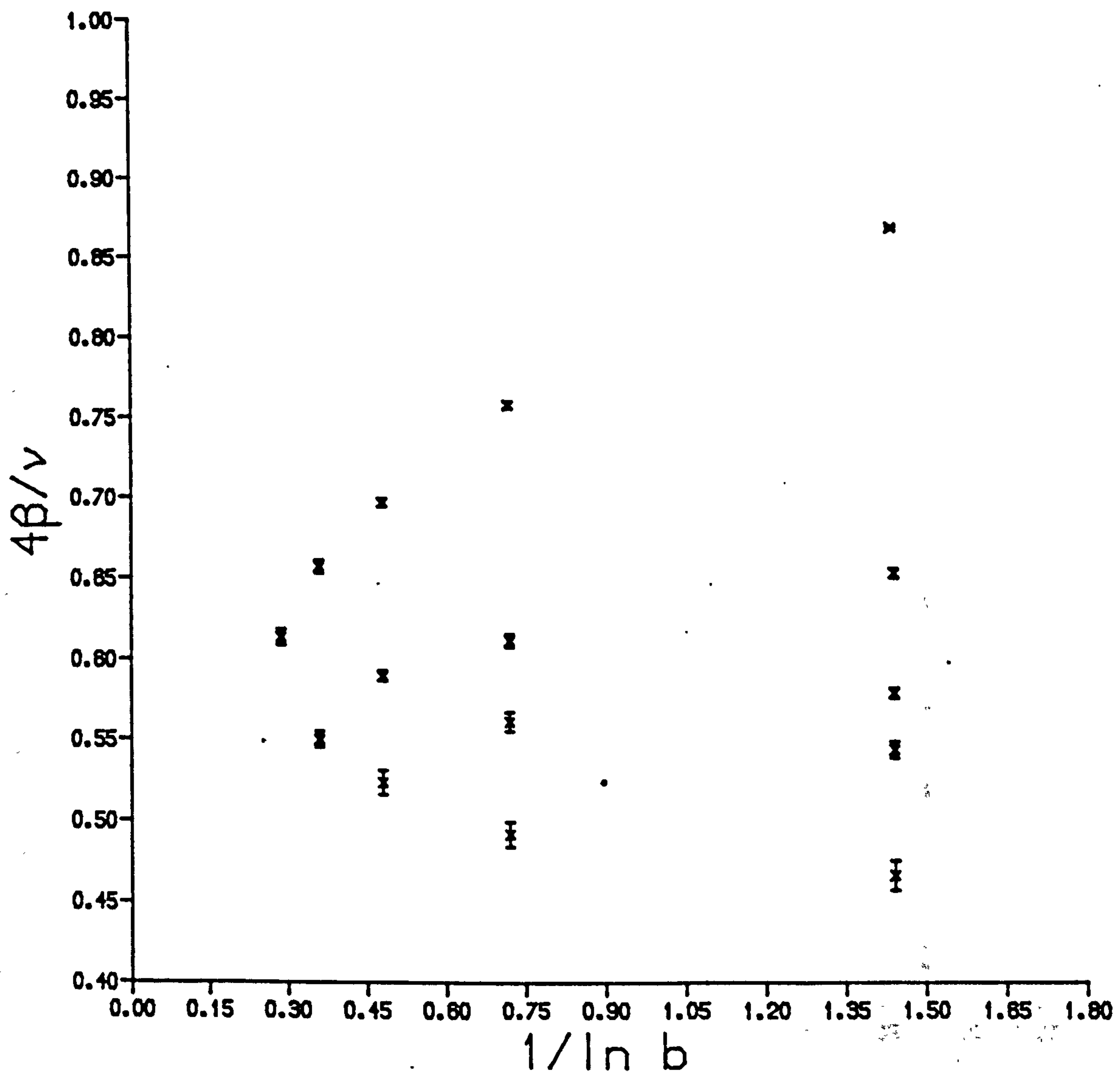


Figure 4-9g: $4\beta/v$ estimates for $p=0.65$.

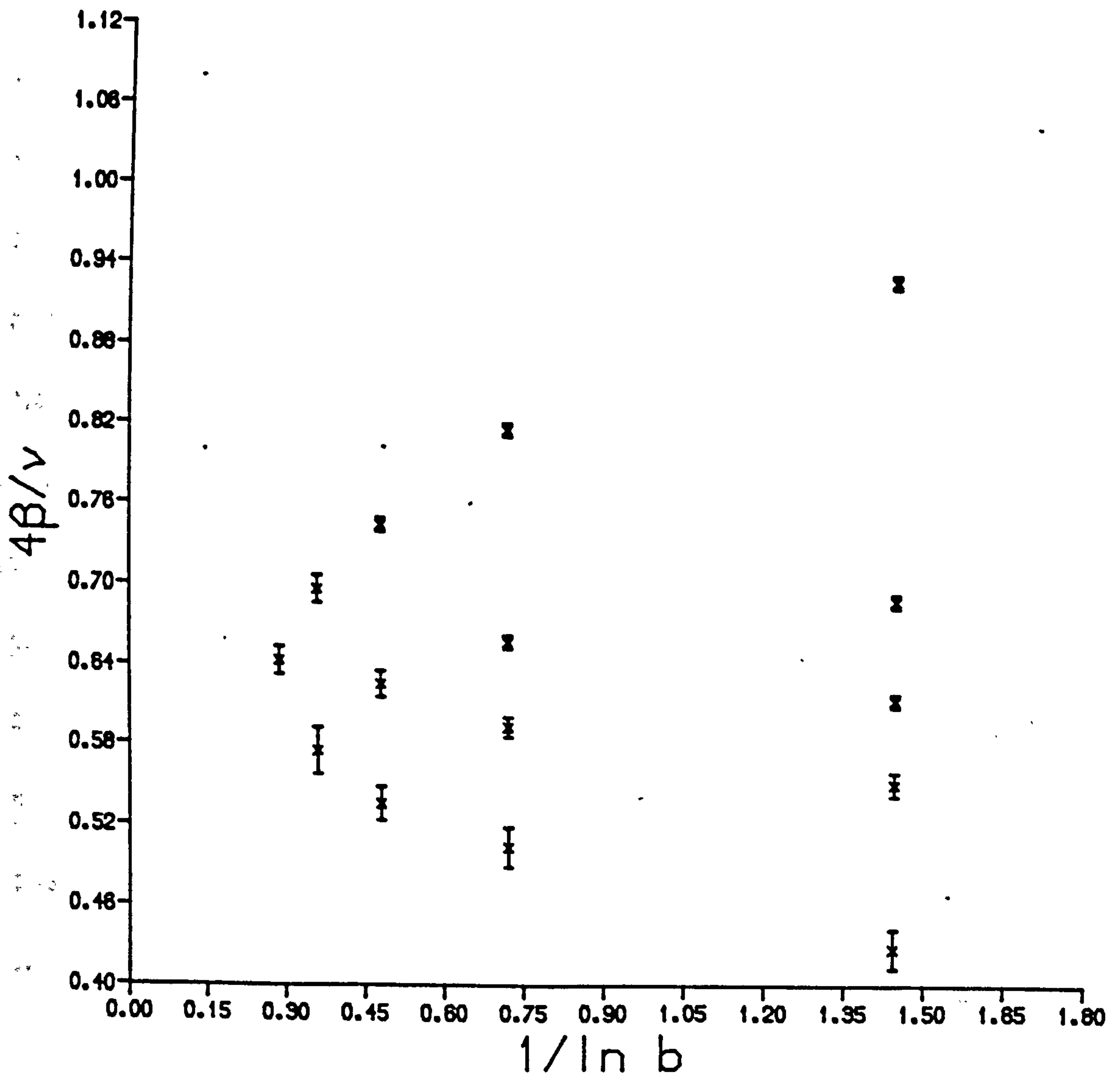


Figure 4-9h: $4\beta/v$ estimates for $p=0.625$

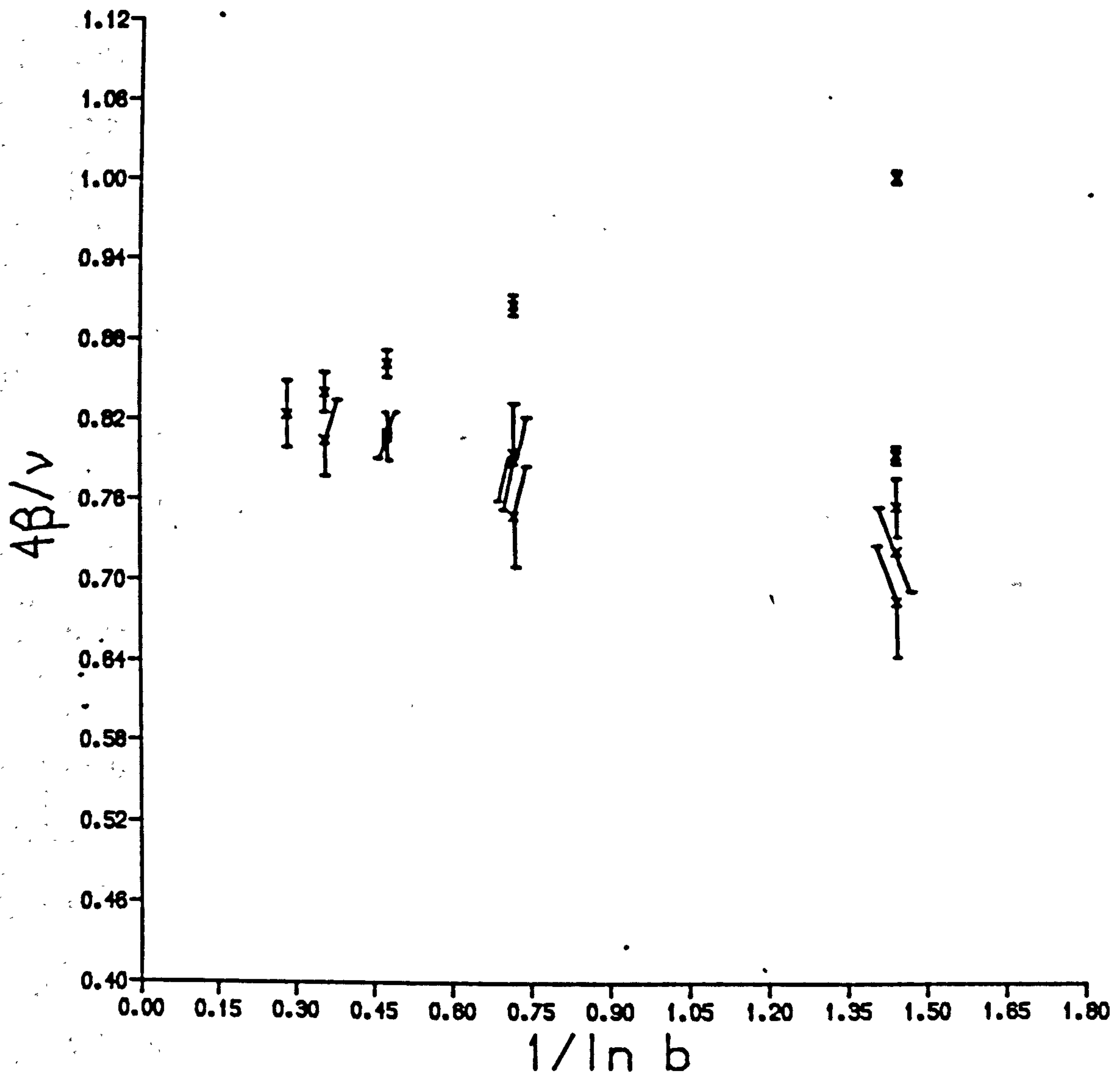


Figure 4-9i: $4\beta/v$ estimates for $p=0.6$

clearly consistent with the expected pure Ising $4\beta/\nu$ value of $\frac{1}{2}$. However, even after disregarding the two sets of data for $L=2$ and $L=64$, we observe a pronounced increase in the estimated value for the exponent ratio β/ν as we move down the critical curve, increasing the dilution. This observed evolution is mirrored in the fixed point values of the cumulant, G^* , which show a systematic decrease in value as we introduce greater amounts of dilution. This behaviour, which is a reflection of a decrease in the extent of the short-range order, is consistent with the picture emerging from droplet-based studies of critical phenomena in $d=1+\epsilon$ (Bruce and Wallace, 1983) which show that the deviation of G^* from 1 (in the $d=1$ limit) is a direct measure of the β/ν index.

Finally, we comment briefly on the possible explanations for the observed behaviour. In the phase diagram being studied we expect to observe the effects of competition amongst the three fixed points present; the pure Ising fixed point on the $p=1$ axis, the percolation fixed point on the $T=0$ axis, and the random Ising fixed point for non-zero T and $p_c < p < 1$. The scaling behaviour of the moments at any point on the critical curve apart from the percolation and pure Ising limits should be that of the random Ising fixed point since it is the attractive fixed point of the three. For "small" values of impurity concentration, c ($=1-p$), we expect to see a crossover from pure Ising behaviour to random Ising exponents as we approach the critical curve. Similarly, for small T values the crossover should occur from percolation to random Ising behaviour as we change the dilution and approach the critical temperature. Thus, for example, by rewriting the sum over configurations in the impurity average of the moments of the block distribution function in terms of a sum over clusters of occupied sites and invoking finite-size scaling forms for cluster averages, it is easy to show that, in the percolation limit, the

moments scale as the block size to a power of the percolation index ratio, $(\beta/\nu)_p (= \frac{5}{48})$. Possible explanations for the increase in the index ratio observed in the simulation are therefore:

(a) we could be seeing a crossover from the pure Ising β value to a random Ising β value, where $\beta_{RI} > \beta_I$. The results of $\epsilon^{1/2}$ expansions for the exponent β (see equation (3.47) or Newlove, 1983) indicate that in two dimensions the value of β in the random case is greater than in the pure model. This latter extrapolation from an expansion about four dimensions to the two-dimensional case considered here is to be regarded as being of doubtful legitimacy since the expansion parameter, ϵ , is assumed to be small; here we are setting $\epsilon=2$!

(b) another possibility is that, since we are in a situation where the specific heat exponent is zero, the random Ising behaviour may be the same as for the pure Ising case, but with additional, multiplicative logarithmic factors (Jug, 1983) (c.f., modification of the critical behaviour at a tricritical point in three dimensions (Bruce and Cowley, 1981)). If such logarithmic corrections are present they could show up in an "effective" exponent ratio, differing from the exponent values characterising the true asymptotic behaviour.

(c) the crossover may be from a pure Ising β value to a random Ising β value, where $\beta_{RI} < \beta_I$ but with a non-monotonic behaviour in the crossover region. Non-monotonic behaviour of effective exponents during crossover from the domain of influence of one fixed point to the domain of influence of another has been observed (Barma and Fisher, 1985; Bruce, 1977)

(d) the percolation fixed point may be influencing the behaviour. As for the above case, the β/ν ratio for percolation is less than for the pure Ising and we

may again be observing non-monotonic crossover behaviour.

In conclusion, this thesis has carried the study of the dilute Ising model further than previous work, in several respects. In analytic calculations using field theory methods we have extended the calculation of two critical amplitudes to one higher order in an expansion in $\epsilon^{1/2}$ ($\epsilon=4-d$). In numerical work, we have used state of the art block spin methods with high statistics to explore the phase diagram and critical behaviour in the two dimensional case. Positive results are obtained in both areas. For example, the new term obtained in the susceptibility amplitude ratio goes in the right direction for agreement with experiment, in contrast to the one-loop result. The numerical results pin down the phase diagram, reproducing the expected limiting behaviour. Nevertheless, the main qualitative conclusion from the thesis is that it underlines the difficulty in extracting in a systematically controlled way critical behaviour in even this simplest of random systems. In particular, the quantitatively unreliable nature of the $\epsilon^{1/2}$ expansion is further exposed and the need for very large simulations to control crossover effects is highlighted. The former will probably never be remedied; one may look however, with some optimism, to improvements in the results from simulations in the future.

References

- Aharony,A., *Phys. Rev.* B10 (1974) 3009
- Aharony,A., Bruce,A.D., *Phys. Rev. Lett.* 33 (1974) 427
- Aharony,A., Fisher,M.E., *Phys. Rev.* B27 (1983) 4394
- Aharony,A., Pelcovits,R.A., *Phys. Rev.* B31 (1985) 350
- Amit,D.J., *Field Theory, the Renormalisation Group, and Critical Phenomena (2nd Ed)*, World Scientific (1984)
- Amit,D.J., *J. Phys.* A9 (1975) 1441
- Anderson,P.W., Edwards,S.F., *J. Phys.* F5 (1975) 965
- Baker,G.A., *Phys. Rev.* 126 (1962) 2071
- Balian,R., Maynard,R., Toulouse,G., eds., *III-Condensed Matter, Les Houches 1978, Session XXXI*, North-Holland/World Scientific (1979)
- Barber,M.N., Fisher,M.E., *Phys. Rev. Lett.* 28 (1972) 1516
- Barber,M.N., In: *Phase Transitions and Critical Phenomena, Vol. 8*, Domb,C., Lebowitz,J.L., eds., Academic Press (1983)
- Barma,M., Fisher,M.E., *Phys. Rev.* B31 (1985) 5954
- Berlin,T.H., Kac, M., *Phys. Rev.* 86 (1952) 821
- Binder,K., *Z. Phys.* B43 (1981) 119
- Binder,K., ed., *Monte Carlo Methods in Statistical Physics*, Springer-Verlag (1979)
- Binder,K., Landau,D.P., *Phys. Rev.* B31 (1985) 5946
- Birgeneau,R.J., Boni,P., Cowley,R.A., Mitchell,P.W., Shirane,G., Uemura,Y.J., Yoshizawa,H., (To be published) (1986)
- Birgeneau,R.J., Belanger,D.P., Cowley,R.A., Jaccarino,V., King,A.R., Shirane,G., Yoshizawa,H., *Phys. Rev.* B27 (1983) 6757
- Birgeneau,R.J., Cowley,R.A., Guggenheim,H.J., Shirane,G., *Phys. Rev. Lett.* 37 (1976) 940
- Bowler,K.C., In: *Proc. of Three Day In-Depth Review of the Impact of Specialised Processors in Elementary Particle Physics*, INFN Padua (1983)

- Bowler,K.C., Rebbi,C., In:*Proc. of the 26th Scottish Universities Summer School in Physics*, Bowler,K.C., McKane,A.J., eds., SUSSP (1985)
- Brézin,E., Le Guillou,J.C., Zinn-Justin,J., *Phys. Lett.* 47A (1974) 285
- Brézin,E., Le Guillou,J.C., Zinn-Justin,J., *Phys. Rev.* D8 (1973) 434 and D8 (1973) 2418
- Brézin,E., Wallace,D.J., Wilson,K.G., *Phys. Rev. Lett.* 29 (1972) 591
- Bruce,A.D., *J. Phys.* C10 (1977) 419
- Bruce,A.D., *J. Phys.* C14 (1981) 3667
- Bruce,A.D., Cowley,R.A., *Structural Phase Transitions*, Taylor and Francis (1981)
- Bruce,A.D., Wallace,D.J., *J. Phys.* A16 (1983) 1721
- Carneiro, C.E.I., Jug,G., *Oxford Univ. Preprint 64/82* (1982)
- Derrida,B., *J. Phys.* A14 (1981) 145
- Emery,V.J., *Phys. Rev.* B11 (1975) 239
- Essam,J.W., In:*Phase Transitions and Critical Phenomena, Vol. 2* Domb,C., Green,M.S., eds., Academic Press (1972)
- Fisher,M.E., In:*Critical Phenomena, Proceedings of the 51st Enrico Fermi Summer School, Varenna, Italy*, Green,M.S., ed., Academic Press (1971)
- Goldstein,H., *Classical Mechanics (2nd Ed)*, Addison-Wesley (1980)
- Grinstein,G., Luther,A., *Phys. Rev.* B13 (1976) 1329
- Grinstein,G., Ma,S-k., Mazenko,G., *Phys. Rev.* B15 (1977) 258
- Harris,A.B., *J. Phys.* C7 (1974) 1671
- Hockney,R.W., Jesshope,C.R., *Parallel Computers*, Adam Hilger (1981)
- Hubbard,J., *Phys. Rev. Lett.* 3 (1958) 77
- Jayaprakash,C., Katz,H.J., *Phys. Rev.* B25 (1982) 265
- Jug,G., *Phys. Rev.* B27 (1983) 4518
- Khmel'nitski,D.E., *Zh. Eksp. Theor. Fiz.* 68 (1975) 1960 [English Translation: *Soviet Physics, JETP* 41 (1975) 981]
- Kirkpatrick,S., Shante,V.K.S., *Advan. Phys.* 20 (1971) 325
- Krinsky,S., Mukamel,D., *Phys. Rev.* B13 (1976) 5065

- Lawrie,J.D., *J. Phys.* A9 (1975) 961
- Metropolis,N., Rosenbluth,A.W., Rosenbluth,M.N., Teller,A.H., Teller,E.,
J. Chem. Phys. 21 (1953) 1087
- Mouritsen,O., *Computer Studies of Phase Transitions*, Springer-Verlag (1984)
- Newlove,S.A., *J. Phys.* C16 (1983) L423
- Nightingale,M.P., *Physica* 83 (1976) A561
- den Nijs,M.P.M., *J. Phys.* A12 (1979) 1857
- Onsager,L., *Phys. Rev.* 65 (1944) 117
- Pawley,G.S., Swendsen,R.H., Wallace,D.J., Wilson,K.G., *Phys. Rev.* B29 (1984) 4030
- Ramond,P., *Field Theory: A Modern Primer*, Benjamin-Cummings (1981)
- Stinchcombe,R.B., *J. Phys.* C12 (1979) 4533
- Stinchcombe,R.B., In: *Phase Transitions and Critical Phenomena, Vol. 7*,
Domb,C., Lebowitz,J.L., eds., Academic Press, (1983)
- Stratonovich, R.L., *Doklady Akad. Nauk S.S.R.* 115 (1957) 1097
[English translation: *Soviet Physics-Doklady* 2 (1958) 416]
- Suzuki,M., *Prog. Theor. Phys.* 58 (1977) 1143
- 't Hooft,G., *Nuc. Phys.* B61 (1973) 465
- 't Hooft,G., Veltman,M., *Nuc. Phys.* B44 (1972) 189
- Verbaarschot,J.J.M., Zirnbauer,M.R., *J. Phys.* A17 (1985) 1093
- Wallace,D.J., In: *Phase Transitions and Critical Phenomena, Vol. 6*,
Domb,C., Green,M.S., eds., Academic Press (1976)
- Wallace,D.J., Zia,R.K.P., *J. Phys.* A8 (1975) 1495
- Wegner,F.J., *Phys. Rev.* B5 (1972) 4529
- Weiss,P., In: *Proceedings of 6th Solvay Congress, 1930*, Gauthier-Villars (1932)
- Widom,B., *J. Chem. Phys.* 43 (1965) 3898
- Wilson,K.G., *Phys. Rev. Lett.* 28 (1972) 548